Allele-Specific Polymerase Chain Reaction (ASPCR) to Detect Resistance Mutations in Minor Variants of HIV-1 Subtype C in Patients Failing Highly Active Antiretroviral Therapy (HAART)

by

Shevani Maharaj

Submitted in fulfilment of the requirements for the degree of

Master of Medical Science in Molecular Virology

In the

Faculty of Health Sciences

University of KwaZulu-Natal

2014

PREFACE

The experimental work described in this dissertation was carried out in the Hasso Plattner Research Laboratory, Doris Duke Medical Research Institute, Nelson R. Mandela School of Medicine, University of KwaZulu-Natal, Durban, under the supervision of Dr Michelle Lucille Gordon.

These studies represent original work by the author and have not otherwise been submitted in any form for any degree or diploma to any other University. Where use has been made of the work of others, it is duly acknowledged in the text.

Signed: _____ Date: 07/04/15

Shevani Maharaj (Candidate)

Signed: _____ Date: 07/04/15

Dr Michelle Lucille Gordon (Supervisor)

DECLARATION

Plagiarism

I, Shevani Maharaj, declare that

(i) The research reported in this dissertation, except where otherwise indicated, is my original work.

(ii) This dissertation has not been submitted for any degree or examination at any other university.

(iii) This dissertation does not contain other person's data, pictures, graphs or other information, unless specifically acknowledged as being sourced from other persons.

(iv) This dissertation does not contain other persons' writing, unless specifically acknowledged as being sourced from other researchers. Where other written sources have been quoted, then:

a) their words have been re-written but the general information attributed to them has been referenced.

b) where their exact words have been used, their writing has been placed inside quotation marks and referenced.

(v) Where I have reproduced a publication of which I am an author, co-author or editor, I have indicated in detail which part of the publication was written by myself alone and have fully referenced such publications.

(vi) This dissertation does not contain text, graphics or tables copied and pasted from the internet unless specifically acknowledged, and the source being detailed in the dissertation and in the Reference section.

Signed: Maharaj Date: 07/04/15

Shevani Maharaj (Candidate)

Signed: Date: 07/04/15

Dr Michelle Lucille Gordon (Supervisor)

ETHICAL APPROVAL

Full ethical approval, from the Biomedical Research Ethics Committee of the Nelson R. Mandela School of Medicine, University of KwaZulu-Natal (ref: BE078/09) was obtained for this study.

ACKNOWLEDGEMENTS

First and foremost, I want to thank God for all that I have been blessed with. Thank you for providing me with the strength and perseverance to get through this, and for blessing me with the most amazing husband and awesome sons.

A very special thank you to my wonderful supervisor, Dr Michelle Lucille Gordon, for providing me with this opportunity and for being so understanding and patient. I really appreciate the guidance, advice, motivation and encouragement that you provided during this period.

Thank you to Professor Thumbi Ndung'u for all his great advice, guidance and motivation. I also thank you for always challenging me to think critically so that I can become a better scientist.

Thank you to Dr Vincent Marconi and Dr Roger Paredes for all the expert advice and guidance that you provided.

I am grateful to Emory University for providing financial support for this project.

Thank you to Mrs Keshni Hiramen and Mrs Nothemba Nontala for all the assistance that you provided in the laboratory and for making it a pleasant environment to work in.

Thank you to the University of KwaZulu-Natal (College of Health Sciences), HIV Pathogenesis Programme (HPP), Poliomyelitis Research Foundation (PRF), and the National Research Foundation (NRF) for providing me with financial support during this MMedSc degree.

To my late parents, Ramdutt and Pulmatti Bechoo, I thank you for all the love, support and encouragement that you had provided me with throughout my life and I thank you for always believing in me. I love you very much and miss you immensely.

Thank you to my mother-in-law, Renuka Devi Maharajh, for taking care of my sons while I was at University. It gave me great comfort and peace of mind to know that they were in the loving care of their wonderful, kind-hearted and patient grandmother.

To all my family and friends thank you for the support and encouragement that you provided during this period

I am thankful to my two sons, Kapil and Rohit, for their unconditional love. I am truly blessed to have such wonderful kids and words cannot describe how much I love you both.

This thesis is dedicated to my husband and best friend, Vinay Maharaj. This would not have been possible without you. Thank you for the love, patience, support and encouragement that you have provided me with throughout this process. I am truly blessed to have you in my life and I am extremely grateful to you for all the sacrifices that you have made to enable me to achieve this goal. Thank you for always putting the needs of myself and our sons before your own. I respect you deeply and I love you unconditionally.

ABSTRACT

The World Health Organization (WHO) has recommended Tenofovir disoproxil fumarate (TDF) as one of the preferred first-line antiretrovirals (ARVs). TDF and Abacavir (ABC) were introduced into the South African National Antiretroviral Treatment Guidelines in 2010. However, exposure to TDF and ABC can result in the development of the K65R and L74V resistance mutations, respectively. The K65R mutation occurs preferably in subtype C viruses, due to the unique polymorphisms found at codons 64 and 65 (which are not present in subtype B). This is a cause for concern in South Africa, where subtype C is the most common HIV-1 subtype. In addition, these mutations may be present in the minor viral population (i.e <20% of the viral population) and it has been shown that the presence of a resistance mutation in a frequency as low as <0.5% may be associated with an increase in the risk of virological failure. This study investigated the prevalence of K65R and L74V in the minor viral population, using Allele-specific PCR (ASPCR), in a cohort of subtype C infected patients that failed their first-line treatment regimen that did not include TDF or ABC.

RNA was extracted from stored plasma samples from a subset of the South African Resistance Cohort Study (SARCS) and the pol region was reverse transcribed and amplified using a one-step RT-PCR kit (Invitrogen; California, USA). For both the K65R and L74V mutations, ASPCR was performed using specific and non-specific primers. A specific and non-specific standard curve was optimised for each mutation (using a mutant plasmid control) and these standard curves were used to perform an absolute quantification. Subsequently, the percentage of each mutation (in each sample) was calculated by dividing the quantity of mutant sequences in the sample by the quantity of total viral sequences in the sample and multiplying this ratio by 100.

The Limit of Detection (LOD) of the K65R ASPCR was 0.72%. Of the 84 patients that were assayed, the K65R mutation was detected in 7 (8.33%) of the patients. Five of the 7 samples were detected above 1% (i.e 3 were approximately 2%, 1 was 9.48% and 1 was 100%) and 2 were detected below 1% (i.e 1 was 0.88% and the other was 0.93%). The limit of detection for the L74V ASPCR was 0.013%.We found the L74V mutation to be prevalent in 9 (10.7%) of 84 patients. In 4 of the 9 patients, the L74V mutation was found in ≥1% of the viral population (viz. 2.82%, 10.10%, 12.02% and 18.22%) and in the other 5 patients, the L74V mutation was detected in <1% of the viral population (2 were between 0.5% and1%, while 3 were detected between 0.013% and0.5%).

In this study, ASPCR detected additional K65R and L74V mutations in the minor viral population of TDF and ABC-inexperienced patients that were missed by standard genotyping. These minorityK65R mutations could contribute to treatment failure in these patients when switched to TDF or ABC-containing ARV regimens. ASPCR is a useful tool for screening for minority mutations before starting or switching regimens.

TABLE OF CONTENTS

Chapter 3: Results

LIST OF FIGURES

LIST OF TABLES

ABBREVIATIONS AND ACRONYMS

ABC	-	Abacavir (ABC)
AIDS	-	Acquired Immunodeficiency Syndrome
ARV	-	Antiretroviral
ASPCR	-	Alelle-Specific Polymerase Chain Reaction
cART	-	Combination Antiretroviral Therapy
Cp	-	Crossing point
CRFs	-	Circulating Recombinant Forms
Ct	-	Threshold Cycle
d4T	-	Stavudine
ddl	-	Didanosine
DNA	-	Deoxyribonucleic Acid
dNTPs	-	Deoxynucleotide Triphosphates
dsDNA	-	Double Stranded Deoxyribonucleic Acid
EDTA	-	Ethylenediaminetetraacetic acid
FDA	-	Food and Drug Administration
HAART	-	Highly Active Antiretroviral Therapy
HIV	-	Human Immunodeficiency Virus
HR1	-	Hydrophobic Region 1
HR2	-	Hydrophobic Region 2
INIs	-	Integrase Inhibitors
LC480	-	LightCycler 480
LiPA	-	Lineprobe Assay
LOD	-	Limit of Detection
$MgSO_4$	-	Magnesium Sulfate

mRNAs	-	Messenger Ribonucleic Acids
NNRTIs	-	Non-nucleoside Reverse Transcriptase Inhibitors
NRTIs	-	Nucleoside/Nucleotide Reverse Transcriptase Inhibitors
OLA	-	Oligonuclotide ligation-based Assays
PCR	-	Polymerase Chain Reaction
PIs	-	Protease Inhibitors
RNA	-	Ribonucleic Acid
RT	-	Reverse Transcriptase
SARCS	-	South African Resistance Cohort Study
SD	-	Standard Deviation
SGS	-	Single-genome Sequencing
SIVs	-	Simian Immunodefiency Viruses
TAMs	-	Thymidine Analog Mutations
TBE	-	Tris-Borate-EDTA
TDF	-	Tenofovir Disoproxil Fumarate
TyHRT	-	Ty1/HIV-1 RT Hybrid System
URFs	-	Unique Recombinant Forms
WT	-	Wildtype
ZDV	-	Zidovudine

CHAPTER 1

Introduction

1.1 Human Immunodeficiency Virus (HIV)

1.1.1 HIV Origin and Classification

Human Immunodeficiency Virus (HIV), which is a retrovirus belonging to the genus Lentivirus, is the causative agent of Acquired Immunodeficiency Syndrome (AIDS). There are two types of HIV that exist, viz. HIV-1 and HIV-2 (Butler et al., 2007). HIV-1 was the first HIV type to be isolated in 1983 and it is the type that is most common in the world (Barre-Sinoussi et al., 1983). HIV-2 occurs mostly in HIV-infected people in West Africa, where the virus was first isolated in 1986and it is the less virulent of the two (Santoro and Perno, 2013, Clavel et al., 1986). HIV-1 is believed to have originated through cross-species transmission of Simian Immunodeficiency Viruses (SIVs) affecting non-human primates, in Central Africa, to humans, while HIV-2 is believed to have crossed over to humans from sooty mangabey monkeys in West Africa (Ndung'u and Weiss, 2012, Cohen et al., 2008, Sharp et al., 2005).

HIV-1 has been transmitted from the non-human primates to humans at least four separate times, which has resulted in the development of the four HIV-1 groups, viz. group M (major), group O (outlier), group N (nonmajor and nonoutlier) and group P. Groups N and O have been found in individuals of West Africa, whilst group P has been isolated from two individuals from Cameroon (Santoro and Perno, 2013). HIV-1 group M is responsible for over 99% of the global HIV infections and it includes nine subtypes (or clades), viz. A, B, C, D, F, G, H, J and K (Santoro and Perno, 2013, Jacobs et al., 2014, Ndung'u and Weiss, 2012). These group M subtypes are referred to as non-recombinant types. Two of these subtypes are furthermore separated into sub-subtypes, viz. A (A1, A2,A3, A4 and A5) and F (F1 and F2) (Triques et al., 1999, Triques et al., 2000, Gao et al., 2001, Meloni et al., 2004, Vidal et al., 2006, Vidal et al., 2009, Santoro and Perno, 2013). In addition to the nine subtypes, group M also includes no less than 58 circulating recombinant forms (CRFs) and many unique

recombinant forms (URFs) (Santoro and Perno, 2013, Santos and Soares, 2010). Recombination takes place when a person is co-infected with two or more HIV subtypes and the reverse transcriptase (RT) enzyme is able to switch from one viral ribonucleic acid (RNA) strand to another (of a different subtype) and then back to the initial strand during reverse transcription, thereby producing a new mosaic HIV strain that is a combination of the parent strains (as shown in Figure 1.1) (Blackard et al., 2002). These mosaic strains, or recombinant forms, are referred to as CRFs if they occur in three or more individuals that are epidemiologically unrelated, but if they occur in just one individual they are classified as URFs (Taylor and Hammer, 2008, Santos and Soares, 2010).

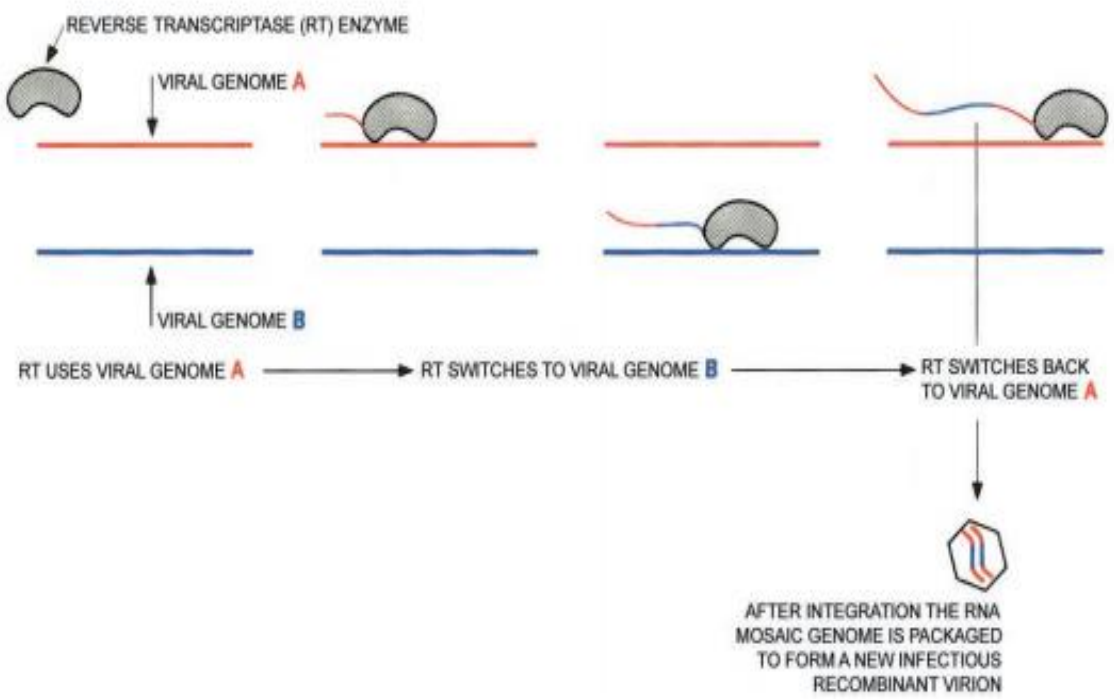

Fig 1.1 The Production of Recombinant Forms of HIV. When a host cell is co-infected by two or more HIV subtypes, the RT enzyme is capable of switching between RNA templates of the different subtypes during the process of reverse transcription, thereby creating a new strain that is a combination of the parent strains. The new strain is referred to as a recombinant form. Taken from (Blackard et al., 2002)

1.1.2 HIV Epidemiology

The UNAIDS World Report for 2013 estimated that in 2012, there were approximately 35.3 (32.2 – 38.8) million people infected with HIV worldwide, approximately 71% of which were in Sub-Saharan Africa. Globally, there were 2.3 (1.9 – 2.7) million new HIV infections in 2012, with 70%of these occurring in Sub-Saharan Africa (UNAIDS, 2013). Since Sub-Saharan Africa only accounts for approximately 12% of the world population, these statistics are especially disconcerting (UNAIDS, 2011). In Sub-Saharan Africa, the most prevalent HIV subtype is subtype C and it is responsible for approximately 50% of the global HIV-1 infections, as shown in Figure 1.2 (Santos and Soares, 2010).

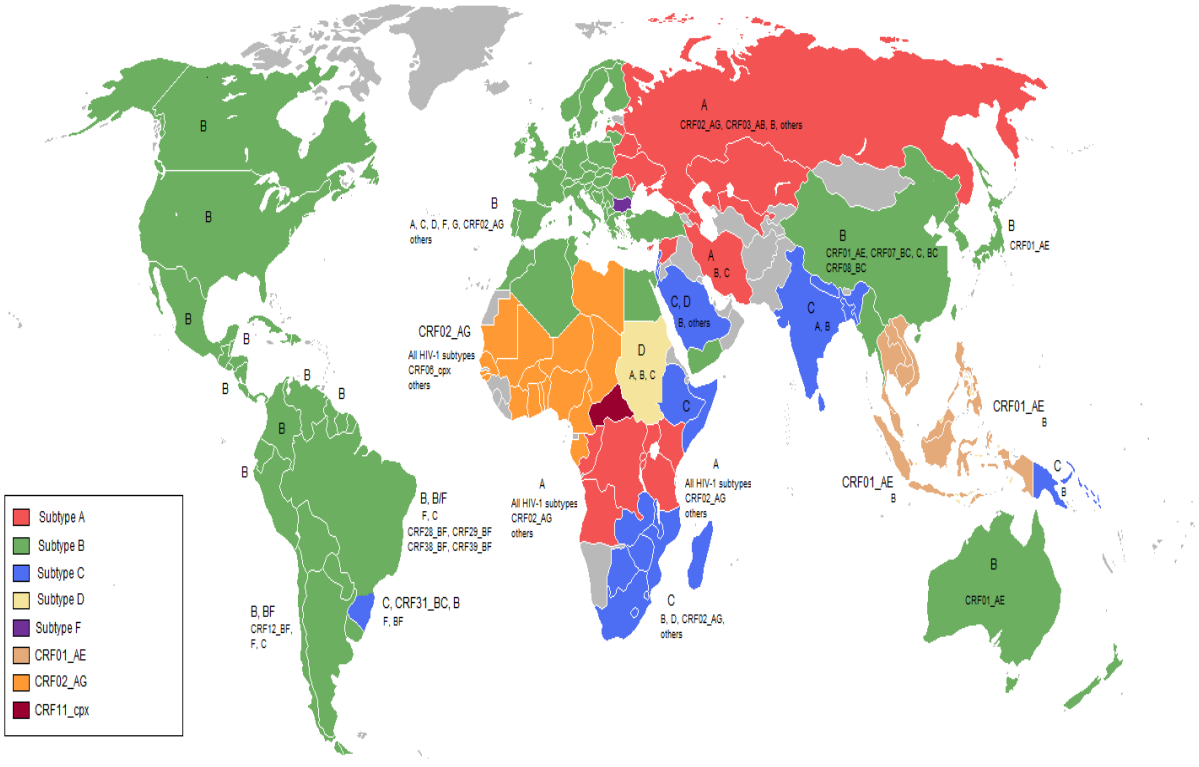

Fig 1.2 Worldwide Distribution of HIV-1. This global distribution of HIV-1 shows that subtype C is the most prevalent HIV-1 subtype, as it is responsible for approximately 50% of the worldwide HIV-1 infections, and that it is the most prevalent subtype in Sub-Saharan Africa. Taken from (Santos and Soares, 2010)

1.1.3 HIV Structure

HIV is a spherical particle (approximately 100nm in diameter) that is surrounded by a lipid bilayer which is host-derived. Each virion's membrane contains trimers of gp120 (a surface glycoprotein), which is bound to gp41 (a transmembrane glycoprotein), which can be seen in Figure 1.3.Within the viral membrane is a p17 matrix protein, that is anchored to the membrane, and the p24 protein capsid, which encloses two copies of the viral RNA, as well as the enzymes reverse transcriptase, integrase and protease (Fanales-Belasio et al., 2010).

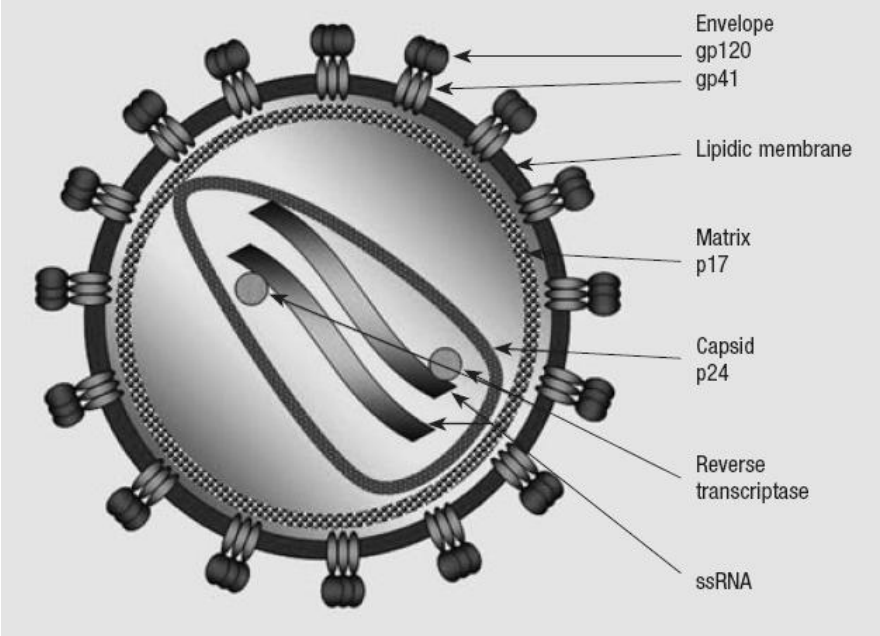

Fig 1.3 Structure of HIV-1. Taken from (Fanales-Belasio et al., 2010)

1.1.4 HIV Life Cycle

The HIV replication cycle begins by entry of the viral particle into the host cell, as shown in Figure 1.4.This occurs when the gp120 surface protein of the virus binds to the CD4 receptor on the host cell, which causes a conformational change in gp120, revealing a particular

domain of gp120 that is capable of binding to the co-receptor (CCR5 OR CXCR4) on the surface of the host cell. This binding then facilitates the penetration of gp41 into the host cell membrane. The gp41 then undergoes a conformational change, which causes the molecule to shorten, which allows the virus and host cell membrane to come into close contact, thereby enabling the two membranes to fuse (Fanales-Belasio et al., 2010).

Once the membranes have fused, the contents of the virus, i.e the viral RNA, reverse transcriptase, integrase and protease, are released into the host cell. The RT enzyme transcribes the viral RNA into double stranded deoxyribonucleic acid (dsDNA) in the cytoplasm and this is then transferred into the nucleus where it is incorporated into the deoxyribonucleic acid (DNA) of the host cell by the viral enzyme integrase (Klimas et al., 2008). When the cell undergoes replication, multiply-spliced viral messenger ribonucleic acids (mRNAs) are produced and this results in the expression of the regulatory proteins, which enable singly-spliced and unspliced mRNA to be transported out of the nucleus into the cytoplasm. In the cytoplasm, translation of the viral mRNA occurs to produce polypeptides, eg. the gag and gag-pol polyprotein. Following translation, the viral proteins, polyproteins and the genomic RNA move towards the cell membrane where assembly and then budding of the immature virion occurs. This is followed by maturation, which involves cleavage of the gag and gag-polpolyproteins by the viral protease enzyme to produce the structural proteins and allows the virion to become an infectious agent (Sierra et al., 2005, Barre-Sinoussi, 1996).

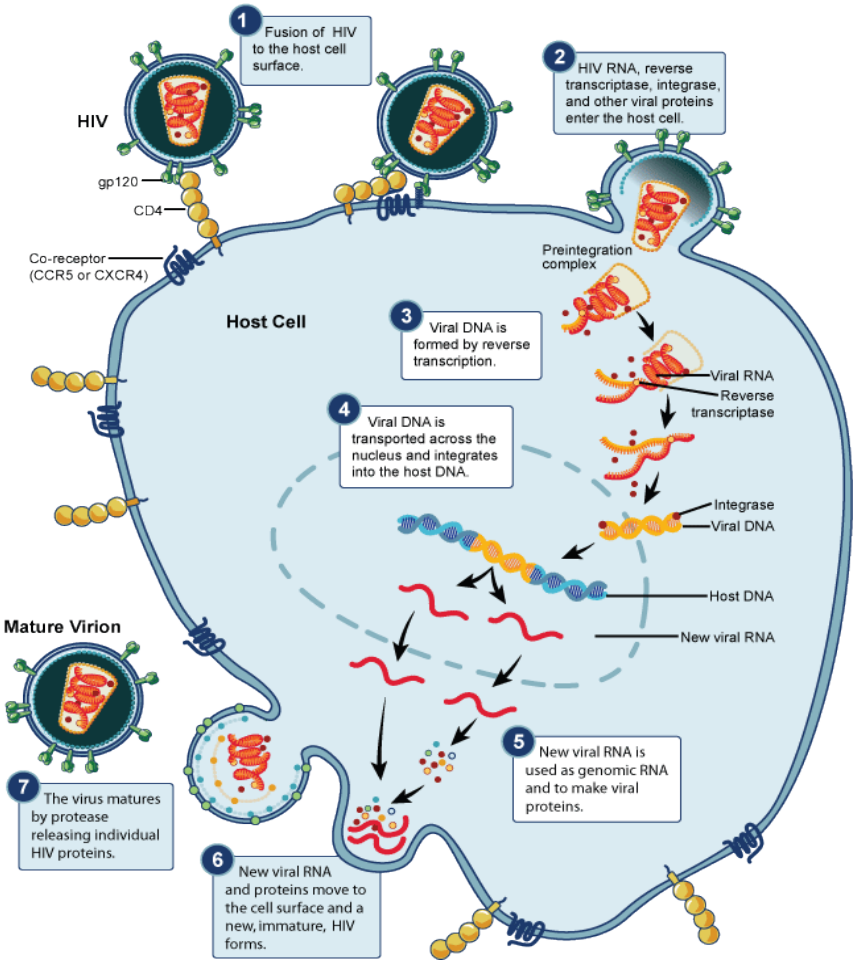

Fig. 1.4 HIV Life Cycle. The life cycle of HIV begins by the binding of the virion to the host cell, followed by the release of the viral contents into the host cell. The viral RNA is then reverse transcribed into DNA and then integrated into the host DNA by integrase. During cell replication, the viral DNA is transcribed and then translated to produce the viral proteins, which moves to the cell membrane where it assembles, together with viral genomic RNA. Assembly is followed by budding of the new, immature virion. Maturation of the virion takes place following cleavage of the polyproteins to produce the structural proteins. http://www.niaid.nih.gov/topics/HIVAIDS/Understanding/Biology/pages/hivreplicationcycle.aspx

1.1.5 HIV Quasispecies

HIV is extremely diverse and this enables the virus to evade the host's immune responses. There are three contributing factors to the vast HIV genetic variability. Firstly, the HIV RT enzyme lacks a proof reading mechanism, which results in approximately one mutation being introduced per genome per replication cycle. Secondly, the virus has a very high replication

rate, generating approximately 10^{10} virions daily in the untreated individual and thirdly, the production of recombinant forms. The combination of all of three factors ensures that each infected individual has a diverse population of HIV, commonly referred to as a quasispecies (Fanales-Belasio et al., 2010, Gianella and Richman, 2010).

1.2 Antiretroviral (ARV) Drugs and Highly Active Antiretroviral Therapy (HAART)

The first reports of AIDS were in 1981, however the causative agent for the disease was unknown and the majority of individuals with AIDS died within two years of becoming infected. This changed in 1983, when HIV-1 was successfully isolated and drug development targeting this retrovirus could begin (Barre-Sinoussi et al., 1983, Gallo et al., 1983, Pomerantz and Horn, 2003). The first US Food and Drug Administration (FDA) approved drug that became available, in 1987, waszidovudine (ZDV). ZDV was administered as a monotherapy and targeted the RT enzyme, which was responsible for reverse transcribing the viral RNA to DNA (Pomerantz and Horn, 2003). Since then many other antiretroviral drugs have been developed, each targeting specific stages in the HIV life cycle (Hartman and Buckheit, 2012).

1.2.1 ARV Drugs

ARV therapy drugs can be classified into six main classes, viz. Nucleoside/Nucleotide Reverse Transcriptase Inhibitors (NRTIs), Non-nucleoside Reverse Transcriptase Inhibitors (NNRTIs), Protease Inhibitors (PIs), Integrase Inhibitors (INIs), small-molecule CCR5 Antagonists and Fusion Inhibitors (Tang and Shafer, 2012).

The first FDA-approved class of ARV drugs to be used was the NRTIs. These drugs target the RT enzyme, which is responsible for the transcription of the viral RNA into dsDNA (for incorporation into the host cell's DNA). The NRTIs are structurally similar to the intracellular deoxynucleotide triphosphates (dNTPs), however they lack the 3'- hydroxyl group that is needed to produce the 5'-3' phosphodiester bond with the incoming 5'-nucleoside triphosphates, thereby leading totermination of DNA synthesis (refer to Figure 1.5a)(Arts and Hazuda, 2012). The NNRTIs also target the RT enzyme, however these inhibitors function by binding to a hydrophobic pocket near the active site of the RT enzyme, causing a spatial conformational change of the active site, impeding RT function (refer to Figure 1.5b) (Arts and Hazuda, 2012, Tang and Shafer, 2012).

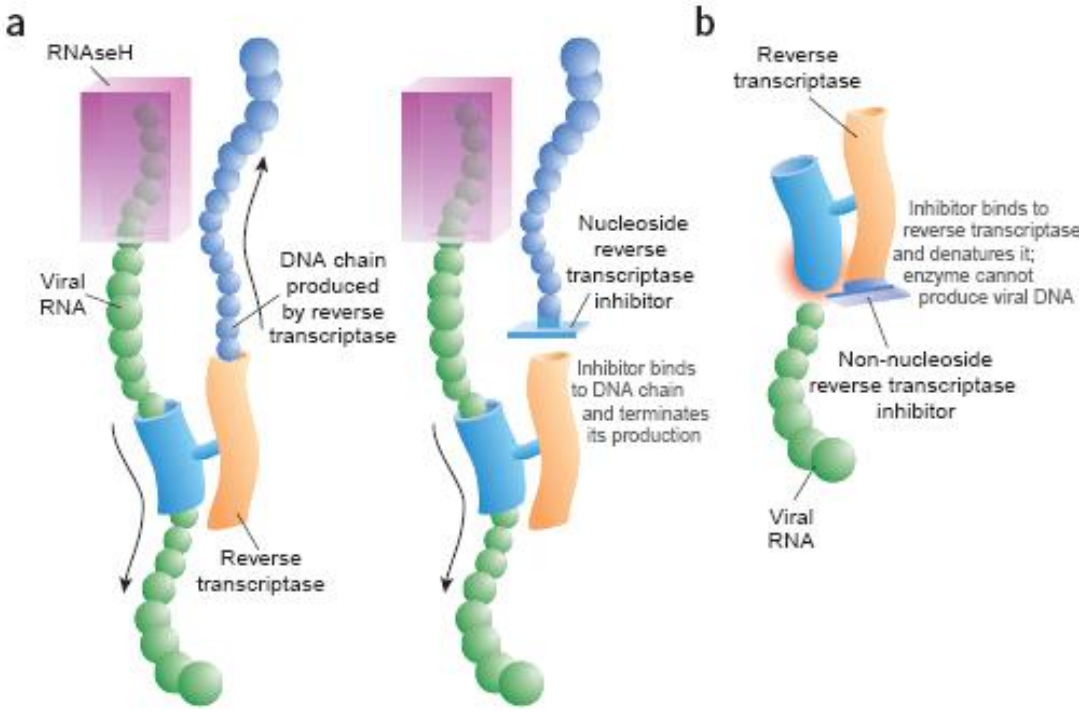

Fig 1.5Mechanism of Action of NRTIs (a) and NNRTIs (b).(a) NRTIs compete with the intracellular dNTPs to be integrated into the DNA chain that is being produced by the RT enzyme. Once the NRTI is incorporated, the RT enzyme is unable to add more dNTPs to the DNA strand as the NRTI lacks the 3'- hydroxyl group needed to produce the 5'-3' phosphodiester bond with the next dNTP.(b) The NNRTI functions by binding near the active site of reverse transcriptase. This results in a conformational change in the active site, thereby inhibiting the activity of the enzyme. Taken from (Pomerantz and Horn, 2003)

Protease inhibitors function by attaching to the protease enzyme's active site, which then inhibits the enzyme from cleaving the virus's gag and gag-polpolyprotein precursors, thereby preventing viral maturation (Cortez and Maldarelli, 2011). Integrase inhibitors target the integrase enzyme, which is responsible for integrating the viral DNA into the host cell's DNA. These inhibitors function by inhibiting the integrase enzyme from forming covalent bonds with the host DNA, which is an essential part of incorporating the viral DNA into the host cell's DNA. This prevents the viral DNA from becoming incorporated into the host DNA, thus preventing the viral proteins from being produced (Hicks and Gulick, 2009). The fusion inhibitors bind to hydrophobic region 1 (HR1) of the viral gp41 protein and prevent HR1 from binding to hydrophobic region 2 (HR2), thereby preventing the formation of the hairpin loop which is essential for the viral cell membrane to fuse with the host cell membrane (Clavel and Hance, 2004, Tang and Shafer, 2012). Small-molecule CCR5 antagonists attach to hydrophobic transmembrane pockets of CCR5. These antagonists do not block the active site of the receptor, but do cause a conformational change in the receptor's second extracellular loop, thereby inhibiting the viral gp120 from binding to the receptor(Arts and Hazuda, 2012).

1.2.2 HAART and Combination Antiretroviral Therapy (cART)

HAART, also referred to as cART, which involves using a combination of ARVs, is currently being used to treat HIV infected individuals. The HAART regimen consists commonly of a combination of three drugs, generally from two different classes (Clavel and Hance, 2004). In South Africa, NRTIs usually make up the backbone of these regimens, as two of the three drugs are generally NRTIs. The main aim of HAART is to reduce HIV-related morbidity and mortality. This combination therapy does not cure HIV, but it does result in suppression of

viral replication, thereby decreasing the patient's viral load to an undetectable level (<400 copies/mm^3) and increasing the CD4 count above baseline. This enables the patient to live a longer and healthier life (DOH, 2004).

1.2.3 HAART in South Africa

ARV therapy has become accessible in many hospitals and clinics in South Africa following the implementation of the Operational Plan for Comprehensive HIV and AIDS Care, Management and Treatment for South Africa in 2003.

The South African National Antiretroviral Treatment Guidelines for 2004, made the following recommendations for first-line and second-line therapy in adults:

Regimen	Drugs
1a	stavudine (d4T), lamivudine (3TC) and efavirenz (EFV)
1b	stavudine (d4T), lamivudine (3TC) and nevirapine (NVP)
2	zidovudine (AZT), didanosine (ddI) and lopinavir/ritonavir (LPV/r)

The recommendations for first-line and second-line therapy for children in 2004 were as follows:

	6 months – 3 years	>3 years old and >10kg
First-line therapy	stavudine (d4T)	stavudine (d4T)
	lamivudine (3TC)	lamivudine (3TC)
	lopinavir/ritonavir (LPV/r)	efavirenz (EFV)
Second-line therapy	zidovudine (AZT)	zidovudine (AZT)
	didanosine (ddI)	didanosine (ddI)
	nevirapine (NVP)	lopinavir/ritonavir (LPV/r)

The NRTIs stavudine (d4T), didanosine (ddI)and, to a lesser degree, ZDV that were included in the above-mentioned treatment regimens have been shown to be correlated with severe metabolic problems, which include lactic acidosis, hepatic steatosis, peripheral neuropathy,

pancreatitis and lipoatrophy (Murphy et al., 2007). Due to these complications, drugs that are linked with less metabolic complications, such as Tenofovir Disoproxil Fumarate (TDF) and Abacavir (ABC), have been made available. Apart from being less toxic, TDF is a preferred drug as it has an extended intracellular half-life and is available as one tablet that is taken once a day(Gallant and Deresinski, 2003). In 2010, the revised South African National Treatment Guidelines included TDF and ABC in the standardised treatment regimens for HIV infected individuals(DOH, 2010).

The standardised national ARV treatment for adults and adolescents in 2010 were as follows:

First-line therapy	All patients needing therapy, including pregnant women	TDF +3TC/FTC +EFV/NVP
	Patients on d4T-based regimen with no side-effects	D4T + 3TC + EFV/NVP
	Contraindication to TDF: renal disease	AZT + 3TC +EFV/NVP
Second-line therapy	Failing on a d4T or AZT-based first-line regimen	TDF + 3TC/FTC + LPV/r
	Failing on a TDF-based first-line regimen	AZT + 3TC + LPV/r
Salvage therapy	Failing any second-line therapy	Specialist referral

The standardised national ARV treatment regimens for children in 2010 were as follows:-

First-line therapy	All infants and children under 3 years	ABC + 3TC + LPV/r
	Children 3 years and over	ABC + 3TC + EFV
	Currently on d4T-based regimen with no side effects	Can continue
Second-line therapy	Children above 3 years Failed ABC + 3TC + EFV	AZT + ddl + LPV/r
	Failed on AZT or ddl-based regimen	ABC + 3TC + LPV/r
	Failed on LPV-based regimen	Refer (Specialist advice necessary and/or hospital referral)
	Infants under 3 years failing first-line therapy	Refer (Specialist advice necessary and/or hospital referral)
Salvage therapy	Failing any second-line therapy	Specialist referral

However, the success of these treatment regimens have been threatened by the emergence of mutations that cause resistance to the drugs (Clavel and Hance, 2004).

1.3 ARV Drug Resistance

The possible explanations for HIV drug treatment failure include patient adherence problems (due to the adverse side effects of the drugs, complex dosing schedules, or lack of counselling on the importance of taking the prescribed medication timeously), as well as pharmacologic issues that are associated with the absorption, metabolism, activation and interactions of the drugs. However one of the most important reasons for drug treatment failure is the emergence of drug resistance mutations (Sen et al., 2006). ZDV was the first ARV drug for which drug resistance mutations were reported and the first report describing this was published in 1989 (Larder et al., 1989). Subsequently, there have been numerous articles illustrating the development of resistance to ARV drugs (Clavel and Hance, 2004). The development of drug resistant mutations is of major concern as resistance to a particular drug can cause cross-resistance to drugs within the same class or to drugs in other classes, which can limit further treatment options. Resistance mutations can also be passed on to newly infected individuals that are treatment-naïve (Little et al., 2002, Wensing and Boucher, 2003, Yerly et al., 2001). In addition, drug-resistant mutations have been detected in the HIV minority variants and these have been found to be associated with poor treatment response in ARV-naive individuals (Gianella and Richman, 2010, Metzner et al., 2005, Johnson et al., 2008). The minority variants are viruses that are present in less than 20% of the total viral population of an individual.

1.4 K65R Resistance Mutation

Tenofovir most frequently selects for one key mutation, viz. the K65R mutation (Gallant and Deresinski, 2003). However, there have been studies that show that TDF may also select for another mutation, viz. the K70E mutation, although if both the K65R and K70E mutations are found in plasma, they do not occur together on a single viral genome (Sluis-Cremer et al., 2007). The K65R mutation is a single-point mutation that occurs on codon 65 in the HIV-1 RT enzyme, which results in a lysine (K) to arginine (R) substitution (Parikh et al., 2006). The lysine at this position is responsible for ensuring correct positioning of the incoming dNTP into the newly synthesised viral DNA strand by interacting with its γ phosphate. However, the K65R mutant is thought to cause NRTI resistance by changing this positioning, thereby enabling the natural dNTP incorporation to be favoured over the NRTI (Parikh et al., 2006). It has been shown that while the K65R mutant causes a slower incorporation rate for the natural dNTP, the incorporation rate of the NRTI is even slower than the natural dNTP (Sluis-Cremer et al., 2007). This was confirmed by Das *et al*. (2009) who have shown that the K65R mutant reduced the dATP incorporation rate by 4.5-fold and the NRTI incorporation rate by >20-fold, when compared to the wild-type (Das et al., 2009).

1.4.1 K65R Occurs Preferentially in HIV-1 Subtype C

The K65R mutation emerges more commonly in subtype C viruses than in subtype B viruses. This could occur because of the difference in nucleotide sequence between the two subtypes at codons 64, 65 and 66 (refer to Figure 1.6) (Coutsinos et al., 2009, Brenner et al., 2006). The subtype C viruses have a homopolymeric adenine stretch at codons 64 and 65, and since the RT enzyme experiences difficulty in synthesizing these adenine stretches, the enzyme undergoes pausing at the end of the adenine stretch. These pause sites could lead to incorrect

alignment of the template and the primer, causing the AAG to AGG point mutation at codon 65 (Santoro and Perno, 2013, Coutsinos et al., 2009).Subtype B, on the other hand, has a homopolymeric adenine stretch at codons 65 and 66 and it therefore frequently experiences pausing at codon 67, resulting in the D67N mutation (Santoro and Perno, 2013).

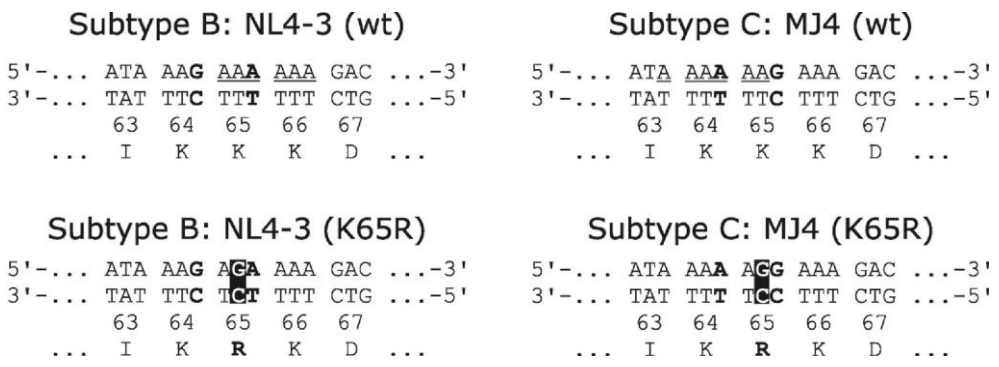

Fig. 1.6 Sequence Difference in Subtype C and Subtype B HIV. This diagram shows the difference in the sequence (that extends across codons 63 to 67) of subtype C and subtype B HIV. The bases that are different between the subtypes appear in bold font and the highlighted bases indicate the site at which the K65R point mutation occurs. The homopolymeric adenine stretches in each sequence is underscored, ending at codon 65 in subtype C and codon 66 in subtype B. Taken from (Coutsinos et al., 2009)

1.4.2 The Antagonistic Relationship of K65R and Thymidine Analog Mutations (TAMs)

Apart from TDF, the K65R mutation can also develop following treatment with ABC, ddI or d4T and it is of particular concern as it causes decreased susceptibility to all the NRTIs, except for ZDV (Das et al., 2009). The primary mutations that result in resistance to ZDV are called TAMs. There are 2 patterns of TAMs, viz. TAM-1 (which is a combination of the M41L, L210W and T215Y mutations) and TAM-2 (which consists of a combination of the D67N, K70R, T215F and the K219Q mutations).

Parikh *et al.* (2006) showed that there was a bidirectional antagonism of K65R and TAMs. In this study HIV-1 recombinants were created with the K65R mutation in a TAM-1 background and also separately in a TAM-2 background. The results showed that when these mutant constructs were exposed to ZDV, the K65R mutation caused a decrease in the TAM-mediated resistance to ZDV (in both backgrounds) from >50-fold to <2.5-fold, when compared to HIV-1 mutants that were carrying the TAMS but no K65R. In addition, it was shown that when exposed to the drug selective pressure of TDF, the TAMs in these mutant constructs (containing K65R in either the TAM-1 or TAM-2 background) reduced K65R-mediated resistance to TDF. In addition, it has been found that TDF maintains partial antiviral activity when a few of the TAMs are present (Trivedi et al., 2008). The K65R mutation developed frequently in patients that were failing ARV treatment that did not include ZDV, and less frequently in patients that were failing treatment that did include ZDV (Parikh et al., 2006). The K65R mutation causes a decrease in the excision rate of ZDV, which counteracts the effects of TAMs, thereby restoring susceptibility to ZDV (Das et al., 2009). Interestingly, the K65R mutation has been shown to cause a diminished replicative fitness in viruses carrying this mutation (Weber et al., 2005). This could also be the reason why the K65R mutation is less favoured than TAMs. Another study revealed that combining TDF with other K65R-inducing drugs should be avoided in settings in which TAMs are less frequent, eg. following commencement of TDF first-line therapy or following prolonged treatment interruptions, as it may increase the risk of the development of the K65R mutation (von Wyl et al., 2008).

1.4.3 The Presence of K65R in the Minority Variants

A study conducted by Svarovskaia *et al.* (2007) suggests that poor response to TDF treatment may be partly due to the presence of K65R in the minor viral population (Svarovskaia et al., 2007). Minority drug resistant variants are variants that are present in less than 20% of the viral population in an individual. Consequently, these minority variants are not detected by standard genotyping techniques, which have a limit of detection of 20%. Studies have shown that the K65R mutation that is present in the minor viral population can be transmitted to treatment-naive patients and could threaten the success of TDF-containing first-line therapy (Bansal et al., 2011). Therefore, to ensure that an effective ARV regimen is selected for HIV-infected individuals, there is a need to introduce an effective and sensitive test to screen for the K65R mutation prior to starting a TDF-containing regimen.

1.4.4 K65R in South Africa

In Sub-Saharan Africa and South Africa, in particular, there have been studies that identified the presence of K65R in patients failing a TDF-containing treatment regimen, using population-based sequencing. However, some studies have produced conflicting results (Hoffmann et al., 2013, Sunpath et al., 2012, Van Zyl et al., 2013, Hamers et al., 2012).

A study performed in Durban, South Africa found that 22 of 33 (69.7%) of patients carried the K65R mutation in subtype C infected patients that were failing a TDF-containing first-line regimen. The study also found that the K65R mutation was present in 1 of 2 patients that were failing a d4T-containing regimen. Despite the small sample size used in this study, the high prevalence (69.5%) of the K65R mutation that was reported may be an indication of a more rapid in-vivo selection of the K65R mutation or the presence of transmitted drug

resistance (Sunpath et al., 2012).In a recent study by Van Zyl *et al.* (2013), the resistance mutations in plasma samples from ARV treated patients that were collected during 2006 to 2012 in South Africa were analysed. The results showed that the K65R mutation was detected in 70 of 153 (45.8%)patients that failed a regimen containing TDF, 3TC and either EFV or NVP(Van Zyl et al., 2013). Another study by Hamers *et al.* (2012), which was conducted in six Sub-Saharan African countries in non-B subtypes, has shown that 0 of 71 (0%) of patients carried the K65R mutation after failing a ZDV-containing regimen, 3 of 20 (15%) of the study participants had the K65R mutation after failing a d4T-containing regimen and 13 of 47 (27.7%) of the study participants carried the K65R mutation after failing a TDF-containing treatment regimen (Hamers et al., 2012).

In contrast to the high prevalence of the K65R mutation reported by Sunpath *et al.* (2012), a study by Hoffmann *et al.* (2013), using a similar sample size (i.e 40), has shown that the K65R mutation was present in 12% of patients that had failed a TDF-based treatment regimen (Hoffmann et al., 2013).

Interestingly, these studies highlight the undeniable increase in the presence of the K65R mutation following the 2010 change in the recommended treatment regimen. Prior to the change in the treatment regimen, patients were not exposed to TDF and the K65R mutation was detected at lower prevalence rates of 4% and 9% as reported by Wallis *et al.* (2010) and Orrell *et al.*(2009), respectively (Orrell et al., 2009, Wallis et al., 2010). Similarly, another study by Marconi *et al.* (2008) reported that the K65R mutation was present in 2.6% of subtype C infected patients that were failing first-line ARV therapy. Furthermore, given that the K65R mutation may be present in the minor viral population a more sensitive test than population-based sequencing needs to be used.

1.5 L74V Resistance Mutation

The L74V mutation commonly arises following exposure to ddI and ABC. In addition, this mutation has also been identified as a predictor of impaired response to TDF (Turner et al., 2004, Wirden et al., 2009, Masquelier et al., 2004).

The L74V mutation results from a leucine (L) to Valine (V) substitution on codon 74 in the HIV-1 RT enzyme(Shah et al., 2000). The mechanism by which L74V confers resistance is by preferentially incorporating the natural dNTP over the NRTI (Wainberg et al., 2005).

1.5.1 L74V and M184V

The presence of the L74V mutation by itself causes low level resistance to ABC. However, this level of resistance increases when M184V, K65R or Y115F coexist with the L74V mutation (Turner et al., 2004). Individually, the L74V and M184V mutations causes reduced viral fitness, diminished DNA synthesis by RT and increased susceptibility to ZDV. However, these outcomes are further intensified when these two mutations coexist (Wainberg et al., 2005, Sharma and Crumpacker, 1999). Diallo *et al.* (2003) showed that reduced RNA primer usage caused by the presence of the L74V or the M184V mutation could account for the poor viral replication capacity of viruses carrying these mutations. The commencement of RNA-primed minus- and plus-strand DNA synthesis is associated with pause sites, which requires the RT enzyme to repeatedly dissociate from the template. The presence of the L74V or M184V mutation has been shown to be associated with reduced rates of dissociation from these pause sites, which results in a decrease in the rate of DNA synthesis. When both these mutations are present, there is an increase in this effect, thereby contributing to reduced viral replication capacity (Diallo et al., 2003).

1.5.2 L74V and TAMs

HIV has 2 mechanisms of resistance to NRTIS, viz. the discriminatory mechanism and the ATP-mediated excision mechanism. The first mechanism involves the development of mutations (eg. the L74Vmutation) that enables the RT enzyme to favour the incorporation of the natural dNTPs over the NRTIs, thereby preventing chain termination. The second mechanism of resistance involves the development of TAMs, which leads to ATP-mediated excision of the chain-terminating NRTI. The presence of the TAMs enables ATP to bind to a site next to the incorporated NRTI, where the ATP is able to break the phosphodiester bond that attaches the NRTI to the DNA. This results in the removal of the NRTI, thereby allowing reverse transcription to continue (Clavel and Hance, 2004).

The L74V mutation can cause an increase in the susceptibility to ZDV (Wainberg et al., 2005). ZDV is an NRTI, so its mechanism of action (as discussed in 1.2.1) is through inhibition of RT by binding to the newly synthesized viral DNA, thereby causing termination of DNA synthesis (Clavel and Hance, 2004). Frankel *et al.*(2005) showed that the presence of the L74V mutation resulted in a decrease in ATP-dependent excision of ZDV-monophosphate from newly produced DNA, which could possibly explain why L74V increases sensitivity to ZDV, even in the presence of TAMs(Frankel et al., 2005).

As the mechanism of action of L74V is similar to K65R, the presence of TAMs appears to decrease or inhibit the emergence of L74V. It has been shown that the L74V mutation hardly ever occurs in patients that are failing ABC-containing ARV therapy that also included ZDV, as compared to those ABC-containing regimens that did not include ZDV. A possible reason for this could be that as the L74V mutation causes increased susceptibility to ZDV, there is reduced selection of viruses expressing this mutation (Wainberg et al., 2005).

1.5.3 L74V in South Africa

According to Marconi *et al.* (2008), the L74V mutation was found in 1.7% of the patients that were failing their first-line ARV therapy, showing that there was a very low occurrence of the L74V mutation in this study population. ABC was not included in the adult treatment guidelines at that time and therefore was rarely used. It was usually used as part of the second-line regimen in paediatric patients when a fridge was not available for the storage of the ddI syrup. However, since the implementation of the newer guidelines (2010 onwards), ABC has been introduced in the first and second-line regimens for paediatric patients. This could therefore lead to an increase in the occurrence of the L74V mutation, particularly in paediatric patients. In a recent study by Van Zyl *et al.* (2013), it was reported that the L74VI mutation was prevalent in 13 of 153 (8.5%) patients receiving a TDF-containing regimen and 30 of 54 (55.6%) paediatric patients receiving an ABC-containing regimen. Another study carried out in paediatric patients that were failing ARV therapy in KwaZulu-Natal, South Africa, reported that the prevalence of the L74VI mutation was 5.5% in patients on a NNRTI-based regimen and 6.3% in patients on a PI-based regimen (Pillay et al., 2014).

1.6 K65R/L74V Double Mutants

The K65R and L74V mutations hardly ever arise simultaneously in the same viral population due to the poor replicative capacity associated with this double mutant.

Deval *et al.* (2004) compared the replicative capacity of wild-type, K65R, L74V and K65R/L74V viruses and they found that the K65R/L74V viruses replicated at a significantly slower rate than the wild-type, K65R or L74V viruses. These results suggest that the presence of the K65R/L74V confers diminished replicative fitness to viruses carrying this

mutation and is possibly the reason why these mutations do not commonly occur on the same viral genome (Deval et al., 2004). As a result of the poor replicative capacity of viruses that have the K65R mutation, as well as the K65R/M184V and K65R/TAM mutual bidirectional antagonism, conventional genotyping methods may be unable to detect the presence of the K65R mutation if present in the minor viral population, as discussed in 1.4.3. A publication by Henry *et al.*(2006) has shown the simultaneous occurrence of these two mutations on the same HIV-1 genome. The results of the study showed that even in the presence of this double mutant, the viral load was still high (Henry et al., 2006). These results are in contrast to the study by Deval *et al.* (2004), which was carried out in vitro. A possible explanation for the contrasting results could be the presence of potential compensatory mutations, in vivo.

It has also been found that, with the use of single-genome sequencing, the presence of the L74V mutation has been shown to be linked to a "hidden" K65R mutation that is undetectable by standard genotyping (Waters et al., 2008).

1.7 Methods to Detect ARV Resistance

There are 2 methods for detection of ARV resistance, i.e phenotyping and genotyping. Phenotypic resistance testing involves measuring how susceptible the virus is to different concentrations of drugs, whilst genotypic resistance testing is used to determine the presence of resistance mutations (Harrigan and Cote, 2000).

The most common genotyping method that is used for detection of resistance mutations is population-based sequencing (Sen et al., 2006). The advantage of using this method of detection of resistance mutations is that it analyses the complete sequence of the gene that is amplified and provides a list of mutations that could cause resistance to the specific drugs

(Cortez and Maldarelli, 2011). However, the problem with this method is that it has a limit of detection of ≥20% of the viral population. As a result, mutations that are present in the minor viral population (<20%) are not being detected (Hauser et al., 2009). Numerous studies have shown that many of the viruses that are present in the minority in the viral population are being missed by conventional genotyping methods (Leitner et al., 1993, Schuurman et al., 2002, Gianella and Richman, 2010). It is therefore necessary to use more sensitive methods for the detection of ARV resistance.

Many different technologies have been developed to detect resistance mutations in the minor HIV viral population, including next generation sequencing, real-time allele-specific polymerase chain reaction (ASPCR), oligonucleotide ligation-based assays (OLA), a Ty1/HIV-1 RT hybrid system (TyHRT), single-genome sequencing (SGS), and the lineprobe assay (LiPA). A study comparing these tests concluded that ASPCR and Ty1HRT had a limit of detection as low as 0.1 to 0.4% (Halvas et al., 2006).Ty1HRT test is a sensitive phenotyping test that is used to detect the drug-resistant RTs present in a viral population. However, the disadvantage of using this method is that it is used specifically for RT, and drug resistance in protease, integrase, envelope or other viral targets cannot be established using this test (Halvas et al., 2006, Nissley et al., 2005).

1.7.1 ASPCR

The initial report describing the application of an allele-specific nested Polymerase Chain Reaction (PCR) for the identification of resistance mutations in HIV-1 was in 1991. Subsequently, real-time PCR technology has been applied to ASPCR, greatly increasing the sensitivity of this assay and enabling this method to be used to quantify PCR products. ASPCR is currently a sensitive and reproducible assay that is used to detect drug-resistant

mutations that are present in the minority variants of a viral population (Paredes et al., 2007, Rowley et al., 2008, Metzner et al., 2005). This method has the advantage of being less laborious and time-consuming than other methods used for the same intention (Paredes et al., 2007). Although ASPCR has been shown to be a highly sensitive assay, the disadvantage of using this assay is that each assay can only be used to analyse a single mutation. In addition, polymorphisms that occur in the primer binding sites (near the 3' end) can hinder the binding of the primer, thereby producing false negatives (Halvas et al., 2006).

Allele-specific PCR involves preparing two separate PCR reactions, viz. a mutant-specific reaction and a non-specific reaction. For the mutant-specific reaction, a mutant-specific primer (i.e Sp in Figure 1.7) is designed, which contains the target mutant sequence at the 3' end, which will bind to the drug-resistant sequence. In addition, it also contains an intentional mismatch at the -1 to -3 positions to further reduce the possibility of non-specific amplification of the mutant-specific primer occurring, thereby increasing the specificity of the reaction. The non-specific reaction involves the design of a primer that is identical to the specific primer, however, the sequence stops just before the target mutant sequence and lacks the intentional mismatch (i.e Ns in Figure 1.7). Each of these reactions contains a common antiparallel primer (i.e CA in Figure 1.7). The two reactions are prepared in the same way, except that each reaction has their own primers (Paredes et al., 2007).

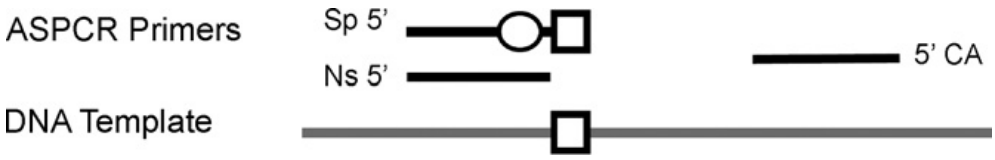

Fig.1.7 Principle of ASPCR. ASPCR involves the use of 2 reactions, viz. a specific reaction and a non-specific reaction. For the specific reaction, a specific primer (Sp) is designed, which contains the target mutant sequence at the 3' end (represented by the square). The Sp also contains an intentional mismatch (represented by the circle) at the -1 to -3 positions. The non-specific reaction involves the design of a non-specific primer (Ns), which is the same as Sp with the exception that it ends before the target sequence and it lacks an intentional mismatch. Each of the reactions uses a common antiparallel primer (CA). Taken from (Paredes et al., 2007)

1.8 Real-Time PCR

Real-time PCR is a reliable and sensitive method to amplify nucleic acids. This amplification method allows for the simultaneous detection and quantification of PCR products as they are generated at each cycle of the PCR program (Arya et al., 2005).

In a typical PCR reaction, each reaction cycle involves three important steps, viz. denaturation of the dsDNA, annealing of the primer to the DNA template and extension of the DNA template. Therefore, after each PCR reaction cycle, each DNA molecule that was present at the beginning of the cycle is duplicated. Real-time PCR allows this process to be monitored as it occurs and displays the information as an amplification curve. This amplification curve consists of three phases, i.e the initial lag phase, the exponential (log-linear) phase and the final plateau phase as shown in Figure 1.8. The initial lag phase, or background phase, refers to the number of cycles that passes before the fluorescent signal from the PCR product can be detected above the background fluorescence of the detection system that is being used. The cycle number at which the PCR product's fluorescent signal rises above the background signal (thus allowing the PCR product's fluorescence to be initially visible in the data) is referred to as the threshold cycle (Ct) or crossing point (CP).

Following the lag phase is the exponential phase, which displays the fluorescence of the PCR product as it amplifies at each cycle, until the plateau phase is reached. Typically, in the exponential phase, each PCR product that is present is duplicated after each PCR cycle, resulting in a rapid increase in the PCR products. The plateau phase begins when the rate of PCR product amplification slows down, due to depletion of reaction components, until no more PCR product is being generated (Arya et al., 2005).

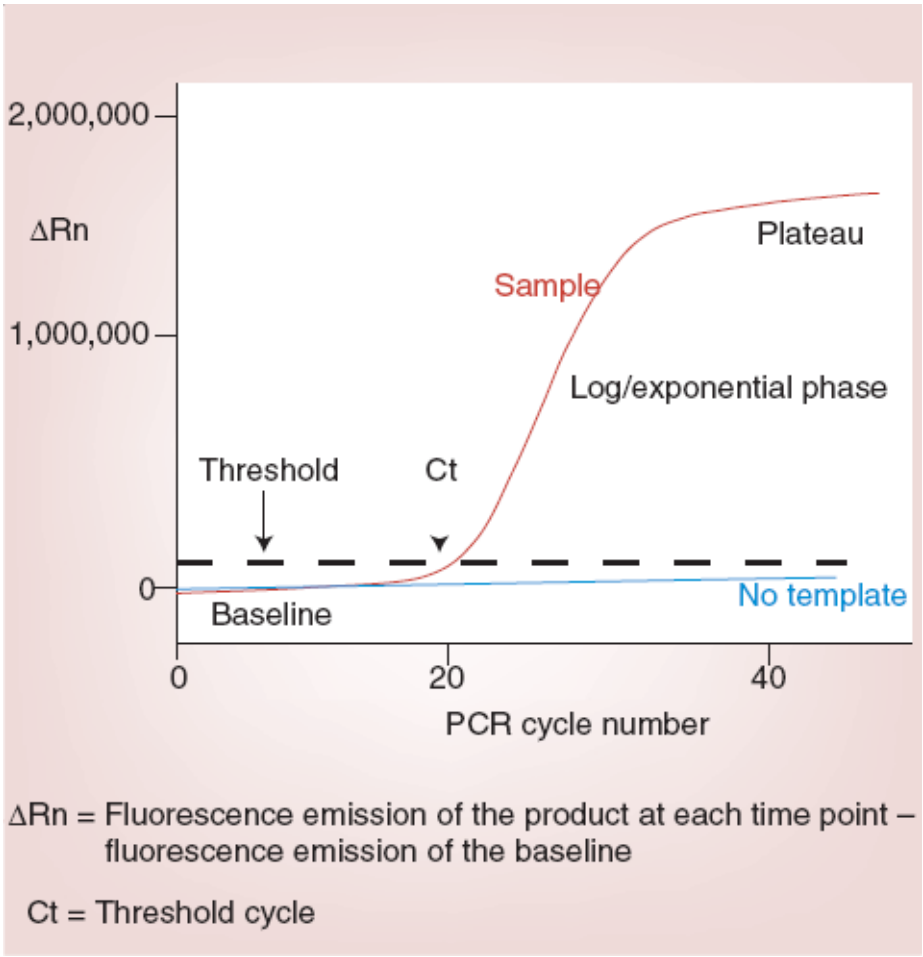

Fig.1.8 Amplification Phases of an Amplification Curve in Real-time PCR. This diagram presents a typical amplification curve produced by real-time PCR. The amplification curve is made up of three phases, viz. the lag-phase (the phase during which the fluorescent signal from the PCR product cannot be detected above background fluorescence), the exponential phase (i.e the phase that begins when the fluorescence from the PCR product rises above the background fluorescence and continues to increase) and the plateau phase (which is the phase at which the increase in PCR products decreases and then finally stops or reaches a plateau). The threshold cycle (Ct) is the cycle number at which the fluorescence from the sample can be detected above background fluorescence. Taken from (Arya et al., 2005)

1.8.1 Detection Chemistries for Real-time PCR

There are two types of detection chemistries for real-time PCR, viz. the non-probe based and the probe-based chemistries.

The probe-based chemistries include hydrolysis probes, hybridisation probes, molecular beacons and scorpion probes. Probe-based chemistries involve the design and development of specific probes which will target only the regions of interest. These probes only fluoresce when bound to the specific target sequence on the template. The use of probes has many advantages, eg. it increases the specificity of the reaction, since there is no non-specific amplification caused by mispriming or primer-dimer formation, and each probe can be labelled with different reporter dyes which enables them to be used in a multiplex PCR. However, the disadvantage of using probes is that it is requires the careful design of each probe that is required for each experiment to ensure that the probes are able to attach and function optimally, and this process is both time-consuming and costly.

The other type of chemistry is the non-probe based chemistry, which includes SYBR Green I, PicoGreen, RiboGreen, EvaGreen, SYTO dyes and BEBO (Reiter and Pfaffl, 2011). SYBR Green I is a DNA-intercalating agent that fluoresces only when bound to dsDNA (as shown in Figure 1.9)and it is the most commonly used non-probe based chemistry (Bustin and Mueller, 2005).

The disadvantage of using the SYBR Green I method (as with all the non-probe based chemistries) is that it will bind non-specifically to all dsDNA (including the target PCR products, non-specific PCR products and primer-dimers) that are generated during the PCR process. However, the advantage of using this method of detection is that it is a more cost-effective and simple means of DNA detection than using probes, as it does not require the

design and development of different probes for the detection of specific sequences (Arya et al., 2005).

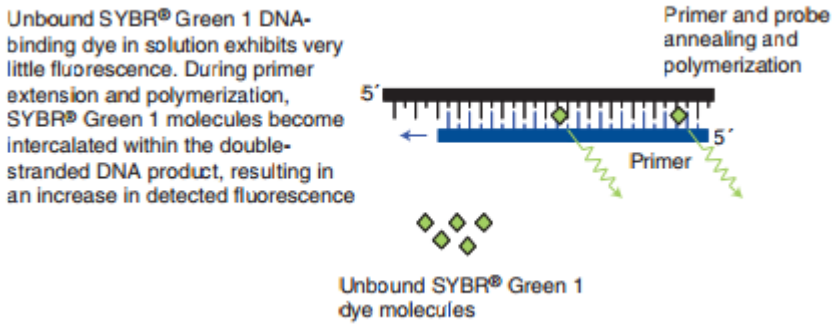

Fig.1.9 SYBR Green I. This diagram illustrates that there is very little fluorescence when unbound SYBR Green I is present in the reaction mix. This changes during the annealing and extension step of the PCR reaction, when SYBR Green I becomes intercalated in the double stranded DNA, resulting in an increase in fluorescence from SYBR Green I. Taken from (Arya et al., 2005)

1.8.2 Quantification Methods using Real-time PCR

There are two main quantification methods in real-time PCR. These are the absolute quantification method (or standard curve method) and the relative quantification method.

Relative quantification is usually used in gene expression studies to compare changes in the expression of a particular gene (or target gene) compared to a reference gene. The reference gene is usually a gene that has the same copy number in all the samples and would therefore be an endogenous control, allowing for normalization of sample-to-sample variation. The results from a relative quantification are shown as a ratio of the target gene over the reference gene for each sample.

The absolute quantification method (refer to Figure 1.10) involves the use of a standard curve, which is produced by amplifying a serially diluted standard, with a known concentration. The standard curve is produced by plotting the concentration of each standard against the Ct (at which the standard was first detected). This standard curve is then used to calculate the concentration of the unknown samples that are amplified by using the Ct of the unknown sample to determine what the concentration would be at that cycle number. Therefore, this method of quantification allows for the calculation of the exact concentration of each target in the sample (Wong and Medrano, 2005, Hoffmann-La Roche)

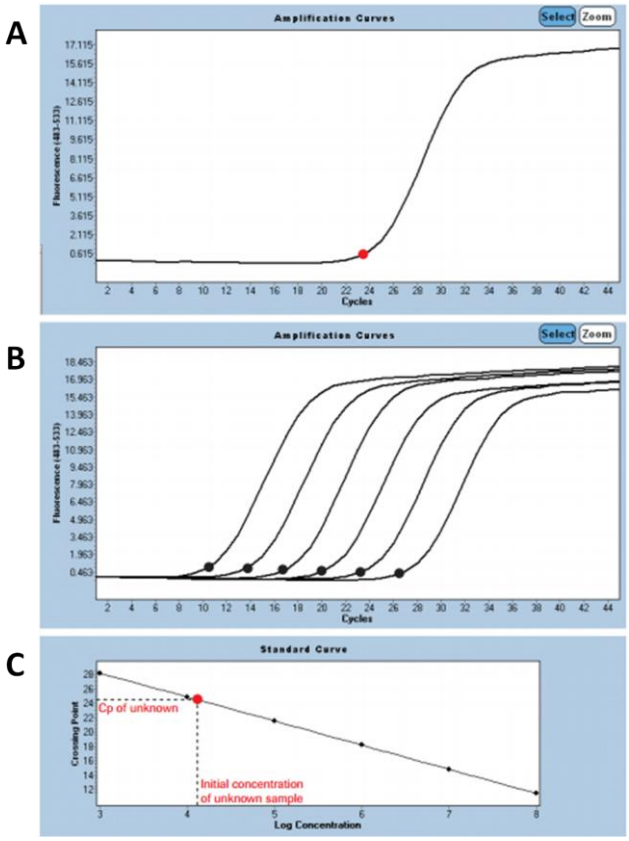

Fig 1.10 Absolute Quantification. The standard curve is produced by serially diluting a standard with a known concentration and amplifying the dilutions on the Lightcycler instrument. The amplication curves and the standard curve that is produced can be seen in B and C, respectively. The concentration of the unknown (A) can be calculated using the standard curve by using the crossing point of the unknown to determine what the concentration would be (as seen in C). Taken from (Hoffmann-La Roche)

1.9 Project Aims and Objectives

The aim of this project was to determine the prevalence of the K65R and L74V resistance mutations in minor variants in HIV-1 subtype C infected patients using ASPCR. ASPCR was used as it is a sensitive and reproducible method that has the added advantage of being less time consuming and laborious than other assays used to detect resistance mutations in minor variants of HIV. This assay could have many applications in the HIV drug resistance, viz. it could allow for the early and sensitive detection of the K65R and L74V resistance mutations, improved detection of transmitted K65R and L74V drug-resistant mutations and a better understanding of drug resistance mutations following prophylactic treatment regimens, eg TDF prophylactic gel.

The Objectives of this project was:

- To optimise a Real-Time PCR assay to detect the K65R and L74V mutations.
- To determine the prevalence of the K65R and L74V mutations in a subset of the South African Resistance Cohort Study (SARCS) cohort. The patients from this cohort were patients that were failing first-line HAART that did not include TDF or ABC.

CHAPTER 2

Materials and Methods

2.1 Study Population

Plasma samples were obtained retrospectively from participants enrolled in the SARCS. The patients that were recruited for the SARCS were failing their first-line HAART that did not include TDF or ABC. All patients were on their first HAART regimen that included either d4T, 3TC and EFV/NVP or AZT, 3TC and EFV/NVP. A subset of the SARCS cohort was used for this study. The original cohort included 115 patients, however only 101 of these samples were available for this study. Table 2.1 contains patient characteristics of this study. The samples had been processed within 24 hours of collection and the plasma was stored at -80°C.Ethical approval for the use of the stored plasma was obtained from the UKZN Biomedical Research Ethics Committee (Reference No: BE078/09).

Table 2.1 Patient Characteristics of this Study Population.

Characteristic	Patients (n=101)
Age, mean years ±SD	37.1 ±9.4
CD4 Cell Count, Median cells/mm^3 (IQR)	155 (104.8 – 230.5)
VL Ranges	
1 000 - 10 000	31
10 000 - 100 000	36
100 000 - 1 000 000	20
1 000 000 - 10 000 000	1
VL unavailable	13
***Duration of ART prior to enrolment, median months (IQR)**	10.8 (6.7 – 18.6)
***Reported >95% treatment adherence**	82.7%
***Treatment Regimen at Time of Enrollment**	
D4T, 3TC and EFV/NVP	53.9%
AZT, 3TC and EFV/NVP	37.4%
2NRTI plus LPV/r	4.4%
Other	4.4%

* This information was obtained from Marconi *et al.* (2008)

2.2 RNA Extraction

RNA was extracted from the stored plasma samples using the QIAamp Viral RNA Mini Kit (Qiagen; Venlo, Netherlands). The volume of plasma used for this step was dependent on the viral load of the sample. If the viral load of the sample was less than 5 000 copies/mL, then 1000 µL of plasma was centrifuged, however, for samples with viral loads ≥5 000 copies/mL, 500 µL of plasma was centrifuged. The plasma was centrifuged at 25,000 x g at 4°C for 1 hour in a refrigerated Jouan MR22i centrifuge (Scientific Group, South Africa). The above step resulted in the formation of a pellet at the bottom of the microcentrifuge tube. The supernatant was then carefully removed, leaving behind 140 µL of the supernatant and the pellet. During this process, caution was taken not to dislodge the pellet containing the important viral material. Viral RNA was thereafter extracted using the QIAamp Viral RNA Mini Kit, according to the manufacturer's instructions. The basic principle underlying this procedure involved first resuspending the pellet in 560 µL of a strong denaturing buffer, which lyses the sample, inactivates RNases and facilitates the isolation of intact RNA. Thereafter, the RNA was combined with absolute ethanol to provide proper binding conditions and mixed thoroughly to facilitate efficient binding of the RNA to the QIAamp membrane. The sample was then transferred to the QIAamp Mini spin columns and centrifuged. Following this step, the RNA which was bound to the membrane, was washed during two wash steps and finally eluted in 50µL elution buffer. The extracted RNA was then used to prepare cDNA and the remainder of the RNA was stored at -80°C.

2.3 Reverse Transcription and Amplification of Samples

Extracted RNA was reverse transcribed and amplified in the same reaction using the Superscript™ III One-Step RT-PCR System with Platinum®*Taq* High Fidelity kit

(Invitrogen; California, USA), according to the manufacturer's instructions. Basically, this method involves the use of two key components, viz. the Superscript RT/Platinum Taq High Fidelity Enzyme Mix(which enhances RT-PCR yields and fidelity) and the 2X Reaction Mix, which contains Magnesium (Mg^{2+}), dNTP's, and stabilizers. The primers that were used in the PCR were forward primer AV150 (5'-GTGGAAAGGAAGGACACCAAATGAAAG-3') and reverse primer 3753L20 (5'-GCTTGCCAATAATCTGTCCACCA-3') to obtain a 1736bp RT-PCR product. The optimisation of the one-step RT-PCR is described below (2.3.1).

2.3.1 Optimisation of the RT-PCR Reaction Mix

The reagent components were used as per the manufacturer's instructions, however, to determine if additional Magnesium Sulfate ($MgSO_4$) was required, a $MgSO_4$ titration was performed. This was done by adjusting the $MgSO_4$ concentration in each of 3 tubes, while keeping the remaining reagent concentrations the same. The first tube contained no additional $MgSO_4$ (final concentration 1.2mM), the second tube contained 1 µL of 5mM $MgSO_4$ (final concentration 1.4mM) and the last tube contained 2 µL of 5mM $MgSO_4$ (final concentration 1.6 mM). The water was adjusted accordingly for each reaction to obtain a final volume of 25 µL. The reaction mix for each can be seen in Table 2.2.

Table 2.2 Reaction Mix for $MgSO_4$ Titration.

	No additional $MgSO_4$	1 µL $MgSO_4$	2 µL $MgSO_4$
2x Reaction Mix (with 0.4 mM of each dNTP, 2.4 mM $MgSO_4$)	12.5 µL	12.5 µL	12.5 µL
Final $MgSO_4$ Concentration [ ]	[1.2 mM]	[1.4 mM]	[1.6 mM]
Forward primer AV150 (10 pmol/µL)	0.5 µL	0.5 µL	0.5 µL
Final Concentration [ ]	[0.2 µM]	[0.2 µM]	[0.2 µM]
Reverse primer 3753L20 (10 pmol/µL)	0.5 µL	0.5 µL	0.5 µL
Final Concentration [ ]	[0.2 µM]	[0.2 µM]	[0.2 µM]
Superscript™ III RT/Platinum® *Taq*HiFi Enzyme Mix	0.5 µL	0.5 µL	0.5 µL
Autoclaved distilled water	3.5 µL	2.5 µL	1.5 µL
5 mM $MgSO_4$	-	1 µL	2 µL
RNA	7.5 µL	7.5 µL	7.5 µL
Total Volume	**25 µL**	**25 µL**	**25 µL**

The prepared reaction mixes were run on a thermal cycler under the conditions described in Table 2.3.

Table 2.3 Cycling Conditions for MgSO4 Titration.

	Temperature	Time	Number of Cycles
cDNA Synthesis	55°C	25 min	1
Pre-denaturation	94°C	3 min	1
Denaturation	94°C	40 sec	
Annealing	60°C	40 sec	40
Extension	68°C	2 min	
Final Extension	68°C	5 min	1
	8°C	Hold	-

2.3.2 Optimisation of the Cycling Conditions

To optimise the cycling conditions, the RT-PCR was prepared using the standard $MgSO_4$ and primer concentrations of1.2 mM and 0.2 µM, respectively, and standard template volumes. This was then run at different cycling conditions, which was achieved by adjusting the pre-

denaturation time, as well as the annealing temperature. These were referred to as cycling conditions 1 (2 min pre-denaturation and 58°C annealing step) and cycling conditions 2 (3 min pre-denaturation and 60°C annealing step) can be seen in Table 2.4 and Table 2.5, respectively.

Table 2.4 Cycling Conditions 1.

	Temperature	Time	Number of Cycles
cDNA Synthesis	55°C	25 min	1
Pre-denaturation	94°C	2 min	1
Denaturation	94°C	40 sec	
Annealing	58°C	40 sec	40
Extension	68°C	2 min	
Final Extension	68°C	5 min	1
	8°C	Hold	-

Table 2.5 Cycling Conditions 2.

	Temperature	Time	Number of Cycles
cDNA Synthesis	55°C	25 min	1
Pre-denaturation	94°C	3 min	1
Denaturation	94°C	40 sec	
Annealing	60°C	40 sec	40
Extension	68°C	2 min	
Final Extension	68°C	5 min	1
	8°C	Hold	-

2.4 Purification of the RT-PCR Product

The RT-PCR product was purified using the QIAquick PCR Purification Kit (Qiagen; Venlo, Netherlands). The protocol briefly involved mixing 125µL of Buffer PB to 25µL of the RT-PCR product to obtain a yellow mixture. If the colour of the mixture was orange or violet, this indicated that the pH of the mixture was not optimal to facilitate proper adsorption of the DNA to the silica membrane, so 10µL 3M sodium acetate, pH 5.0, was added to obtain the

correct pH. This mixture was then transferred to a QIAquick spin column and the column was centrifuged at 13 000 rpm for 60 seconds at room temperature, to enable the DNA to be adsorbed by the membrane of the spin column. The columns were then washed with 750µL of Buffer PE and centrifuged at 13 000 rpm for 60 seconds. To remove any residual wash buffer, the column was centrifuged at 13 000rpm for 60 seconds. The spin column was transferred to a clean 1.5 mL microcentrifuge tube and 25µL of elution buffer was added to the spin column. This was allowed to stand for 1 minute before being centrifuged at 13 000rpm for 1 minute at room temperature. The purified PCR product was then run on a 1% agarose gel to verify that the correct size product had been amplified and to verify the integrity of the product. The concentration of the purified PCR product was obtained by quantification on the Nanodrop 2000 (Thermo Scientific; Massachusetts, USA).

2.5 Gel Electrophoresis

The 1% agarose gel was prepared by dissolving an agarose tablet (Bioline Reagents Ltd; London, UK), containing 0.5g of agarose, in 50 mL of 1X Tris-Borate-EDTA (TBE) buffer for 5 minutes at room temperature. To prepare the 1X TBE, 100 mL of a 10XTBE buffer concentrate (Sigma; Missouri, USA) was diluted with 900 mL of distilled water to obtain a final volume of 1 litre of 1X TBE buffer. The agarose and TBE buffer mixture was then heated in a microwave until boiling point was reached. It was thereafter removed from the microwave, swirled (to mix) and then reheated. This process was repeated until no agarose particles were visible and a clear liquid was obtained. The liquid was allowed to cool, and prior to it polymerising, it was poured into an appropriately sized gel casting tray, with inserted combs, and allowed to polymerise. Once the gel had set, the combs were carefully removed and the gel, supported by the gel casting tray, was placed into an Electrophoresis

tank containing 1X TBE buffer. Care was taken to ensure that the gel was completely submerged by the 1X TBE buffer. Each sample was prepared for loading onto the gel by first mixing 1µL of gel loading buffer with 5µL of purified PCR product on a piece of parafilm. The loading dye was prepared by diluting 1µL of GelRed 10000X concentrate (Sigma; Missouri, USA) in 50µL gel loading buffer to obtain a 6x working solution. The prepared sample was then loaded onto the gel and electrophoresis was carried out at 100V for 30 minutes. In addition to the samples, a 1kb DNA ladder was also loaded onto the gel and this was prepared by mixing 2µL of gel loading buffer with 2µL of the DNA ladder on a piece of parafilm. Upon completion of electrophoresis, the gel was viewed in the SynGene Gel Documentation system, which used a UV light to illuminate the bands containing DNA. The bands obtained for the sample were compared to the ladder to determine if the correct size product was obtained.

2.6 cDNA Synthesis and Nested PCR

A different method of RT-PCR was used to amplify samples that were unsuccessfully amplified using the RT-PCR method described in 2.3. This alternative method involved firstly producing cDNA from the RNA followed by amplification of the cDNA using a nested PCR, in separate reactions.

2.6.1 cDNA Synthesis

The cDNA master mix was prepared as described in Table 2.6 in a 1.5 mL microcentrifuge tube.

Table 2.6 cDNA Synthesis Mastermix.

Reagent	Volume per reaction	Final concentration
5x First Strand Buffer	4	2X
0.1M DTT	1	10mM
DEPC Treated Water	1	
RNase OUT (40 U/µL)	1	40U
Superscript III (200 U/µL)	1	200U
Final Volume	8	

The cDNA synthesis master mix was kept at room temperature until it was required, however, the mix could not stand at room temperature for more than 30 minutes, so care was taken to perform the following steps quickly.

In a 0.2 mL PCR tube, 1 µL of dNTP mix and 1 µL of IN3 Primer were mixed. Ten microlitres of RNA was added to this and the tube was run on a thermal cycler under the conditions described in Table 2.7. Following the 4°C step for 1 minute, the PCR reaction was paused and 8µL of cDNA master mix was added to each PCR tube and the reaction is resumed.

Table 2.7 Cycling Conditions for cDNA Synthesis.

Temperature	Time	
65°C	5 min	Relaxes the RNA Structure
4°C	1 min	Cool to Optimal Enzyme Activity Temperature
Pause manually, add cDNA master mix and continue reaction		
50°C	60 min	Reverse Transcription
70°C	15 min	Inactivation of Superscript III
4°C	Hold	

2.6.2 Amplification of cDNA using a Nested PCR

To amplify the cDNA, a nested PCR was performed. The master mix for the first round of PCR was prepared as shown in Table 2.8.

Table 2.8 First Round PCR.

Reagent	Volume per reaction (µL)	Final concentration
DEPC Treated Water	16.3	
10x Buffer + $MgCl_2$	2.5	1X
10mM dNTPs	0.88	0.35 mM
G25REV (10pmol/µL)	0.25	0.125 µM
IN3 (10pmol/µL)	0.25	0.125 µM
Expand Long Template (5 U/µL)	0.38	1.9 U
Final Volume	**20.5**	

Twenty and a half microlitres (20.5 µL) of the PCR mastermix was then added into 0.2 mL PCR tubes and 4.5 µL of cDNA was added to the appropriately labelled tube. The PCR tubes were then run placed in the thermal cycler and run under the conditions mentioned in Table 2.9.

Table 2.9 Nested PCR Cycling Conditions.

	Temperature	Time	Number of Cycles
Initial Denaturation	94°C	2 min	1
Denaturation	94°C	10 sec	
Annealing	52°C	30 sec	10
Extension	68°C	2 min	
Denaturation	94 °C	15 sec	
Annealing	52°C	30 sec	25
Extension	68°C	2 min + 20 sec/cycle	
Final Extension	68°C	7 min	1
	4°C	Hold	

The master mix for the second round of PCR was prepared as shown in Table 2.10.

Table 2.10 Second Round PCR.

Reagent	Volume per reaction (µL)	Final concentration
DEPC Treated Water	39	
10x Buffer + $MgCl_2$	5	1X
10 mMdNTPs	1.75	0.35 mM
AV150 (10pmol/µL)	0.5	0.125 µM
Pol M4 (10pmol/µL)	0.5	0.125 µM
Expand Long Template (5 U/µL)	0.75	1.9 U
Final Volume	**47.5**	

Forty seven and a half microlitres (47.5 µL) of the second round mastermix was added to PCR tubes. To this, 2.5 µL of the first round PCR product was added to each appropriately labelled tube and caution was exercised to ensure that only 1 first round PCR tube was open at a time. The PCR tubes were placed in a thermal cycler and run under the conditions listed in Table 2.9.

2.7 Preparation of Sample Dilutions for Real-Time PCR

The purified samples were prepared for real-time PCR by diluting the RT-PCR products in 1mMEthylenediaminetetraacetic acid (EDTA) to obtain the desired concentration. This calculation was based on the equation:

$$\text{Number of copies} = \frac{(\text{amount X } 6.022\text{x}10^{23})}{(\text{length X } 1\text{x}10^{9} \text{ X } 650)}$$

Note: In this equation, the amount refers to the concentration of the template (in ng), $6.022\text{x}10^{23}$ is Avagadro's number (which is the number of molecules/mole), length is the number of base pairs of the template, $1\text{x}10^{9}$ is used to convert the number of molecules from g to ng and 650 is the average weight of a base pair. An online calculator is based on this equation. Taken from http://cels.uri.edu/gsc/cndna.html

Each sample was diluted to a standard concentration of 1 ng/µL and then serially diluted to obtain 10^6copies, which was used as the template in the real-time reactions.

2.8 Preparation of Plasmid DNA for Creating Standard Curves on the LightCycler 480 (LC480)

2.8.1 Amplification of Plasmid DNA

The standards for creating the K65R and L74V standard curves were prepared from the K65R and L74V plasmid DNA, respectively, using AmpliTaq Gold (Applied Biosystems, California, USA). Mutant constructs (K65R-C10 and L74V-C10), which were obtained from the Retrovirology Laboratory *irsiCaixa*, in Barcelona, Spain, were used for this purpose. The primers that were used in the PCR were forward primer AV150 (5'-GTGGAAAGGAAGGACACCAAATGAAAG-3') and reverse primer 3753L20 (5'-GCTTGCCAATAATCTGTCCACCA-3') to obtain a 1736bp product. The PCR reaction mix was prepared as shown in Table 2.11.

Table 2.11 PCR Reaction Mix for Amplification of Plasmid DNA.

Reagent	Volume per reaction	Final concentration
AmpliTaq Gold 10x buffer	2.5 µL	1X
10mM dNTPs	0.5 µL	0.2mM
50mM $MgSO_4$	1 µL	2mM
Forward Primer AV150 (10pmol/µL)	0.5 µL	0.2 µM
Reverse Primer 3753L20 (10pmol/µL)	0.5 µL	0.2 µM
AmpliTaq Gold enzyme (5 U/uL)	0.2 µL	1U
Water	18.8 µL	
Plamid DNA	1 µL	
Total Volume	**25 µL**	

The prepared reaction mix was then run on the thermal cycler under the conditions described in Table 2.12.

Table 2.12 Cycling Conditions for Plasmid DNA Amplification.

	Temperature	Time	Number of Cycles
Pre-denaturation	94°C	12 min	1
Denaturation	94°C	30 sec	35
Annealing	58°C	30 sec	
Extension	68°C	2 min	
Final Extension	68°C	5 min	1
	8°C	Hold	-

2.8.2 Purification and Gel Electrophoresis of Plasmid DNA

The PCR products were purified as mentioned in 2.4 using the QIAquick PCR Purification Kit, as per the manufacturer's instructions. The purified PCR product was then run on a 1% agarose gel with a 1kb DNA ladder as described in 2.5 in order to confirm that the correct product had been amplified. Thereafter, the purified PCR product was quantified using the Nanodrop 2000 instrument and the K65R and L74V amplicons were diluted to obtain a 1ng/µL concentration, which was then further diluted to prepare the dilutions required to produce the standard curve for ASPCR.

2.8.3 Dilution of Plasmid DNA

The purified plasmid controls were prepared for real-time PCR by diluting each PCR product in 1mM EDTA to achieve the desired concentration. This calculation was based on the equation in 2.6. All plasmid control PCR products were initially diluted to a standard concentration of 1ng/µL and serially diluted to obtain 10^7 to 10^2 dilutions. These dilutions were used as the template for creating the standard curves for the real-time PCR reactions.

2.9 Quantification using ASPCR

2.9.1 Optimisation of the LC 480 Real-Time PCR Standard Curve for the K65R Mutation

The K65R ASPCR was performed on the LC 480. A set of specific and non-specific primers were used for the K65R mutation. The forward primer used for the mutant-specific reaction was K65R-SP3 and for the non-specific reaction, K65R-NS was used. The same reverse primer, K65R-R, was used for both the specific and non-specific reactions. The sequences for the K65R primers can be seen in Table 2.13.

Table 2.13 K65R Primer Sequences.

Primer	Primer sequence (5'----3')	Number of bases
K65R-R	CTT CCC AAA AGT CTT GAG TTC T	22
K65R-NS	CTC CAG TAT TTG CCA TAA AAA	21
K65R-SP3	CTC CAG TAT TTG CCA TAA ATA G	22

Note: The codon indicated in the red box represents the codon 65 nucleotides in both the non-specific and specific primers.

2.9.1.1 Optimisation of the Primer Concentration for the K65R ASPCR

To determine what the optimal primer concentration for the ASPCR was, a primer titration was performed. This was achieved by preparing the mastermix for each of three reactions for both the K65R specific and the K65R non-specific reactions, as per the manufacturer's instructions, but using a different final primer concentration in each mastermix, i.e 0.25 µM, 0.375 µM and 0.5 µM (as seen in the Table 2.14, Table 2.15 and Table 2.16, respectively). The volume of water used for each mastermix was adjusted accordingly to obtain a final volume of 10 µL. To prepare the ASPCR mastermix, the water (PCR-grade), the primers and the SYBR Green I Master Mix were first thawed. The SYBR Green I Master Mix is light sensitive, so precautions were taken to keep the SYBR Green I Master Mix away from light

exposure. Once thawed, the primers were vortexed and then centrifuged briefly and the reactions were prepared for the specific and non-specific reactions separately.

Table 2.14 Mastermix with 0.25 µM Final Primer Concentration.

Reagents		Final Concentration
Water, PCR grade	2 µL	
Forward primer (10 pmol/µL)	0.25 µL	0.25 µM
Reverse primer (10 pmol/µL)	0.25 µL	0.25 µM
SYBR Green Master Mix, 2x conc.	5 µL	1X
Total Volume	**7.5 µL**	

Table 2.15 Mastermix with 0.375 µM Final Primer Concentration.

Reagents		Final Concentration
Water, PCR grade	1.75 µL	
Forward primer (10 pmol/µL)	0.375 µL	0.375 µM
Reverse primer (10 pmol/µL)	0.375 µL	0.375 µM
SYBR Green Master Mix, 2x conc.	5 µL	1X
Total Volume	**7.5 µL**	

Table 2.16 Mastermix with 0.5 µM Final Primer Concentration.

Reagents		Final Concentration
Water, PCR grade	1.5 µL	
Forward primer (10 pmol/µL)	0.5 µL	0.5 µM
Reverse primer (10 pmol/µL)	0.5 µL	0.5 µM
SYBR Green Master Mix, 2x conc.	5 µL	1X
Total Volume	**7.5 µL**	

Each of the above mastermixes was prepared separately with the specific and non-specific primers. The components of the mastermix were mixed by gently pipetting up and down a few times. Seven and a half microlitres (7.5µL) of the mastermix was then transferred to the appropriate well of the same plate, to which 2.5µL of the DNA template was added. The plate was sealed with the sealing foil, followed by centrifugation at 3000rpm for 2 minutes.

The plate was loaded into the LC 480 instrument and then run under the conditions shown in Table 2.17.

Table 2.17 Cycling Conditions for Optimisation of Primer Concentration for K65R ASPCR.

Programs	Acquisition mode	Temperature	Time	Number of cycles
Pre-incubation	None	95°C	5 minutes	1
Amplification	None	95°C	15 seconds	40
	None	60°C	15 seconds	
	Single	72°C	15 seconds	
Melting Curve	None	95°C	5 seconds	1
	None	65°C	1 minute	1
	Continuous	97°C	-	1
Cooling	None	40°C	None	1

2.9.1.2 Optimisation of the Annealing Temperature for the K65R ASPCR Reaction

The K65R standard curve was run with different annealing temperatures to determine what the optimal annealing temperature of the primers should be. The different primer annealing temperatures that were selected were 57°C, 60°C and 62°C. This experiment was performed by amplifying the K65R standard dilutions, viz. 10^7 DNA copies to 10^2 DNA copies, using a different primer annealing temperature in 3 separate experiments. For each annealing temperature, the K65R standard dilutions were used to generate a standard curve for both the K65R specific and the K65R non-specific reactions. The PCR Reaction Mix for the optimisation of the annealing temperature for the K65R ASPCR can be seen in Table 2.18.

Table 2.18 PCR Reaction Mix for Optimisation of the Annealing Temperature for the K65R ASPCR.

Reagents	0.375 pmol/µL
Water, PCR grade	1.75 µL
Forward Primer (10 pmol/µL)	0.375 µL
Reverse Primer (10 pmol/µL)	0.375 µL
SYBR Green Master Mix, 2x conc.	5 µL
Total Volume	7.5 µL

The components of the mastermix were mixed by gently pipetting up and down a few times. Seven and a half microlitres (7.5µL) of the mastermix was then transferred to the appropriate well of the plate, to which 2.5µL of the template was added. The plate was sealed with the sealing foil, followed by centrifugation at 3000rpm for 2 minutes. The plate was loaded into the LC 480 instrument and then run under the conditions described in Table 2.19.

Table 2.19 Cycling Conditions for the Optimisation of the Annealing Temperature for the K65R ASPCR.

Programs	Acquisition mode	Temperature	Time	Number of cycles
Pre-incubation	None	95°C	5 minutes	1
Amplification	None	95°C	15 seconds	40
	None	x °C*	15 seconds	
	Single	72°C	15 seconds	
Melting Curve	None	95°C	5 seconds	1
	None	65°C	1 minute	1
	Continuous	97°C	-	1
Cooling	None	40°C	None	1

*The annealing temperature was adjusted to 57°C, 60°C and 62°C for each ASPCR run.

2.9.2 Generation of the Standard Curves

The standard curves for the specific reactions, as well as the standard curves for the non-specific reactions were created by amplifying the standard dilutions (prepared in 2.8.3) using

the optimised ASPCR conditions. Basically, the mastermix for each of the specific and the non-specific reactions were prepared and 7.5 µL of this mastermix was aliquoted into the respective wells on the same plate. To this, 2.5 µL of the standard dilutions (i.e the 10^7 – 10^2standard dilutions) were added to the appropriate well. The plate was centrifuged and then loaded onto the LC 480, as described in 2.9.1.2. Following completion of the run, the LC 480 software was used to group each set of dilutions together into the specific and non-specific standard curve subsets and the software was then used to analyse the results to obtain the efficiency, slope and error value for each standard curve.

2.9.3 Quantification of Patient Samples with ASPCR

ASPCR was carried out on the patient samples using the sample dilution prepared in 2.7. The mastermix for the K65R specific and non-specific reactions were prepared and 7.5 µL of this was transferred to the respective wells on the plate. Two and a half microlitres (2.5 µL) of the sample dilution prepared in 2.6 was added to the corresponding wells and the plate was loaded onto the LC480, as explained in 2.9.1.2. The standard dilutions for the specific and non-specific reactions were included on every plate. At the end of the run, the standard curve was used to extrapolate the concentration of the sample, based on the crossing point at which the sample started amplifying. The percentage of viruses carrying the mutation for each sample was calculated using the following formula:

$$\% \text{ mutant sequences} = \frac{\text{(quantity of mutant sequences in the sample)}}{\text{(quantity of total viral sequences in the sample)}} \times 100$$

In this formula, the quantity of mutant sequences in the sample refers to the copies of the viruses that contained the mutant specific sequences (which was calculated using the mutant-specific standard curve). The quantity of total viral sequences in the sample refers to the copies of all the viruses in the sample (which was calculated using the non-specific standard curve). The percentage of mutant sequences in each sample was then calculated by dividing the concentration of the viruses carrying the mutant sequence by the concentration of the total viruses in the sample and this ratio was then multiplied by 100.

2.9.4 Sensitivity Test / Limit of Detection (LOD) Test

The sensitivity of the ASPCR was determined as described by Paredes *et al.*(2007). Briefly, the Wildtype (WT) plasmid amplicons were used as the template in 18 replicate reactions, separately, for both the specific and the non-specific K65R reactions. This was done to determine the percentage at which this assay starts producing unreliable results. The WT amplicons were amplified, purified and diluted using the same procedure described in 2.8.1 to 2.8.3. Briefly, the mastermix for the specific and non-specific mastermixes were prepared and 7.5 µL was aliquoted into the respective wells on the plate. The $WT10^6$ dilution was added to this and the plate was loaded onto the LC480 Instrument using the optimised run conditions, as described in 2.9.1.2. Once completed, an external standard curve was imported into the run using a 10^6 WT dilution as a calibrator for the standard curve in the run and used to calculate the percentage of mutant sequences using the formula in 2.9.3. The sensitivity of the assay was determined by calculating the mean plus 3 standard deviations (S.D) above the copy number of the 18 replicates of the wild-type plasmid dilution prepared in mutant specific reaction mix, as described by Paredes et al. (2007).

2.9.5 Accuracy test

The accuracy test was also performed as described by Paredes *et al*. (2007). Here, the percentage of the mutant plasmid amplicons were measured in a background of WT plasmid amplicons. Preparation of the serial dilutions was done by making 10-fold dilutions of a K65R 10^6 dilution (100%)until a 0.001% dilution was obtained and these dilutions were referred to as the nominal (or hypothetical) proportions. The serial dilutions for the accuracy test were prepared as shown in Table 2.20.

Table 2.20 Preparation of Serial Dilutions for Accuracy Test.

Nominal Proportions	Method
100% mutant	100 µL of K65R 10^6 dilution
10% mutant	10 µL of 100% mutant + 90 µL of WT 10^6 dilution
1% mutant	10 µL of 10% mutant + 90 µL of WT 10^6 dilution
0.1% mutant	10 µL of 1% mutant + 90 µL of WT 10^6 dilution
0.01% mutant	10 µL of 0.1% mutant + 90 µL of WT 10^6 dilution
0.001% mutant	10 µL of 0.01% mutant + 90 µL of WT 10^6 dilution

These dilutions were amplified in triplicate, for both the K65R specific and non-specific reactions and were run on the same plate. The plate was loaded as described in 2.8.1.2 and run on the LC480 machine using the optimised run conditions.

2.9.6 Optimisation of the LC 480 Real-Time PCR Standard Curve for the L74V Mutation

ASPCR for the L74V mutation was carried out on the LC480 instrument. This involved the use of both a specific and non-specific reaction. The primers for each of these reactions included a common forward primer (L74V-F). A separate reverse primer was used for each reaction, viz. L74V-SP5 for the specific reaction and L74V-NS2 for the non-specific reaction. The sequences for the L74V primers can be seen in Table 2.21.

Table 2.21 L74V Primer Sequences

Primer	Primer sequence (5'----3')	Number of bases
L74V-F	CCT GAA AAT CCA TAT AAC ACT CCA	24
L74V-NS2	T TGA GTT CCC TGA AAT CTA CTA	22
L74V-SP5	T TGA GTT CCC TGA AAT CTA CGA C	23

Note: The codon indicated in the red box represents the codon 74 nucleotides in both the non-specific and specific primers.

The optimisation procedures for the L74V ASPCR were performed following the same methods as for the K65R ASPCR, as described in 2.9.1.2. The same procedures that were used for the K65R ASPCR (to generate the standard curves, quantify the patient samples and perform the LOD and accuracy test) were performed for the L74V ASPCR (as discussed from 2.9.1.2 to 2.9.5).

CHAPTER 3

Results

3.1 Optimisation of the RT-PCR

3.1.1 Optimisation of the RT-PCR Reaction Mix

To optimise the RT-PCR reaction mix as explained in 2.3.1, the $MgSO_4$was titrated to final concentrations of 1.2 mM $MgSO_4$, 1.4 mM $MgSO_4$ and 1.6 mM $MgSO_4$. The PCR products were then run on a 1% agarose gel and the bands were visualised, as described in 2.5.The results obtained, following gel electrophoresis, can be seen in Figure 3.1. The $MgSO_4$ concentration that produced the best RT-PCR product was the reaction mix that contained a final concentration of 1.2 mM $MgSO_4$.

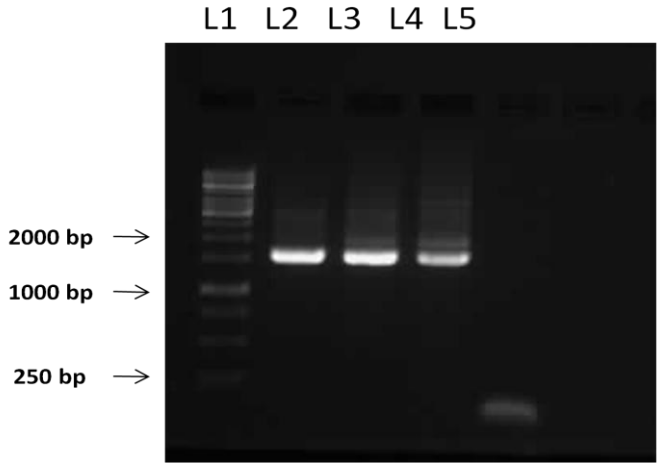

Fig 3.1 A $MgSO_4$ titration for the RT-PCR reaction mix. Lane 1 (L1) contains a 1 kb DNA ladder and lanes 2 to 4 (i.e L2 – L4) contains the 1.2 mM $MgSO_4$, 1.4 mM $MgSO_4$ and 1.6 mM$MgSO_4$final concentrations, respectively. The bands were visualised on a 1% agarose gel. The 1.2 mM $MgSO_4$ final concentration produced the optimal band of interest. Lane 5 (L5) contains the negative control.

3.1.2 Optimisation of the Cycling Conditions for the RT-PCR

The optimal cycling conditions for the RT-PCR reaction mix was determined as described in 2.3.2. The results for cycling conditions 1 (2 min pre-denaturation and 58°C annealing step) and cycling conditions 2 (3 min pre-denaturation and 60°C annealing step) can be seen in Figure 3.2 and Figure 3.3, respectively. The optimal band of interest was obtained with

cycling conditions 2 (Figure 3.3), as there was no smear below the sample band and the negative control did not contain a primer dimer band.

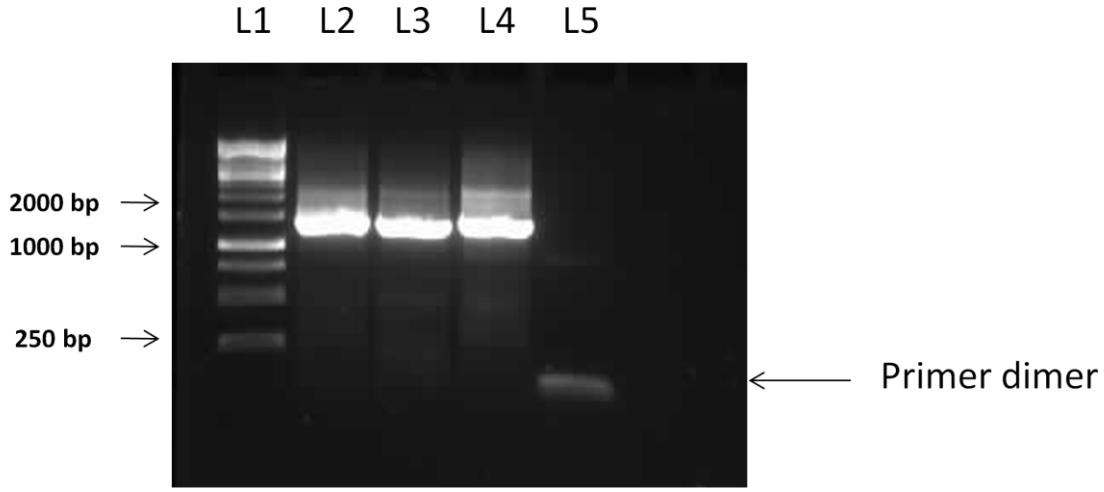

Fig 3.2 RT-PCR Results using Cycling Conditions 1. The gel picture showing the results using a pre-denaturation step of 94°C for 2 min and 58°C annealing. Lane 1 (L1) contains the 1 kb DNA ladder, lane 2 (L2) and lane 3(L3)contains the RT-PCR products of 2 different samples, lane 4 (L4) contains the positive control and Lane 5 (L5) contains the negative control, which contained a primer dimer band.

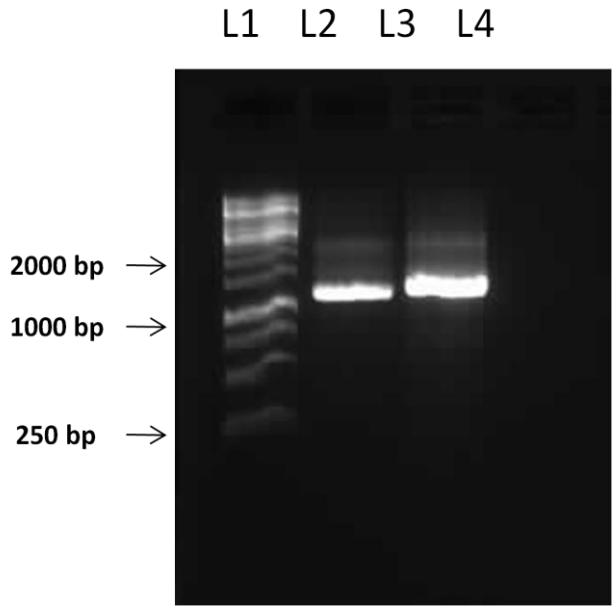

Fig 3.3 RT-PCR Results using Cycling Conditions 2. The picture of the gel showing the results using a pre-denaturation step of 94°C for 3 min and 60°C annealing. Lane 1 (L1) contains the 1 kb DNA ladder, lane 2 (L2) and lane 3 (L3) contains the RT-PCR products of 2 different samples and lane 4 (L4) contains the negative control.

3.1.3 Amplification of Patient Samples using the Optimised RT-PCR Reaction

The extracted RNA was reverse transcribed and amplified using the optimised RT-PCR reaction mix and cycling conditions, as discussed in 3.1.1 and 3.1.2. A representative gel can be seen in Figure 3.3, which shows the band of interest obtained using the optimised RT-PCR conditions (i.e a final $MgSO_4$concentration of 1.2 mM, pre-denaturation at 94°C for 3 min and 60°C annealing step).

Of the 101 extracted RNA samples, 74 samples amplified and 27 samples did not amplify. For the 27 samples that did not amplify, the RT-PCR was repeated several times by increasing the total reaction volumes used from 25 µL to 50 µL or by using different RNA extracts that were isolated using the same extraction method (some of which were previously extracted RNA, while others were freshly isolated RNA) and a further 10 samples amplified. A subset was also tested using a different cDNA synthesis and PCR method (i.e an in-house resistance genotyping assay), but these samples still did not amplify. Table 3.1 shows the RNA samples that did and did not amplify and their respective viral load ranges. As seen in the table, the samples that did not amplify were in the lower viral load ranges. It is possible that these samples were degraded and were therefore not amplifiable or that the RT-PCR assay was not sensitive enough.

Table 3.1 RNA Amplification Related to Viral Load Ranges

Viral Load (VL) ranges	Number of Samples	RNA that Amplified (number of samples)	RNA that Did Not Amplify (number of samples)
1 000 - 10 000	31	23	8
10 000 - 100 000	36	31	5
100 000 - 1 000 000	20	20	0
1 000 000 - 10 000 000	1	1	0
VL unavailable	13	9	4
Total	**101**	**84**	**17**

3.2 Amplification of Plasmid DNA

The K65R and L74V plasmid DNA was used to prepare the K65R and L74V standard curves, respectively. However, as mentioned in 2.8.1 to 2.8.2, the plasmid DNA was first amplified, purified and then run on a 1% agarose gel to confirm that the correct band had been amplified. The results following visualisation of the gel showing the amplification of the expected 1736bp band can be seen in Figure 3.4.

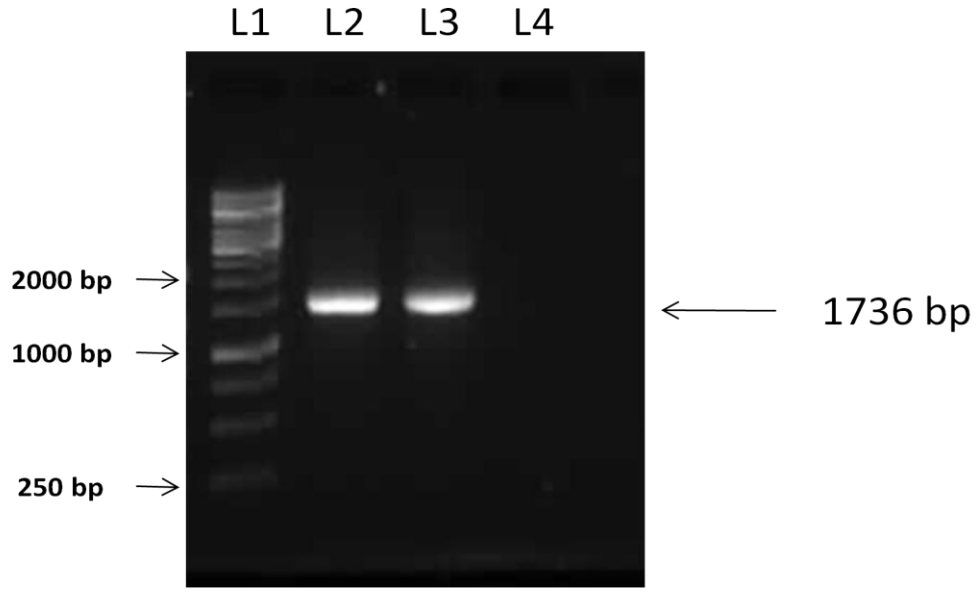

Fig3.4 PCR Products of K65R and L74V Plasmid DNA. Results obtained following amplification and purification of the K65R (L2) and L74V (L3) plasmid DNA, as visualised on a 1% agarose gel. Lane 1 (L1) contains the 1kb DNA ladder and lane 4 (L4) contains the negative control.

3.3 Optimisation of the K65R ASPCR

3.3.1 Optimisation of the Primer Concentration

The optimal primer concentration was determined by comparing the ASPCR results obtained using 3 different primer concentrations, i.e 0.25 µM, 0.375 µM and 0.5 µM (refer to 2.9.1.1). For each standard curve, each of the dilutions were run in triplicate. As seen in Figure 3.5, the final primer concentration that produced the best results was 0.375 µM.

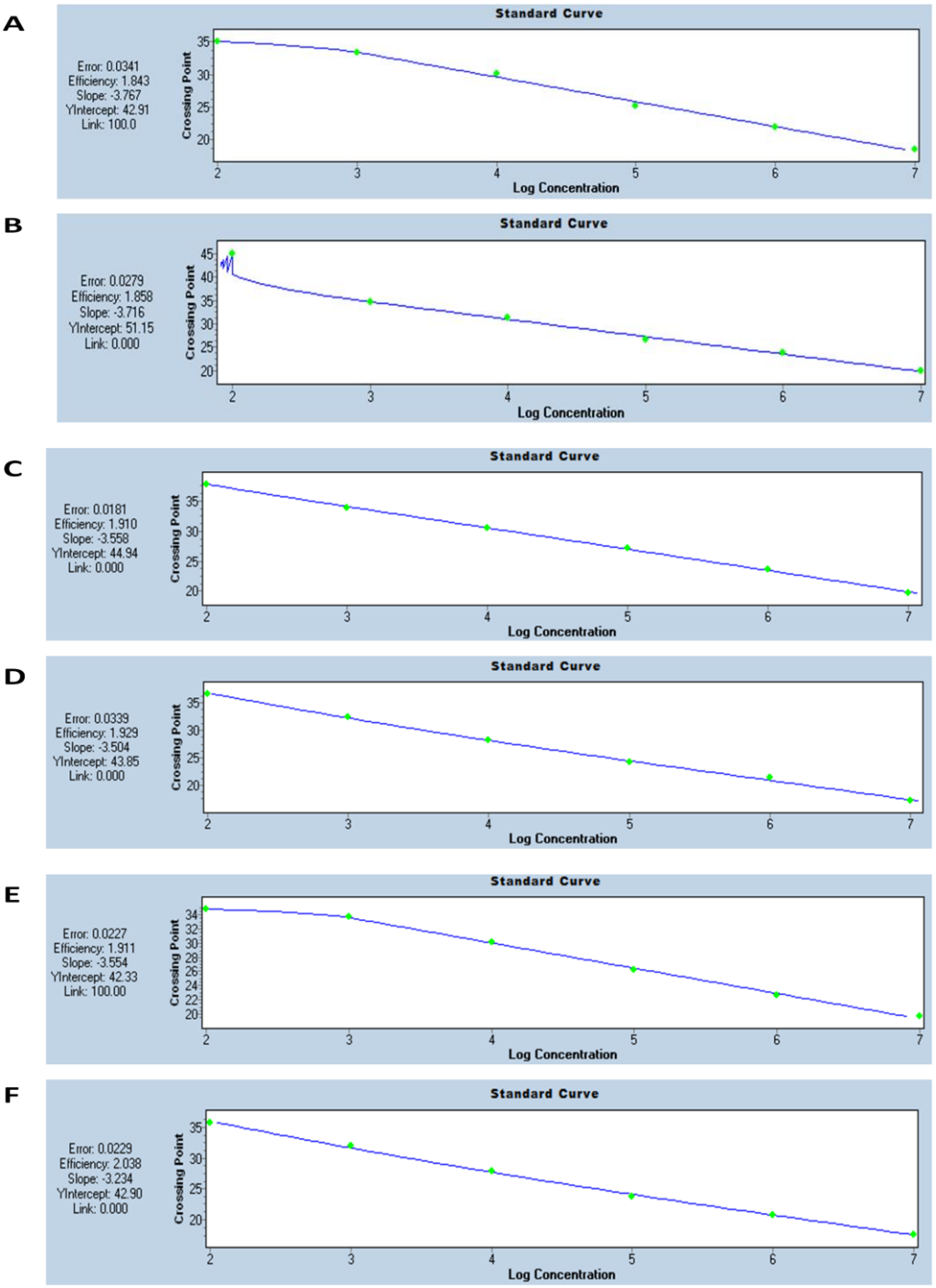

Fig3.5 Standard Curves Produced by using Different Primer Concentrations. The standard curves that were obtained with the primer concentration of 0.25 µM (final) for the K65R specific reaction (A) and the K65R non-specific reaction (B).The standard curves that were obtained with the primer concentration of 0.375 µM (final) for the K65R specific reaction (C) and the K65R non-specific reaction (D). The standard curves that were obtained with the primer concentration (final) of 0.5 µM for the K65R specific reaction (E) and the K65R non-specific reaction (F). The best error, efficiency and slope for both the specific and the non-specific standard curves were produced by the primer with the final concentration of 0.375 µM (C and D).

3.3.2 Optimisation of the Annealing Temperature for the K65R ASPCR

To determine the optimal annealing temperature for the K65R ASPCR, the K65R standard dilutions, prepared in 2.7.3, were used to create a standard curve in 3 separate experiments that differed only in the primer annealing temperature (i.e 57°C, 60°C and 62°C). The standard dilutions (used to generate each standard curve) were run in triplicate. The results obtained for an annealing temperature of 57°C, 60°C and 62°C can be seen in Figure 3.6 (A, B, C and D), Figure 3.7 (A, B, C and D) and Figure 3.8 (A, B, C and D), respectively.

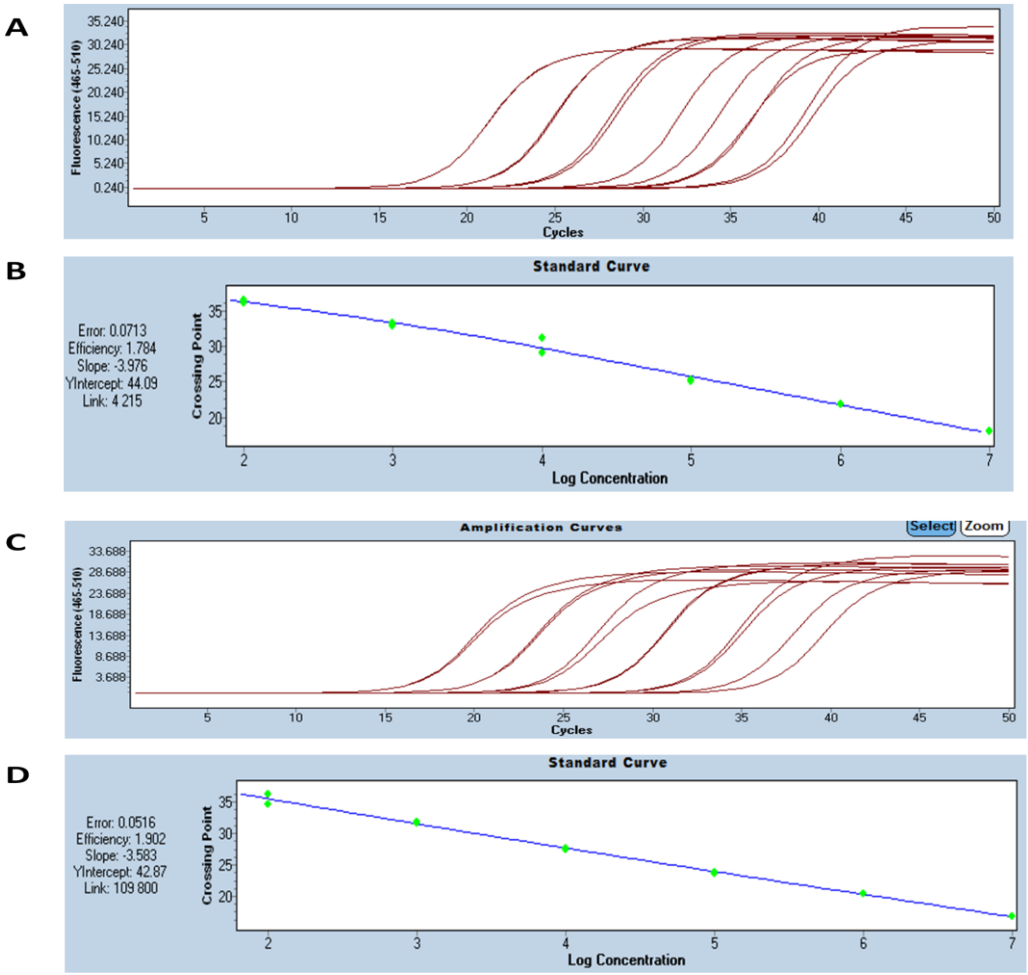

Fig3.6Amplification and Standard Curves with an Annealing Temperature of 57°C. The results show the amplification curves (A) and the standard curves (B) for the K65R standard dilutions using a primer annealing temperature of 57°C. The error of the standard curve (B) was 0.0713, the efficiency was 1.784 and the slope was -3.976. C and D show the amplification curves and the standard curve, respectively, for the K65R non-specific reaction. As seen in D, the error was 0.0516, the efficiency was 1.902 and the slope was -3.583.

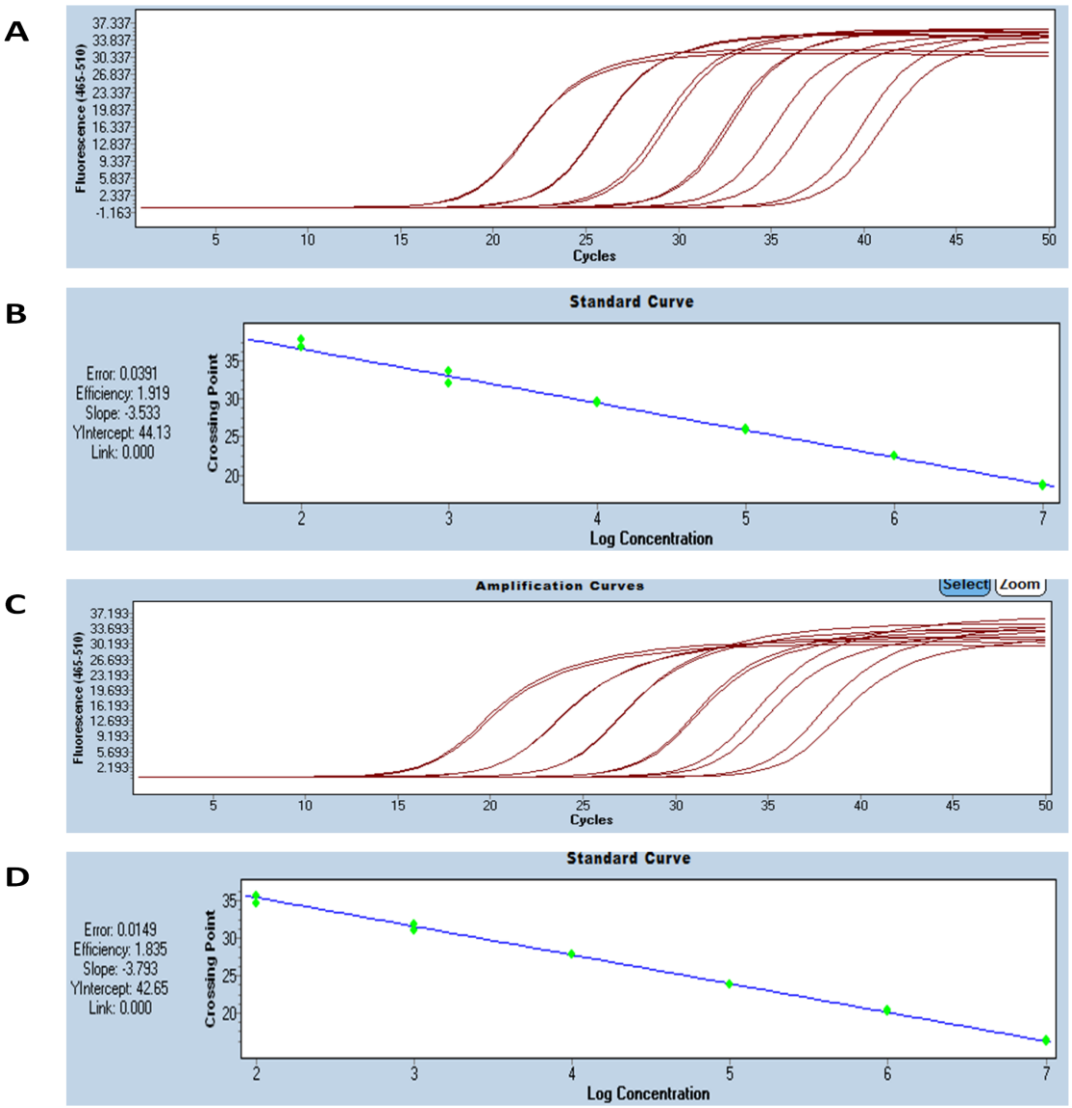

Fig 3.7 Amplification and Standard Curves with an Annealing Temperature of 60°C. The amplification curves (A) and the standard curves (B) for the K65R specific reaction using an annealing temperature of 60°C can be seen above. The error of the standard curve (B) was 0.0391, the efficiency was 1.919 and the slope was -3.533.C and D show the amplification curves and the standard curve, respectively, for the K65R non-specific reaction. As seen in D, the error was 0.0149, the efficiency was 1.835 and the slope was -3.793.

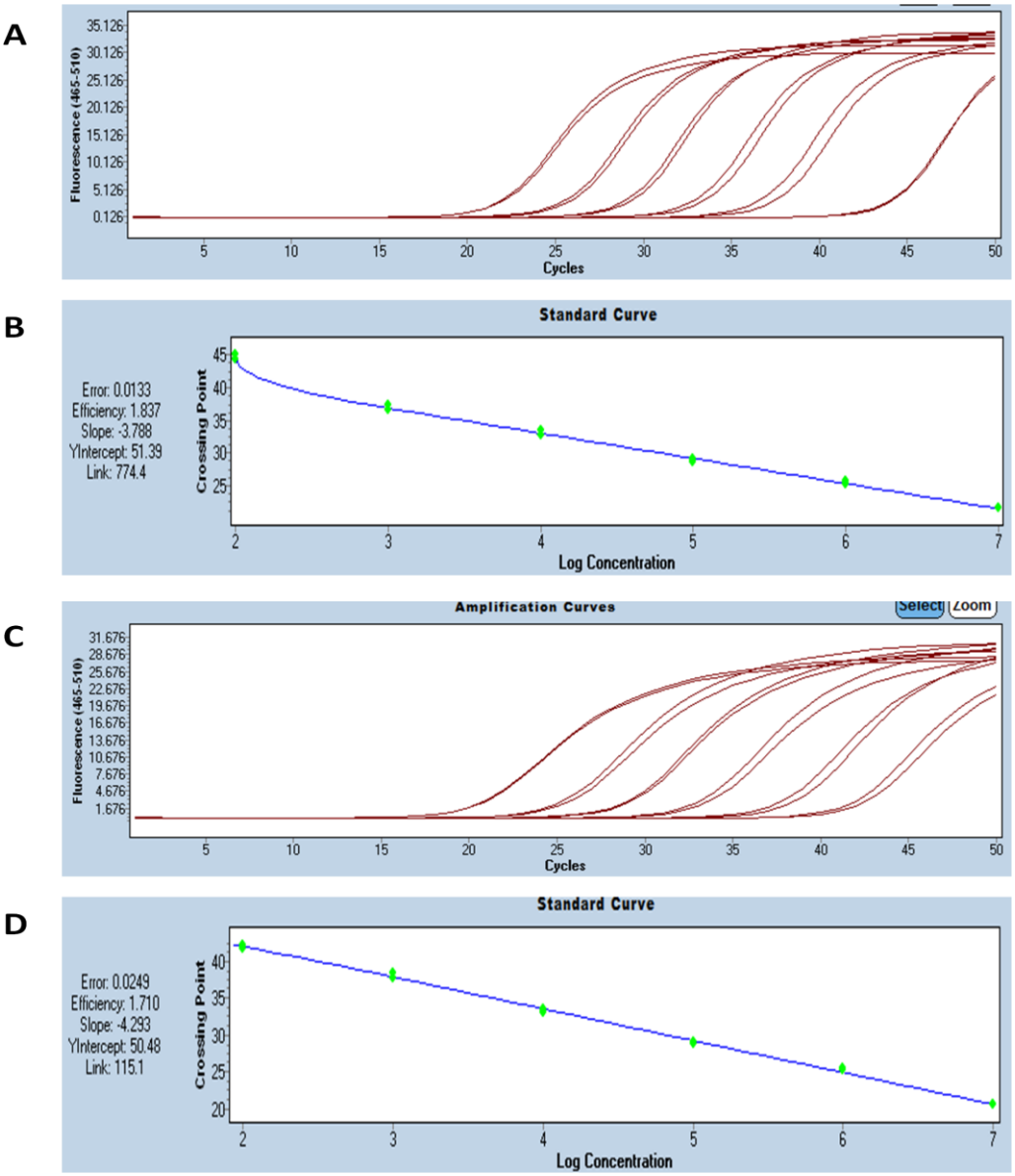

Fig 3.8 Amplification and Standard Curves with an Annealing Temperature of 62°C. The results obtained for the amplification curves (A) and the standard curve (B) for the K65R specific reaction using an annealing temperature of 62°C. The error of the standard curve was 0.0133, the efficiency was 1.837 and the slope was -3.788. C and D show the amplification curves and the standard curve, respectively, for the K65R non-specific reaction. As seen in D, the error was 0.0249, the efficiency was 1.710 and the slope was -4.293.

For a standard curve, the error value obtained should be less than 0.2 and the slope should be -3.3. As can be seen from the results of Figure 3.6, Figure 3.7 and Figure 3.8, the annealing temperature that produced the best standard curve was 60°C, as the best efficiency for both the specific and non-specific reactions was obtained with this temperature.

3.3.3 K65R Standard Curves

The K65R specific and non-specific standard curves, Figure 3.9 (B and C), were constructed with the 10^7 to 10^2 DNA copies standard dilutions, prepared in 2.8.3, and using the optimised ASPCR conditions (refer to 3.3.1 and 3.3.2). For each standard curve, each of the standard dilutions were run in triplicate.

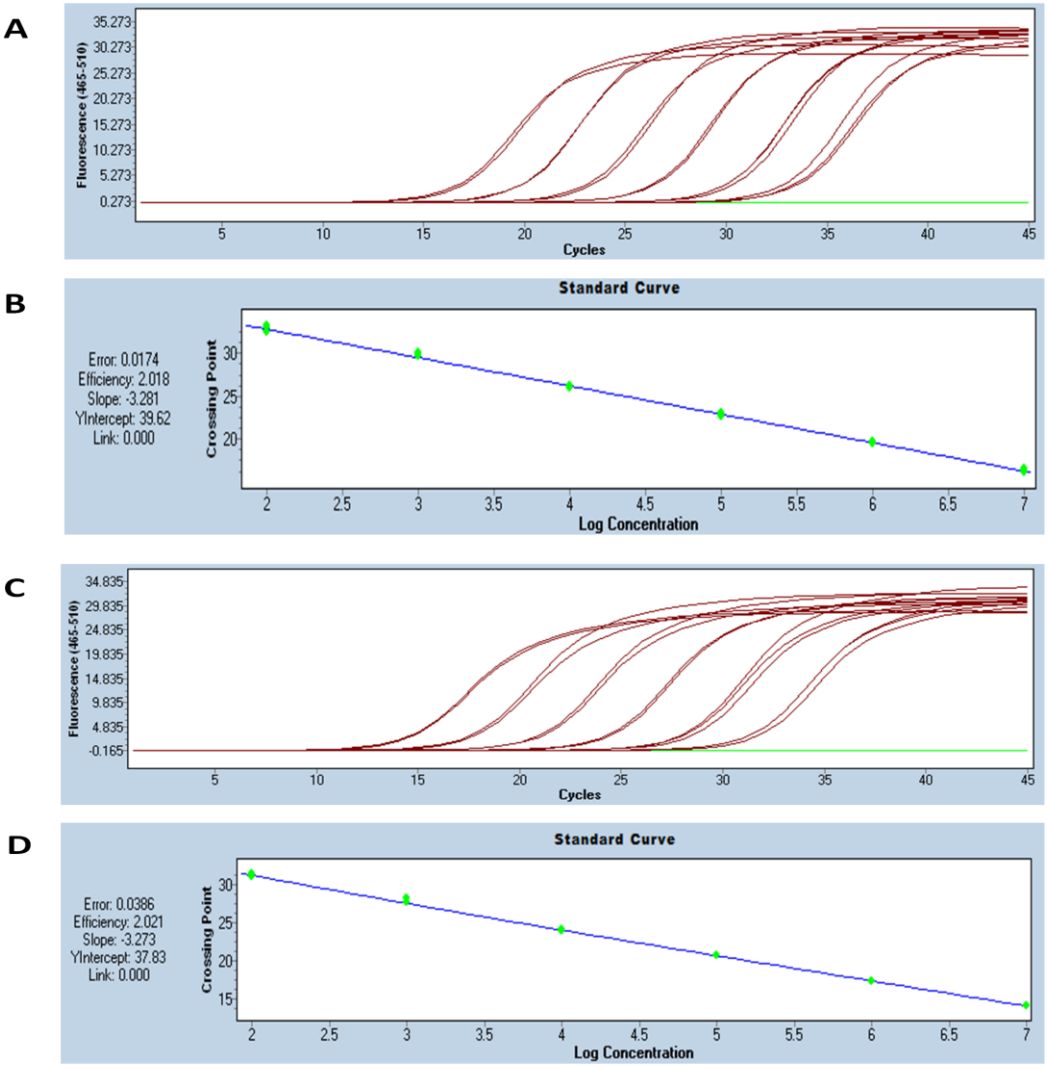

Fig 3.9 The Amplification Curves and Standard Curve Obtained with the Optimised K65R ASPCR. The amplification curves (A) and standard curve (B) obtained with the optimised ASPCR conditions for the K65R specific standard curve. The amplification curves (C) and standard curve (D) obtained with the optimised ASPCR conditions for the K65R non-specific standard curve. The error values, efficiency values and the slope for both the K65R specific and non-specific standard curves were very close to the ideal values for ASPCR standard curves. The green lines in B and C represent the negative control.

3.4 Sensitivity/ LOD Test

For the sensitivity test, 18 replicates of WT DNA were prepared for each of the specific and non-specific reactions, as described in 2.9.4. The K65R standard curve was imported into the run and this was used to determine the mean concentration of the 18 K65R specific replicates. The K65R non-specific standard curve was also imported into the run in order to calculate the mean concentration of the 18 K65R non-specific replicates. Included in the run was a 10^6 dilution WT plasmid DNA prepared with both the K65R specific and non-specific reaction mixes, separately, and this served as internal standards that allowed for the K65R specific and non-specific external standard curves to be imported into the run. The LC 480 software was then used to perform these calculations and then to determine the ratio of the mean concentration of the K65R specific reaction divided by the mean concentration of the K65R non-specific reaction. The sensitivity of the assay was determined as described in 2.9.4. The sensitivity obtained was 0.72%. Therefore, this is the percentage at which the assay begins to produce false positives.

3.5 Accuracy Test

The accuracy test was performed by preparing 10-fold serial dilutions of the 10^6 K65R plasmid DNA in a background of the 10^6dilution WT plasmid DNA, as explained in 2.9.5. Each of the dilutions was run in triplicate. For the K65R specific reaction, Figure 3.10 (A), the 100% mutant amplicons started amplifying between 19.9 and 20 cycles, the dilution containing 10% mutant amplicons started amplifying between 23.5 and 23.90 cycles, the dilution containing 1% mutant amplicons started amplifying between 26.10 and 26.7 cycles. The remaining dilutions (i.e 0.1%, 0.01% and 0.001%) all amplified between 27.7 and 28.60 cycles. The dilution at which accuracy was lost was the 1% dilution. For the non-specific

reaction, Figure 3.10 (B), each of the dilutions was prepared using the primers for the non-specific reaction and run in triplicate. All the dilutions started amplifying at 17.56 cycles, which is the cycle number that the 10^6 dilution usually starts amplifying at on the K65R non-specific standard curve. The K65R specific and non-specific standard curves were imported into the run to determine if the calculated percentage matched the nominal proportion, as shown in Table 3.2. The measured proportions were plotted against the nominal proportions and the results obtained can be seen in Fig 3.11. The results show that the percentage calculated for each dilution using the LC480 software is similar to the theoretical perfect match for the measured and nominal proportions from the 1% dilution and above.

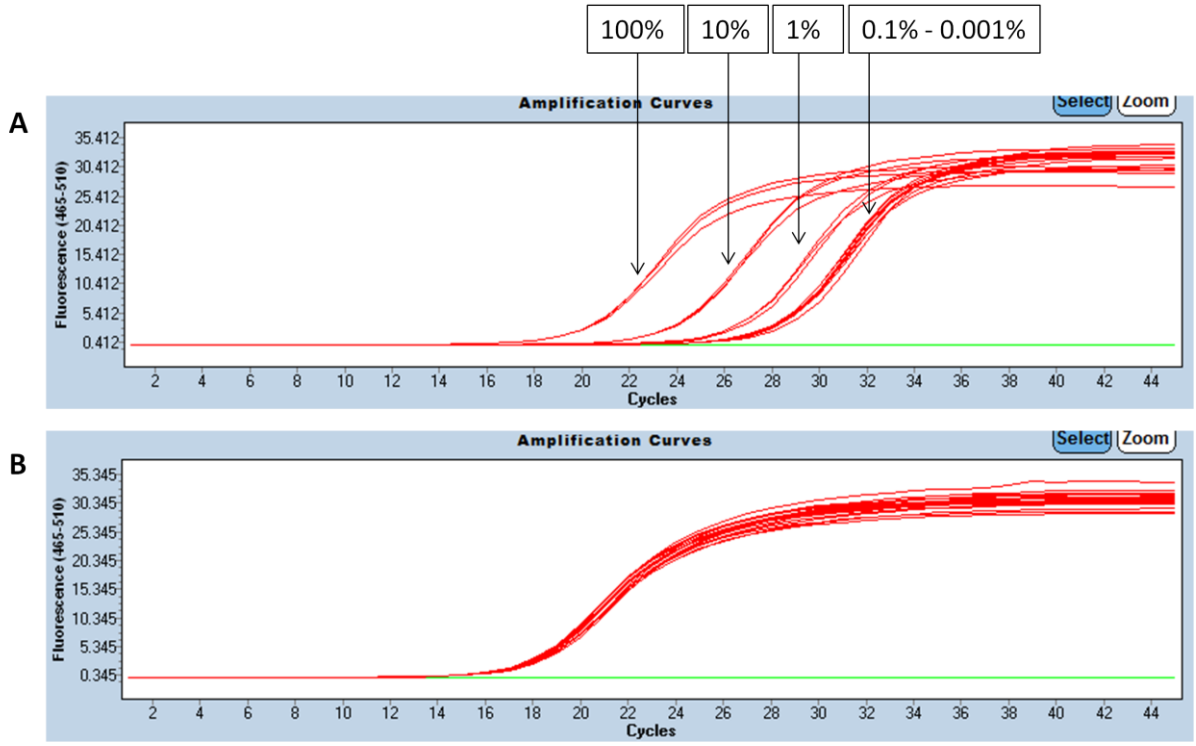

Fig 3.10 Amplification Curves for the Accuracy Test. Results showing the amplification curves for the 10-fold serial dilutions of the K65R specific reaction (A) and the non-specific reaction (B).

Table 3.2 Measured against Nominal Proportion for K65R Accuracy Test. The table shows the nominal proportions (which is the percentage of the K65R 10^6 dilution plasmid DNA prepared in a background of WT DNA) of the samples prepared and the measured proportion as calculated on the LC480.

Nominal Proportion	Measured Proportion
100	100
10	7
1	1
0.1	0.33
0.01	0.34
0.001	0.3

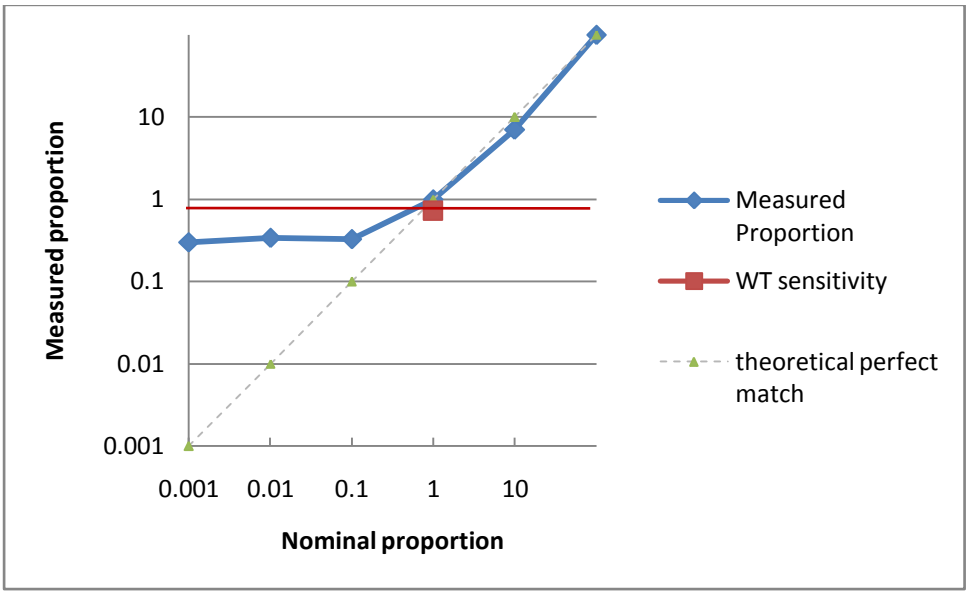

Fig 3.11 Graph Showing the Measured Proportion Plotted against the Nominal Proportion for K65R. This graph shows the measured proportion (on the y-axis) plotted against the nominal (hypothetical) proportion (on the x-axis). The green dotted line represents the theoretical perfect match of the measured proportion against the nominal proportion. As it can be seen, the results obtained from the experiment (represented by the blue line) behaves similarly to the theoretical perfect match from the 1% dilution upwards. However, the percentage at which the WT starts to produce false positives results (the red line) is 0.72%. Therefore, the limit of detection of the test is 0.72%.

3.6 Quantification of the Patient Samples using K65R ASPCR

The ASPCR results that were obtained for the 84 patient samples (that amplified using the RT-PCR) can be seen in Table 3.3. Positive results (i.e the samples in which the mutation was detected above the limit of detection of 0.72%) were obtained for 7 out of the 84samples (8.33%). Five samples were detected above 1% (i.e 3 were approximately 2%, 1 was 9.48% and 1 was 100%) and 2 were detected below 1% (i.e 1 was 0.88% and the other was 0.93%). Table 3.4 contains a list of the samples that did not amplify using the RT-PCR.

Table 3.3 ASPCR Results for 84 Samples Amplified by RT-PCR

	Sample Name	K65R specific reaction mean concentration (copies)	K65R non-specific reaction mean concentration (copies)	Ratio of specific / non-specific mean concentration (copies)	Percentage of the Ratio
1	Sw1	342	6.04×10^{6}	5.66×10^{-5}	0.0057%
2	Sw2	176.5	6.26×10^{5}	2.84×10^{-4}	0.028%
3	Sw3	63.2	2.35×10^{5}	2.67×10^{-4}	0.027%
4	Sw6	4.475	9.80×10^{3}	4.56×10^{-4}	0.046%
5	Sw7	19.5	1.07×10^{4}	1.81×10^{-3}	0.18%
6	Sw8	58.85	4.64×10^{4}	1.25×10^{-3}	0.13%
7	Sw9	206	2.47×10^{6}	4.33×10^{-5}	0.0043%
8	Sw10	* >40 cycles	8.19×10^{4}	0	0%
9	Sw11	0.435	1.12×10^{5}	3.88×10^{-6}	0.00039%
10	Sw12	641.5	3.90×10^{6}	1.66×10^{-4}	0.017%
11	Sw14	* >40 cycles	6.67×10^{4}	0	0%
12	Sw15	7.08	1.36×10^{5}	4.22×10^{-5}	0.0042%
13	Sw16	93.2	3.41×10^{5}	2.74×10^{-4}	0.027%
14	Sw17	3.2	4.76×10^{4}	6.28×10^{-5}	0.006%
15	Sw18	7.435	3.27×10^{3}	2.73×10^{-3}	0.27%
16	Sw19	* >40 cycles	5.60×10^{4}	0	0%
17	Sw20	13.015	4.27×10^{5}	3.24×10^{-4}	0.032%
18	Sw21	0.2717	1.07×10^{5}	1.81×10^{-6}	0.0002%
19	Sw23	15.2	2.29×10^{5}	4.90×10^{-5}	0.0049%
20	Sw24	11.75	1.09×10^{4}	1.07×10^{-3}	0.11%
21	Sw25	28.3	9.54×10^{4}	2.96×10^{-4}	0.03%
22	Sw26	11.675	5.49×10^{4}	2.14×10^{-4}	0.02%
23	Sw27	1620	5.48×10^{5}	1.54×10^{-3}	0.154%
24	Sw28	6000	8.01×10^{6}	7.72×10^{-4}	0.077%
25	Sw29	1.08	3.87×10^{4}	3.30×10^{-5}	0.003%
26	**Sw30**	**500**	**5.64×10^{4}**	**8.83×10^{-3}**	**0.88%**
27	Sw31	231	1.76×10^{5}	1.45×10^{-3}	0.15%

	Sample Name	K65R specific reaction mean concentration (copies)	K65R non-specific reaction mean concentration (copies)	Ratio of specific / non-specific mean concentration (copies)	Percentage of the Ratio
28	Sw33	156.5	3.14×10^{6}	5.08×10^{-5}	0.0051%
29	Sw34	151	1.37×10^{5}	1.11×10^{-3}	0.11%
30	Sw35	192	1.18×10^{6}	1.64×10^{-4}	0.016%
31	Sw36	5.38	2.62×10^{4}	0	0%
32	Sw37	(>40 cycles)	1.72×10^{3}	0	0%
33	Sw38	48.25	5.21×10^{5}	8.13×10^{-5}	0.0081%
34	Sw41	289	1.85×10^{5}	1.71×10^{-3}	0.17%
35	Sw42	490.5	1.16×10^{6}	3.97×10^{-4}	0.04%
36	Sw43	770	1.24×10^{5}	6.20×10^{-3}	0.62%
37	**Sw44**	**58.7**	**2.93×10^{3}**	**2.03×10^{-2}**	**2.03%**
38	Sw45	8.295	2.12×10^{4}	3.66×10^{-4}	0.04%
39	Sw46	7.065	9.60×10^{3}	7.15×10^{-4}	0.07%
40	Sw47	82.6	2.00×10^{5}	4.14×10^{-3}	0.41%
41	Sw48	(>40 cycles)	1.23×10^{3}	0	0%
42	Sw49	298	2.31×10^{6}	1.28×10^{-4}	0.013%
43	Sw50	1.955	3.57×10^{5}	5.73×10^{-6}	0.00057%
44	Sw52	160	9.76×10^{5}	1.62×10^{-4}	0.016%
45	Sw53	1.23×10^{3}	1.20×10^{7}	1.05×10^{-4}	0.01%
46	Sw54	1.125×10^{3}	3.60×10^{5}	3.14×10^{-3}	0.31%
47	Sw55	137	1.71×10^{5}	7.90×10^{-4}	0.079%
48	Sw57	110.65	8.55×10^{5}	1.30×10^{-4}	0.013%
49	Sw58	0.647	5.11×10^{4}	8.05×10^{-6}	0.00081%
50	Sw59	100.4	6.39×10^{5}	1.69×10^{-4}	0.017%
51	Sw60	13.6	2.31×10^{5}	5.68×10^{-5}	0.0057%
52	Sw61	4.28×10^{3}	9.51×10^{5}	5.49×10^{-4}	0.055%
53	Sw63	2875	2.90×10^{6}	1.14×10^{-3}	0.11%
54	Sw65	437.5	1.17×10^{5}	3.74×10^{-3}	0.37%
55	Sw66	9.625	1.81×10^{4}	4.68×10^{-4}	0.047%
56	Sw67	1410	4.90×10^{6}	2.88×10^{-4}	0.029%
57	**Sw69**	**1250**	**4.65×10^{4}**	**2.67×10^{-2}**	**2.67%**
58	Sw71	1180	$5\ 73 \times 10^{5}$	2.06×10^{-4}	0.021%
59	Sw72	1290	7.57×10^{6}	1.67×10^{-4}	0.017%
60	**Sw73**	**8410**	**8.89×10^{4}**	**9.48×10^{-2}**	**9.48%**
61	Sw74	0	5.73×10^{3}	0	0%
62	Sw75	1070	3.11×10^{6}	3.51×10^{-4}	0.035%
63	Sw76	140.5	2.43×10^{6}	5.74×10^{-5}	0.0057%
64	**Sw77**	**36.9**	**1.35×10^{3}**	**2.73×10^{-2}**	**2.73%**
65	Sw78	396.5	1.75×10^{6}	2.29×10^{-4}	0.023%
66	**Sw79**	**191×10^{5}**	**1.74×10^{3}**	**110.5**	**100% ****
67	Sw80	1.09×10^{3}	7.34×10^{5}	1.48×10^{-3}	0.15%
68	Sw81	74.2	1.57×10^{5}	4.83×10^{-4}	0.048%
69	Sw82	4.20×10^{2}	3.20×10^{5}	1.33×10^{-3}	0.13%
70	Sw83	3.155×10^{2}	2.55×10^{5}	1.23×10^{-3}	0.123%
71	Sw84	9.455×10^{2}	5.18×10^{5}	1.84×10^{-3}	0.18%

	Sample Name	K65R specific reaction mean concentration (copies)	K65R non-specific reaction mean concentration (copies)	Ratio of specific / non-specific mean concentration (copies)	Percentage of the Ratio
72	Sw88	5.725×10^{2}	3.12×10^{5}	1.8×10^{-3}	0.18%
73	Sw89	0.375	9.65×10^{2}	3.92×10^{-4}	0.039%
74	Sw90	* >40 cycles	2.97×10^{2}	0	0%
75	Sw91	2.58×10^{2}	1.985×10^{5}	1.3×10^{-3}	0.13%
76	Sw92	0.7955	4.535×10^{4}	1.58×10^{-5}	0.0016%
77	Sw93	48.15	1.02×10^{6}	4.77×10^{-5}	0.0048%
78	Sw94	150.0	4.05×10^{5}	3.72×10^{-4}	0.037%
79	**Sw97**	**1.415×10^{3}**	**1.54×10^{5}**	**9.3×10^{-3}**	**0.93%**
80	Sw98	875	3.84×10^{6}	2.19×10^{-4}	0.022%
81	Sw99	4240	7.18×10^{5}	5.86×10^{-3}	0.59%
82	Sw100	1070	2.98×10^{5}	3.64×10^{-3}	0.36%
83	Sw101	0	111.85	0	0%
84	Sw102	5355	2.63×10^{6}	2.04×10^{-3}	0.2%

* >40 cycles denotes that the K65R specific samples amplified after 40 cycles. This means that the percentage of the mutant in the specific reaction was very low, since the K65R non-specific reactions were amplifiable within the standard curve range for these samples. The LC480 software assigns a common number to any samples that amplify after 40 cycles, which means that the calculated percentage was incorrect.
** This sample was taken as 100% since the specific reaction produced a higher concentration than the non-specific reaction, resulting in a high ratio.
Samples that appear in bold font are the samples in which the K65R mutation was detected.

Table 3.4. List of Samples that were Not Amplifiable by RT-PCR.

	Sample Name	Viral Load (VL)
1	Sw4	unavailable
2	Sw5	2 000
3	Sw13	unavailable
4	Sw22	6 800
5	Sw32	5 300
6	Sw39	13 000
7	Sw40	80 000
8	Sw51	1 300
9	Sw56	29 853
10	Sw62	1 100
11	Sw64	1 300
12	Sw68	17 000
13	Sw85	4 200
14	Sw86	unavailable
15	Sw87	49 900
16	Sw95	unavailable
17	Sw96	2 400

3.7 Optimisation of the L74V ASPCR

3.7.1 Optimisation of the Annealing Temperature for the L74V ASPCR

The optimal annealing temperature for the L74V ASPCR was determined as described for K65R in 2.8.1.2. Briefly, the standard dilutions used to generate the standard curve were amplified at 3 different annealing temperatures, viz. 57°C, 60°C and 62°C, in different experimental runs. The results can be seen in Figure3.12, Figure 3.13 and Figure 3.14.

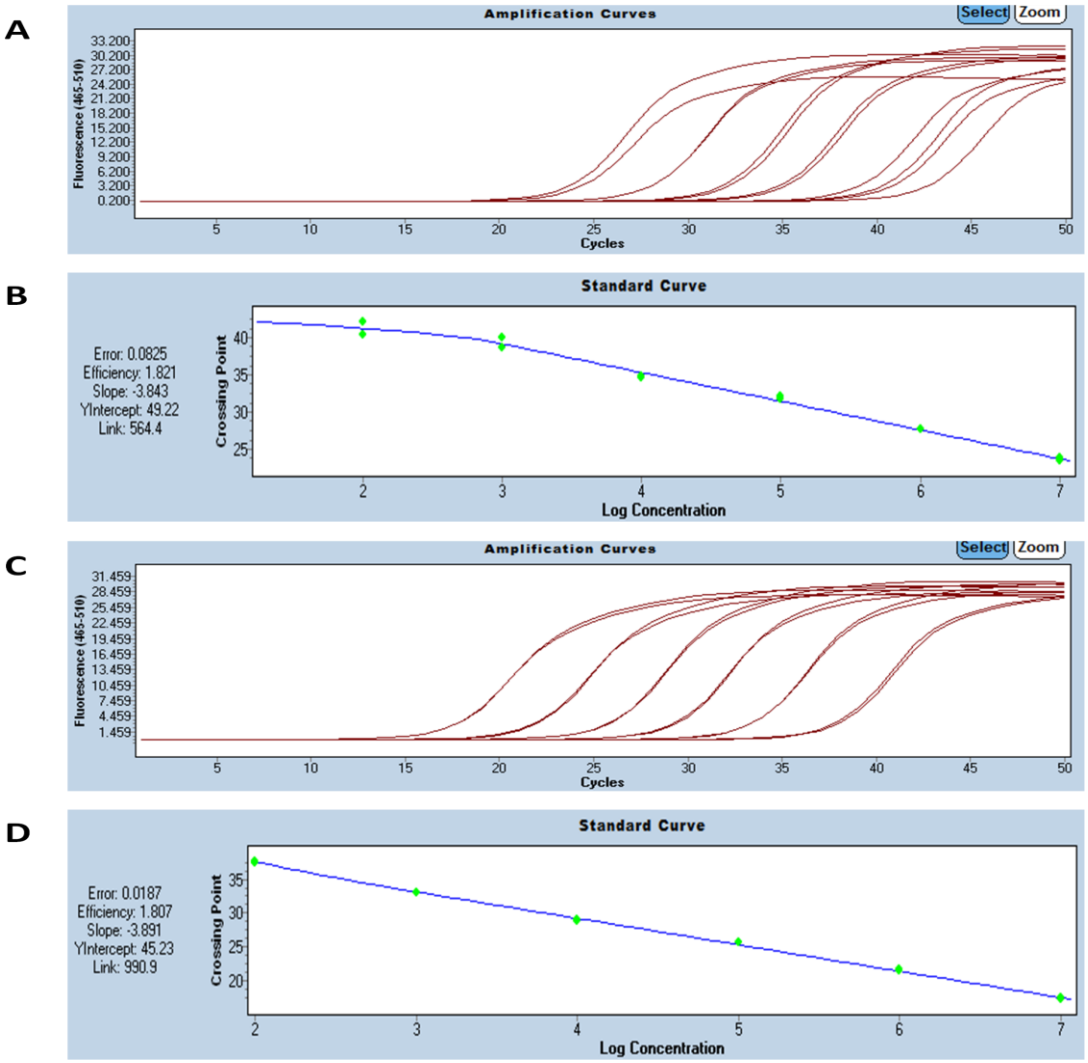

Fig 3.12 Amplification and Standard Curves for L74V with an Annealing Temperature of 57°C. The amplification curves and standard curve for the L74V specific reaction can be seen in A and B, respectively. The error of the standard curve was 0.0825, the efficiency was 1.821 and the slope was -3.843. C contains the amplification curves for the L74V non-specific reaction and D shows the standard curve for the non-specific standard curve. The error of the standard curve was 0.0187, the efficiency was 1.807 and the slope was -3.891.

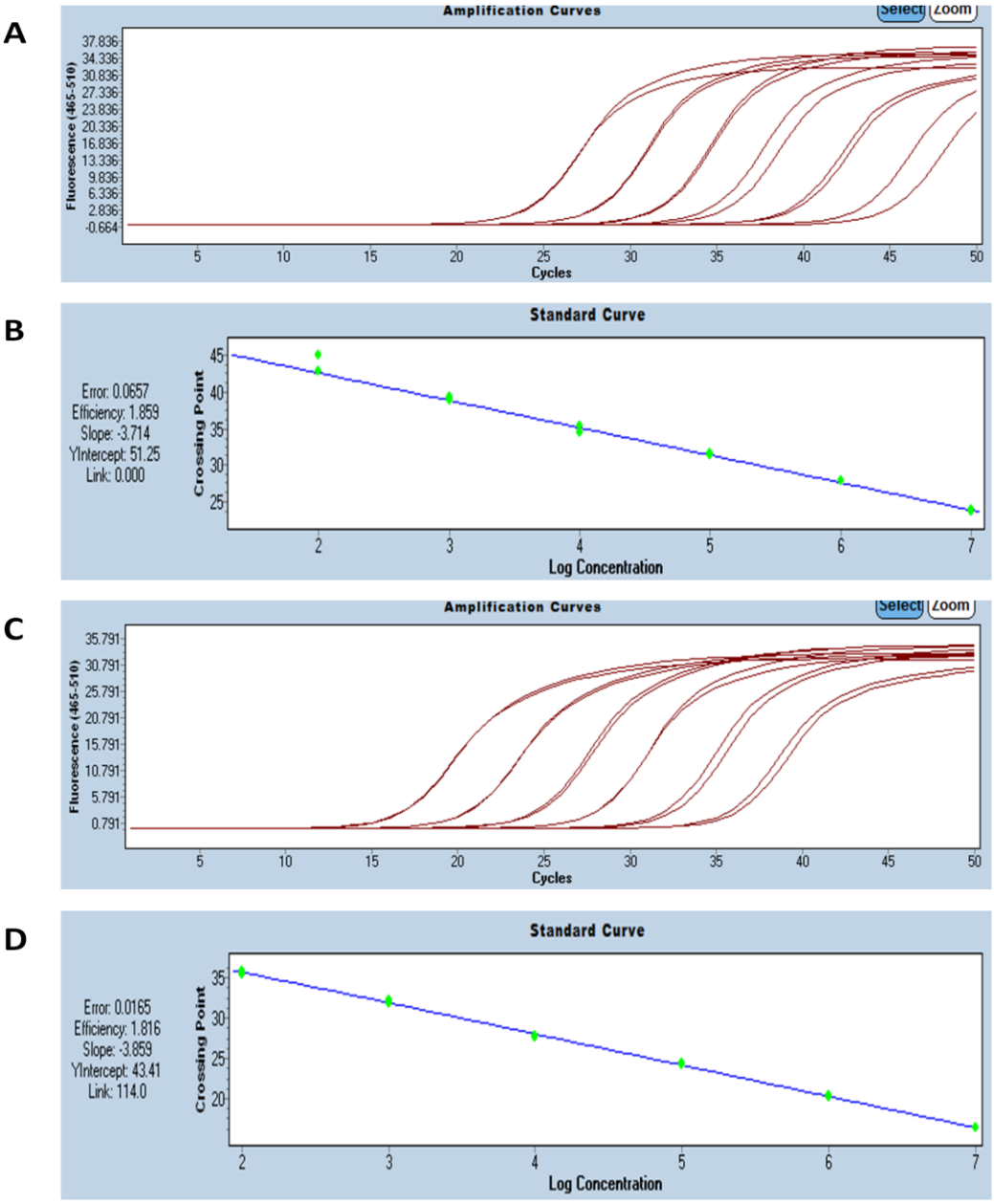

Fig 3.13 Amplification and Standard Curves for L74V with an Annealing Temperature of 60°C. The amplification curves and standard curve for the L74V specific reaction can be seen in A and B, respectively. The error of the standard curve was 0.0657, the efficiency was 1.859 and the slope was -3.714. C contains the amplification curves for the L74V non-specific reaction and D shows the standard curve for the non-specific standard curve. The error of the standard curve was 0.0165, the efficiency was 1.816 and the slope was -3.859.

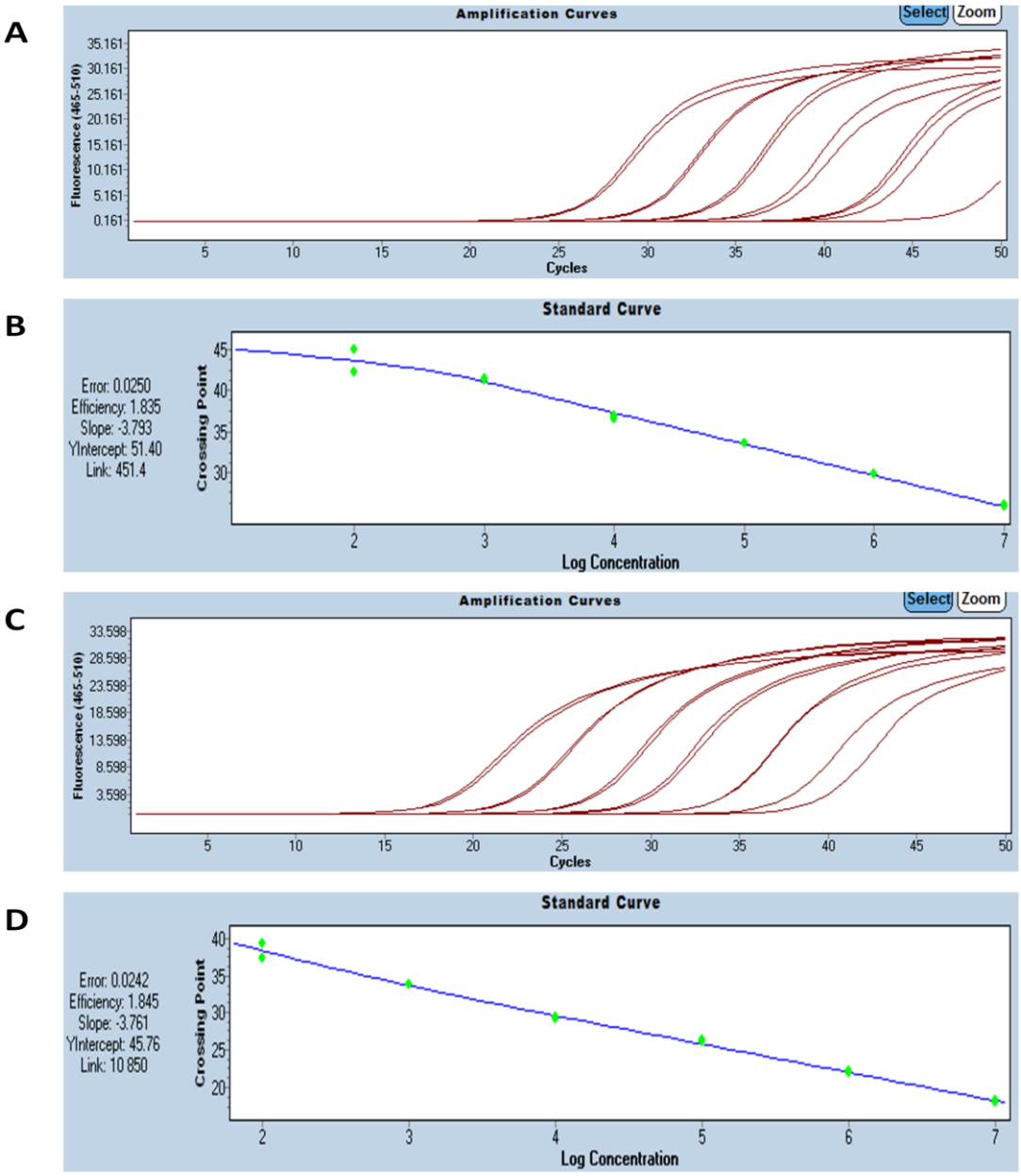

Fig 3.14Amplification and Standard Curves for L74V with an Annealing Temperature of 62°C. The amplification curves and standard curve for the L74V specific reaction can be seen in A and B, respectively. The error of the standard curve was 0.0250, the efficiency was 1.835 and the slope was -3.793. C contains the amplification curves for the L74V non-specific reaction and D shows the standard curve for the non-specific standard curve. The error of the standard curve was 0.0242, the efficiency was 1.845 and the slope was -3.761.

3.7.2 L74V Standard Curves

The optimised L74V ASPCR conditions were used to amplify the standard dilutions (i.e 10^7 to 10^2) and the results can be seen in Figure 3.15.

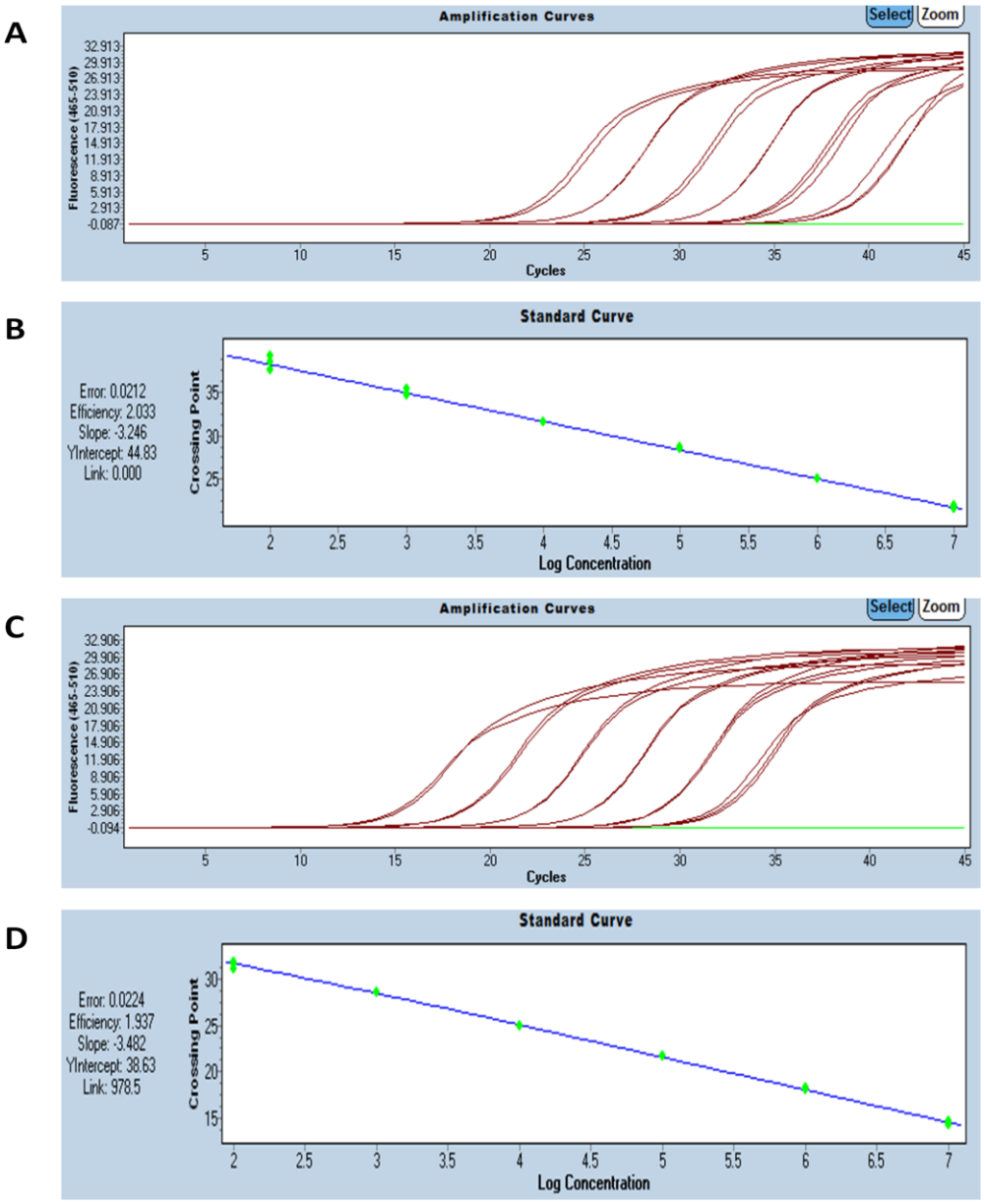

Fig 3.15 Optimised L74V Standard Curves. The optimised standard curve can be seen in A and B. Figure A shows the amplification curves for the L74V specific standard curve and B shows the actual standard curve with the log concentration of the standard dilutions on the x-axis plotted against the crossing point on the y-axis. The results for the optimised L74V non-specific amplification curves and the standard curve can be seen in C and D, respectively.

3.8 Sensitivity/ LOD Test

The sensitivity test was performed by preparing 18 replicates of the 10^6 dilution WT DNA in the specific and non-specific mastermix, separately, as described in 2.9.4 for K65R. Following completion of the run, external specific and non-specific standard curves were imported into the run using a 10^6 dilution WT DNA (prepared in the appropriate mastermix) as an internal standard. The specific and non-specific standard curves were used to calculate the mean concentration of the 18 replicates in the specific and non-specific reactions, respectively. The sensitivity of the assay was determined as described in 2.9.4. The sensitivity obtained was 0.013%. Therefore, this is the percentage at which the assay begins to produce false positives.

3.9 Accuracy Test

The accuracy test was carried out by preparing 10-fold serial dilutions of the 10^6dilution L74V plasmid DNA with the 10^6dilution WT plasmid DNA, as explained in 2.9.5 (for K65R). Each of the dilutions was run in triplicate. For the L74V specific reaction, Figure 3.16 (A), the 100% mutant amplicons started amplifying between 25.2and 26cycles, the dilution containing 10% mutant amplicons started amplifying between29.4 and 29.6 cycles, the dilution containing 1% mutant amplicons started amplifying between 32.5 and 33 cycles and the dilution containing the0.1% mutant amplicons began amplifying between 35.9 and 36.5 cycles . The remaining dilutions (i.e 0.01% and 0.001%) started amplifying from 35.94 cycles. The dilution at which accuracy was lost was the 0.1% mutant dilution. For the non-specific reaction, Figure 3.16 (B), each of the dilutions was prepared using the primers for the non-specific reaction. Each of the dilutions was run in triplicate. All the dilutions started amplifying between18.03 to 18.76 cycles, which corresponds to the cycle number that the

10^6dilution usually starts amplifying at on the L74V non-specific standard curve. The L74V specific and non-specific standard curves were imported into the run to determine if the calculated percentage matched the nominal proportion, as shown in Table 3.5. The measured proportions were plotted against the nominal proportions and the results obtained can be seen in Figure 3.17. Because the calculated nominal proportions were shifted to the right of the theoretical perfect match, the preparation of the dilutions (as explained in 2.9.5) was repeated, using the 10^7mutant dilution with the 10^7 dilution WT DNA, and the accuracy test was performed again. The results of this, which can be seen in Figure 3.18 (A), shows that the dilution at which accuracy was lost was the 0.1% dilution, which is the same as before. The amplification curves for the non-specific reaction can be seen in Figure 3.18 (B). The amplification curves amplified between 14.8 and 15.8 cycles, which corresponds with the cycle number at which the 10^7 dilution usually starts amplifying at in the non-specific standard curve. The table (Table 3.6) shows that the measured proportion compared to the corresponding nominal proportion was similar from the 0.1% dilution upwards. The graph (Figure 3.19) shows the measured proportion plotted against the nominal proportion. These results show that the calculated percentages for the dilutions behave similarly to the theoretical perfect match from the 0.1% dilution upwards.

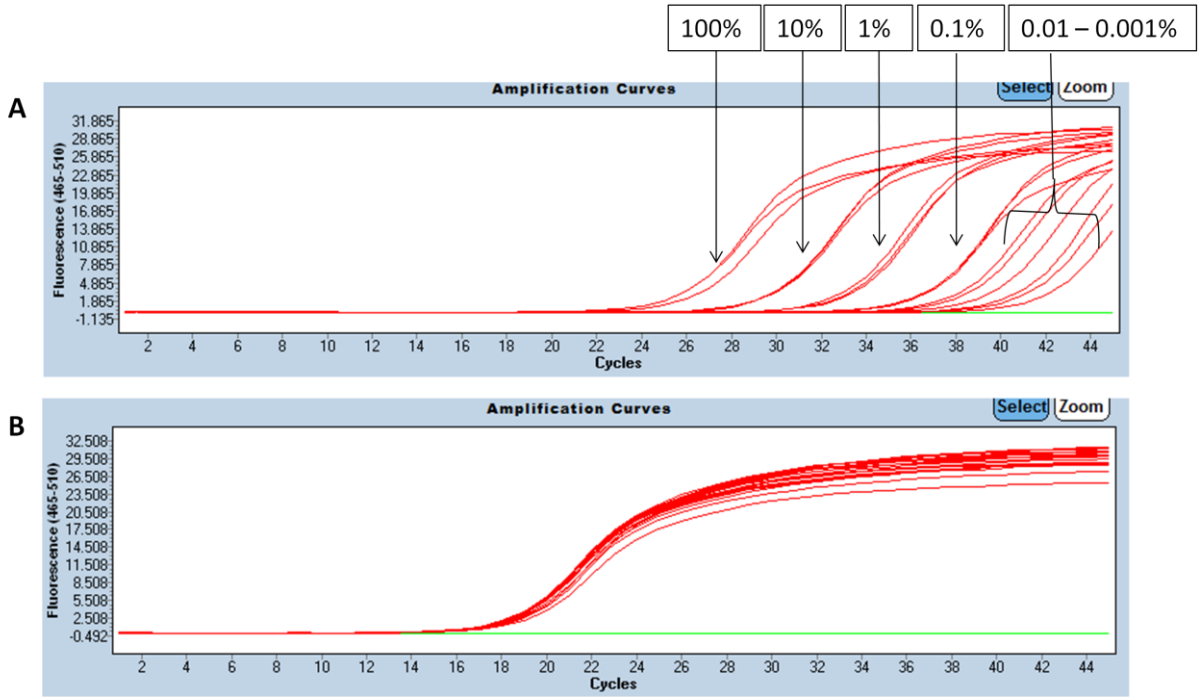

Fig 3.16 Amplification Curves for the L74V Accuracy Test. Results showing the amplification curves for the 10-fold serial dilutions of the L74V specific reaction (A) and the non-specific reaction (B). The green lines in both A and B represent the negative control.

Table 3.5 Measured Proportion against Nominal Proportion for the L74V Accuracy Test. The table shows the nominal proportions (which is the hypothetical percentage of the 10^6 dilution L74V plasmid DNA prepared with 10^6dilution WT plasmid DNA) of the samples prepared and the measured proportion as calculated on the LC480.

Nominal Proportion	Measured Proportion
100	68
10	3.6
1	0.34
0.1	0.03
0.01	0.004
0.001	0.003

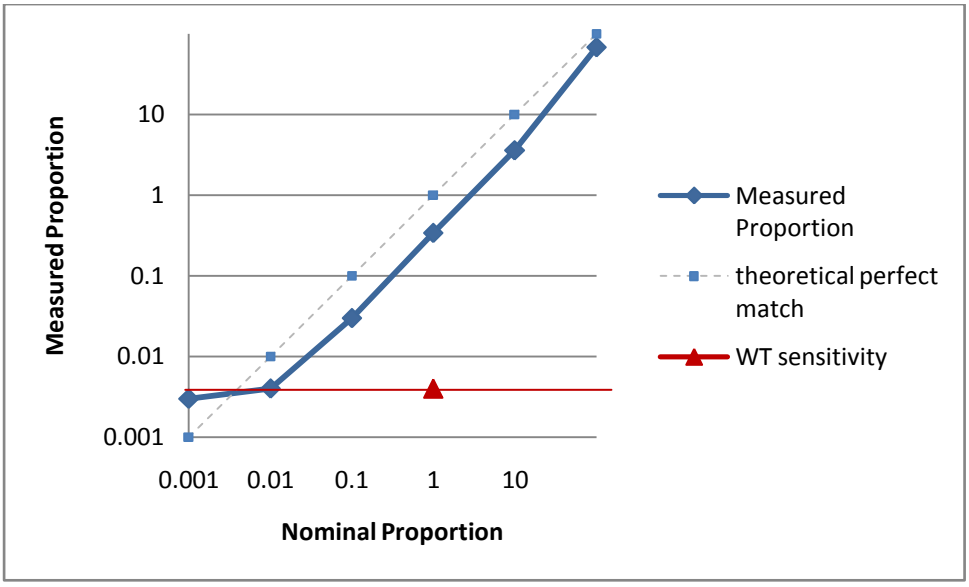

Fig 3.17 Graph Showing the Measured Proportion Plotted against the Nominal Proportion for L74V. This graph shows the measured proportion (on the y-axis) plotted against the nominal (hypothetical) proportion (on the x-axis). The green dotted line represents the theoretical perfect match of the measured proportion against the nominal proportion. As can be seen from the results obtained from the experiment (represented by the blue line), it appears that an error may have occurred in the preparation of the 10% mutant dilution, which was carried forward in the subsequent dilutions. However, the percentage at which the WT starts to produce false positives results (the red line) is 0.004%. Therefore, the limit of detection of the test is 0.004%.

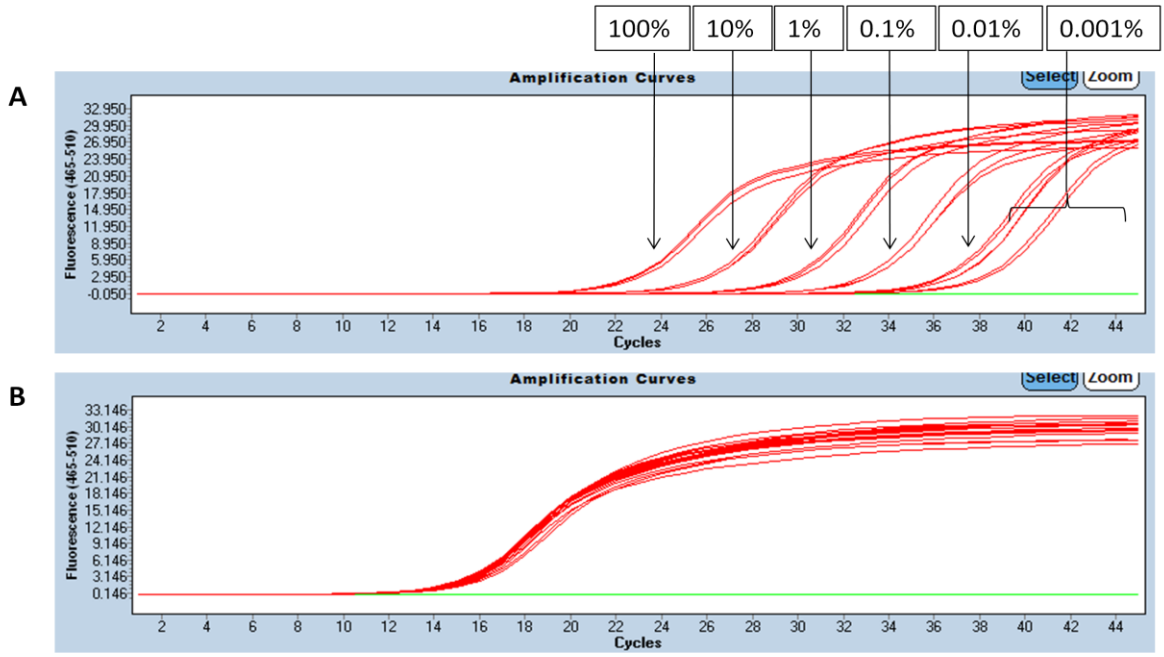

Fig 3.18 Amplification Curves for the L74V Accuracy Test. Results showing the amplification curves for the 10-fold serial dilutions of the L74V specific reaction (A) and the non-specific reaction (B). The green lines in both A and B represent the negative control.

Table 3.6 Measured against Nominal Proportion for L74V Accuracy Test. The table shows the nominal proportions (which is the percentage of the 10^7 dilution L74V plasmid DNA prepared with the 10^7 dilution WT plasmid DNA) of the samples prepared and the corresponding measured proportion (as calculated on the LC480).

Nominal Proportion	Measured Proportion
100	130
10	7.1
1	0.5
0.1	0.051
0.01	0.004
0.001	0.0016

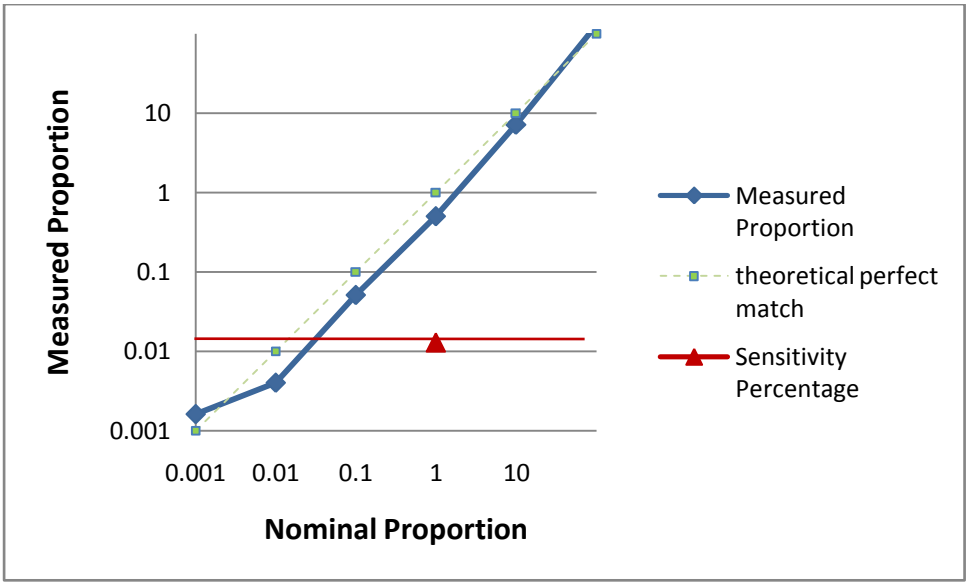

Fig 3.19 Graph Showing the Measured Proportion Plotted against the Nominal Proportion for L74V. This graph shows the measured proportion (on the y-axis) plotted against the nominal (hypothetical) proportion (on the x-axis). The green dotted line represents the theoretical perfect match of the measured proportion against the nominal proportion. As it can be seen from the results obtained from the experiment (represented by the blue line), the measured proportion plotted against the nominal proportion closely matches the theoretical perfect match. However, the percentage at which the WT starts to produce false positives results (the red line) is 0.013%. Therefore, the limit of detection of the test is 0.013%.

3.10 Quantification of the Patient Samples using L74V ASPCR

Table 3.7 contains the L74V ASPCR results for the 84 samples for which RT-PCR products were obtained. Positive results were obtained for 9 out of the 84 samples (10.7%). For 4 samples, the mutation was detected above 1% (viz. 2.82%, 10.10%, 12.02% and 18.22%), while for the remaining 5 samples the mutation was detected below 1% (i.e 2 were 0.5% to <1%, while 3 were >0.013% to <0.5%).

Table 3.7 List of Samples that were Analysed using the L74V ASPCR

	Sample Name	L74V specific reaction mean concentration (copies)	L74V non-specific reaction mean concentration (copies)	Ratio of specific / non specific mean concentration (copies)	Percentage of the Ratio
1	Sw1	0	1.50×10^{3}	0	0%
2	Sw2	0	2.71×10^{9}	0	0%
3	Sw3	0	1.35×10^{5}	0	0%
4	Sw6	0	2.67×10^{9}	0	0%
5	Sw7	* >40 cycles	3.05×10^{6}	0	0%
6	**Sw8**	**1315**	**4.58×10^{4}**	**2.82×10^{-2}**	**2.82%**
7	Sw9	0	1.6×10^{4}	0	0%
8	Sw10	0	3.97×10^{3}	0	0%
9	Sw11	0	5.87×10^{8}	0	0%
10	Sw12	252.5	1.53×10^{7}	1.58×10^{-5}	0.0016%
11	Sw14	* >40 cycles	4.49×10^{7}	0	0%
12	Sw15	0	2.39×10^{5}	0	0%
13	Sw16	0	5.81×10^{8}	0	0%
14	Sw17	0	7.61×10^{8}	0	0%
15	Sw18	0	7509.5	0	0%
16	Sw19	0	5.24×10^{3}	0	0%
17	Sw20	0	6.66×10^{9}	0	0%
18	Sw21	0	3.9×10^{3}	0	0%
19	Sw23	0	7.39×10^{7}	0	0%
20	Sw24	0	2.65×10^{9}	0	0%
21	Sw25	* >40 cycles	1.91×10^{6}	0	0%
22	Sw26	* >40 cycles	1.55×10^{7}	0	0%
23	Sw27	0	9.57×10^{8}	0	0%
24	Sw28	0	1.61×10^{9}	0	0%
25	Sw29	0	1.36×10^{8}	0	0%
26	Sw30	1350	1.255×10^{7}	1.08×10^{-4}	0.011%
27	Sw31	0	6.95×10^{8}	0	0%
28	Sw33	0	1.81×10^{9}	0	0%
29	Sw34	0	1.81×10^{9}	0	0%

	Sample Name	L74V specific reaction mean concentration (copies)	L74V non-specific reaction mean concentration (copies)	Ratio of specific / non specific mean concentration (copies)	Percentage of the Ratio
30	Sw35	* >40 cycles	6.65×10^{5}	0	0%
31	Sw36	0	6.1×10^{8}	0	0%
32	Sw37	0	1.81×10^{3}	0	0%
33	Sw38	0	3.35×10^{7}	0	0%
34	Sw41	0	1.68×10^{8}	0	0%
35	Sw42	* >40 cycles	5.62×10^{4}	0	0%
36	Sw43	0	1.17×10^{8}	0	0%
37	Sw44	0	500	0	0%
38	Sw45	0	1.12×10^{8}	0	0%
39	Sw46	0	5.46×10^{8}	0	0%
40	Sw47	0	2.78×10^{9}	0	0%
41	Sw48	* >40 cycles	5.59×10^{4}	0	0%
42	Sw49	0	3.8×10^{8}	0	0%
43	Sw50	0	2.19×10^{8}	0	0%
44	Sw52	0	12750	0	0%
45	Sw53	0	4.42×10^{7}	0	0%
46	**Sw54**	**177**	**9.15×10^{5}**	**1.94×10^{-4}**	**0.019%**
47	Sw55	0	1.42×10^{9}	0	0%
48	Sw57	* >40 cycles	4.70×10^{5}	0	0%
49	Sw58	0	2.17×10^{8}	0	0%
50	Sw59	0	1.78×10^{5}	0	0%
51	Sw60	* >40 cycles	9.29×10^{5}	0	0%
52	Sw61	0	4.91×10^{4}	0	0%
53	Sw63	0	1.19×10^{9}	0	0%
54	Sw65	0	7.84×10^{8}	0	0%
55	Sw66	0	1.40×10^{8}	0	0%
56	Sw67	0	4.05×10^{8}	0	0%
57	**Sw69**	**9.74×10^{4}**	**9.67×10^{5}**	**0.1010**	**10.10%**
58	Sw71	* >40 cycles	9.51×10^{6}	0	0%
59	Sw72	0	1.75×10^{9}	0	0%
60	Sw73	0	8.16×10^{3}	0	0%
61	Sw74	* >40 cycles	27.4	0	0%
62	Sw75	* >40 cycles	8.74×10^{4}	0	0%
63	Sw76	0	1.06×10^{5}	0	0%
64	Sw77	0	4.16×10^{4}	0	0%
65	Sw78	0	1.17×10^{9}	0	0%
66	**Sw79**	**2.50×10^{3}**	**2.06×10^{4}**	**0.1202**	**12.02%**
67	Sw80	0	3.88×10^{9}	0	0%
68	Sw81	0	6.745×10^{4}	0	0%
69	**Sw82**	**2585**	**5.343×10^{5}**	**5.28×10^{-3}**	**0.53%**
70	**Sw83**	**4.0×10^{5}**	**4.43×10^{7}**	**9.13×10^{-3}**	**0.36%**
71	Sw84	0	1.9×10^{9}	0	0%
72	Sw88	1.38×10^{3}	2.20 10^{7}	6.27×10^{-5}	0.0063%
73	Sw89	0	5.4×10^{5}	0	0%
74	Sw90	0	4.1×10^{9}	0	0%

	Sample Name	L74V specific reaction mean concentration (copies)	L74V non-specific reaction mean concentration (copies)	Ratio of specific / non specific mean concentration (copies)	Percentage of the Ratio
75	Sw91	0	3.5×10^{8}	0	0%
76	**Sw92**	**1.39×10^{4}**	**2.37×10^{6}**	**5.86×10^{-3}**	**0.59%**
77	Sw93	* >40 cycles	1.84×10^{6}	0	0%
78	Sw94	* >40 cycles	5.92×10^{6}	0	0%
79	**Sw97**	334	9.83×10^{6}	3.37×10^{-5}	0.0034%
80	Sw98	* >40 cycles	7.87×10^{5}	0	0%
81	**Sw99**	**1.69×10^{4}**	**9.23×10^{4}**	**0.1822**	**18.22%**
82	**Sw100**	**285.3**	**4.23×10^{5}**	**6.73×10^{-4}**	**0.067%**
83	Sw101	0	1.52×10^{3}	0	0%
84	Sw102	* >40 cycles	5.0×10^{7}	0	0%

* >40 cycles denotes that the L74V specific samples amplified after 40 cycles. This means that the percentage of the mutant in the specific reaction was very low, since the L74V non-specific reactions were amplifiable within the standard curve range for these samples. The LC480 software assigns a common number to any samples that amplify after 40 cycles, which means that the calculated percentage is incorrect.
Samples that appear in bold font are the samples in which the L74V were detected.

CHAPTER 4

Discussion

In 2010, the change in the South African ARV treatment regimen recommended the use of TDF and ABC for the treatment of adult and paediatric patients, respectively, in both the first-line and second-line regimens. However, recent studies have shown that there has been an increase in the presence of the mutations that cause resistance to these drugs, viz. the K65R and L74V mutations (Van Zyl et al., 2013, Sunpath et al., 2012). The K65R mutation, which confers resistance to TDF, has been shown to occur preferentially in subtype C viruses, which is a cause for major concern in South Africa where subtype C is the most common HIV-1 subtype. Furthermore, the K65R mutation has been shown to be present in the minor viral population and can be transmitted to newly infected individuals (Gianella and Richman, 2010, Johnson et al., 2008, Little et al., 2002). In South Africa, resistance testing is commonly performed by population-based sequencing (which can detect mutations that are present in $\geq$ 20% of the viral population) and as a result resistance mutations that are present in the minor viral population may be missed.

While several technologies have been developed to detect resistance mutations in minor variants, ASPCR has been shown to be one of the most sensitive methods and can detect resistance mutations that are present in <1% of the viral population (Halvas et al., 2006). Furthermore, this assay has been found to be less laborious and time-consuming than other methods used for similar functions (Paredes et al., 2007). In this study, ASPCR was used to determine the prevalence of the K65R and L74V resistance mutations in the minor viral population of patients failing HAART (that did not include TDF or ABC) in KwaZulu Natal, South Africa. For the K65R assay, the accuracy test showed that the LC480 was able to detect the measurements accurately down to 1%, but between the 1% dilution and the 0.1%

dilution, this accuracy was lost. The results of the K65R sensitivity test showed that the assay starts to produce false positive results at 0.72%, so this was taken as the sensitivity of the test. For the L74V assay, the accuracy test showed that the lowest dilution that produced accurate amplification curves was 0.01%, but this accuracy was lost between the 0.01% and 0.001% dilution. The results of the L74V sensitivity test was 0.013%, which is the percentage at which this assay starts to produce false positive results. The sensitivity of both ASPCR assays are comparable to the sensitivity obtained from other ASPCR studies, which have reported that the assay is able to detect mutations that are present in <1% of the viral population (Paredes et al., 2007, Halvas et al., 2006). It was recently reported that a mutation that is present at frequencies as low as 0.5% can increase the risk of treatment failure(Li and Kuritzkes, 2013), highlighting the need for sensitive assays such as ASPCR for the detection of resistance mutations.

Where we investigated the prevalence of the K65R and L74V mutations in a cohort that was TDF and ABC-naïve, we found the K65R mutation in 7 (8.33%) of 84 patients. Five of these 7 patients contained the K65R mutation in 1% or more of the viral population (i.e 3 were about 2%, 1 was 9.48% and 1 was 100%), whilst the remaining 2 patients contained the mutation in between 0.5 and 1% of the viral population. It is possible that this could contribute to future virologic failure in these 7 patients. This cohort had been previously genotyped using Sanger sequencing by Marconi *et al.* (2008) who reported the prevalence of the K65R mutation to be 3%. Our assay detected the K65R mutation in 2 (1 at 9.48% and 1 at 100%) out of the 4 patients described in Marconi *et al.* (2008). The other 2 patients were detected with a mixture of WT and K65R mutation (with Sanger sequencing) and was possibly not detected by ASPCR due to RT-PCR amplification bias or it could be possible that these mixtures were a result of incorrect base-calling in Sanger sequencing. However, the ASPCR assay was able to detect the K65R resistance mutation in the minor viral

population that was missed by population-based sequencing in a further 5.3% of the patients. Since the patients in this study were failing their first-line HAART that did not include TDF, these patients would have been switched to the 2010 amended TDF-containing second-line treatment, and the presence of the low-level K65R mutation could have compromised the success of their treatment. There are 2 possibilities for the emergence of this mutation in this TDF-naïve population. Firstly, many of these patients were failing treatment that contained d4T, and even though K65R development usually occurs through TDF exposure, this mutation could also develop when exposed to d4T (Brenner and Coutsinos, 2009). If the development of K65R in these patients occurred through d4T exposure, this would have resulted in cross-resistance to TDF in the second-line HAART. The other possibility is that this mutation could have been pre-existing (i.e it was not selected for by drug selection pressure), which would imply that drug-naïve patients could also have these mutants. This could then compromise the success of treatment in patients starting first-line TDF. The recent report by Sunpath *et al*. (2012) has shown a high prevalence of K65R in patients failing first-line TDF. This therefore emphasizes the importance of introducing a sensitive screening test to identify the K65R mutation in the minor viral population prior to commencing or switching to a TDF-containing first-line or second-line treatment regimen.

For the L74V mutation, 9 (10.7%) of 84 patients harboured this mutation. This was also higher than reported for Sanger sequencing by Marconi *et al.* (2008) who found the mutation in only 2 samples (1.7%) of the study population. Of these 2 samples, 1 contained the L74V mutation and the other contained the L74I mutation. As the L74V ASPCR specifically detects the L74V mutation, it was able to detect the 1 sample carrying the L74V mutation at 18.22%. The patient carrying the L74I mutation was not detected. In 4 of the 9 patients detected by ASPCR, the L74V mutation was found in ≥1% of the viral population. In the other 5 patients, the L74V mutation was detected in 2 isolates ≥0.5% and 3 were between

>0.013% to <0.5%. The clinical relevance of samples detected at frequencies <0.5% are unknown. While the patients in this study were adult patients that were failing ARV first-line treatment that did not include ABC, this assay can be used to test for the L74V mutation in paediatric patients initiating, or failing, an ABC-containing regimen.

In South Africa, there has been an increase in the TDF and ABC resistance mutations. Since the presence of resistance mutations in a frequency of as low as 0.5% can increase the risk of virologic failure (Li and Kuritzkes, 2013), introducing a screening test into the public sector would be of benefit, as it will enable the detection of TDF drug resistance mutations. This type of surveillance would guide policy makers, ensuring the use of effective regimens in the National ARV programme. Due to the high rate of K65R first-line treatment failures, it is possible that the mutations could be naturally occurring, and if this is so then it would be beneficial to test for these mutations prior to starting a first-line treatment regimen. If such a test was to be implemented, the minimum cut-off percentage would be 0.5% or the LOD of the test (i.e if the LOD of the test is higher than 0.5%).

Although ASPCR has many advantages over other methods used for the same purpose, it also has limitations. One of the disadvantages of using this method is that polymorphisms that occur in the primer binding sites (near the 3' end) may affect the binding of the specific primers, leading to underestimation of the mutation in the viral population, although polymorphisms that exist near the 5' end of the specific primer set has not much effect on the accuracy (Paredes et al., 2007). To correct for this, usually these polymorphisms (which may have been detected previously by population-based sequencing) are incorporated into the specific primer set. In addition, appropriate polymorphisms would also have to be incorporated into the standards, since the occurrence of other additional mismatches in the specific primer set (which are not present in the standard sequence) may constrain the amplification of the specific standard curve compared to the non-specific standard curve.

However, it has been suggested that using SYBR Green instead of Taqman probes may help resolve issues introduced by polymorphisms (Paredes et al., 2007). Therefore SYBR Green was used in this study to decrease the effect of polymorphisms on specificity. Another concern with using ASPCR is that to obtain equal amplification efficiencies, it is imperative that both the specific and non-specific primers bind to the same region of the DNA. To achieve this, the non-specific primer used in this study was identical to the specific primer, except that it stopped before the target mutation and lacked the intentional mismatch present in the specific primer.

A few problems were experienced during the course of the project. Firstly, not all of the samples were amplifiable by RT-PCR. Many attempts were made to obtain PCR products for these samples by either using different RNA extracts or increasing the total reaction volumes used, leading to the successful amplification of ten of the problematic samples. A subset of the remaining samples was tested using a different PCR, however, the samples did not amplify, suggesting that the problem was possibly related to the quality of the RNA sample. Secondly, because the LC 480 instrument uses a 96-well plate format, which is an open system, it is more prone to cross-contamination. Therefore, extreme caution had to be exercised when handling the plates and during the process of loading the mastermix and samples onto the plates. Thirdly, initial difficulty experienced in preparing the standard dilutions and optimising the standard curve, was overcome by preparing the standard dilutions in 1mM EDTA, which was found to stabilise the standard dilutions, resulting in them producing an improved standard curve. Finally, the L74V accuracy test had to be repeated since an error occurred in the serial dilution, which was corrected for by repeating the preparation of the dilutions.

In essence, ASPCR had been found to be a valuable assay for detecting the presence of mutations in the minor viral population. Recent reports have shown a high prevalence of the

K65R and L74V mutations in first-line failures, since the introduction of TDF and ABC in the first-line treatment regimens and second-line treatment regimens (Sunpath et al., 2012, Van Zyl et al., 2013). The results of this study show that these mutations are present in the minority variants in patients that have not been exposed to TDF or ABC, which could possibly threaten the success of ARV treatment. This further emphasizes the need to screen patients using a sensitive test, like ASPCR, prior to beginning a first-line or second-line treatment regimen containing TDF or ABC. However, the practicality of implementing these assays would need to be addressed in South Africa due to the large numbers of patients that would have to be screened. Supplier negotiation tactics could be explored to reduce the cost of the reagents and equipment required, thereby reducing the cost of the assays. Furthermore, cheaper point-of-care applications could be implemented to make these assays more accessible in the public-sector, and more specifically in resource-limited settings.

CHAPTER 5

Conclusion

TDF and ABC have been recommended as preferred first-line and second-line drugs in the South African 2013 ARV treatment guidelines. However, the recent increase in the development of the K65R and L74V resistance mutations in South Africa poses a major problem as these mutations cause resistance to TDF and ABC, respectively.

We developed two ASPCR assays, one for K65R and another for L74V, that were able to detect these mutations in 0.72% and 0.013% of the viral population respectively, proving to be far more sensitive than population-based sequencing. In addition, the assays were able to detect more K65R and L74V mutations than were detected by Sanger sequencing in the same cohort of patients. Since the presence of resistance mutations may increase the risk of future virological failure, using a sensitive test like ASPCR would prove to be a valuable tool to detect the presence of the K65R and L74V resistance mutations in the minority variants prior to initiating or switching ARV treatments.

CHAPTER 6

References

ARTS, E. J. & HAZUDA, D. J. 2012. HIV-1 antiretroviral drug therapy. *Cold Spring Harb Perspect Med,* 2**,** a007161.

ARYA, M., SHERGILL, I. S., WILLIAMSON, M., GOMMERSALL, L., ARYA, N. & PATEL, H. R. 2005. Basic principles of real-time quantitative PCR. *Expert Rev Mol Diagn,* 5**,** 209-19.

BANSAL, V., METZNER, K. J., NIEDEROST, B., LEEMANN, C., BONI, J., GUNTHARD, H. F. & FEHR, J. S. 2011. Minority K65R variants and early failure of antiretroviral therapy in HIV-1-infected Eritrean immigrant. *Emerg Infect Dis,* 17**,** 1966-8.

BARRE-SINOUSSI, F. 1996. HIV as the cause of AIDS. *Lancet,* 348**,** 31-5.

BARRE-SINOUSSI, F., CHERMANN, J. C., REY, F., NUGEYRE, M. T., CHAMARET, S., GRUEST, J., DAUGUET, C., AXLER-BLIN, C., VEZINET-BRUN, F., ROUZIOUX, C., ROZENBAUM, W. & MONTAGNIER, L. 1983. Isolation of a T-lymphotropic retrovirus from a patient at risk for acquired immune deficiency syndrome (AIDS). *Science,* 220**,** 868-71.

BLACKARD, J. T., COHEN, D. E. & MAYER, K. H. 2002. Human immunodeficiency virus superinfection and recombination: current state of knowledge and potential clinical consequences. *Clin Infect Dis,* 34**,** 1108-14.

BRENNER, B. G. & COUTSINOS, D. 2009. The K65R mutation in HIV-1 reverse transcriptase: genetic barriers, resistance profile and clinical implications. *HIV Ther,* 3**,** 583-594.

BRENNER, B. G., OLIVEIRA, M., DOUALLA-BELL, F., MOISI, D. D., NTEMGWA, M., FRANKEL, F., ESSEX, M. & WAINBERG, M. A. 2006. HIV-1 subtype C viruses rapidly develop K65R resistance to tenofovir in cell culture. *AIDS,* 20**,** F9-13.

BUSTIN, S. A. & MUELLER, R. 2005. Real-time reverse transcription PCR (qRT-PCR) and its potential use in clinical diagnosis. *Clin Sci (Lond),* 109**,** 365-79.

BUTLER, I. F., PANDREA, I., MARX, P. A. & APETREI, C. 2007. HIV genetic diversity: biological and public health consequences. *Curr HIV Res,* 5**,** 23-45.

CLAVEL, F., GUETARD, D., BRUN-VEZINET, F., CHAMARET, S., REY, M. A., SANTOS-FERREIRA, M. O., LAURENT, A. G., DAUGUET, C., KATLAMA, C., ROUZIOUX, C. & ET AL. 1986. Isolation of a new human retrovirus from West African patients with AIDS. *Science,* 233**,** 343-6.

CLAVEL, F. & HANCE, A. J. 2004. HIV drug resistance. *N Engl J Med,* 350**,** 1023-35.

COHEN, M. S., HELLMANN, N., LEVY, J. A., DECOCK, K. & LANGE, J. 2008. The spread, treatment, and prevention of HIV-1: evolution of a global pandemic. *J Clin Invest,* 118**,** 1244-54.

CORTEZ, K. J. & MALDARELLI, F. 2011. Clinical management of HIV drug resistance. *Viruses,* 3**,** 347-78.

COUTSINOS, D., INVERNIZZI, C. F., XU, H., MOISI, D., OLIVEIRA, M., BRENNER, B. G. & WAINBERG, M. A. 2009. Template usage is responsible for the preferential acquisition of the K65R reverse transcriptase mutation in subtype C variants of human immunodeficiency virus type 1. *J Virol,* 83**,** 2029-33.

DAS, K., BANDWAR, R. P., WHITE, K. L., FENG, J. Y., SARAFIANOS, S. G., TUSKE, S., TU, X., CLARK, A. D., JR., BOYER, P. L., HOU, X., GAFFNEY, B. L., JONES, R. A., MILLER, M. D., HUGHES, S. H. & ARNOLD, E. 2009. Structural basis for the role of the K65R mutation in HIV-1 reverse transcriptase polymerization, excision antagonism, and tenofovir resistance. *J Biol Chem,* 284**,** 35092-100.

DEVAL, J., NAVARRO, J. M., SELMI, B., COURCAMBECK, J., BORETTO, J., HALFON, P., GARRIDO-URBANI, S., SIRE, J. & CANARD, B. 2004. A loss of viral replicative capacity correlates with altered DNA polymerization kinetics by the human immunodeficiency virus reverse transcriptase bearing the K65R and L74V dideoxynucleoside resistance substitutions. *J Biol Chem,* 279**,** 25489-96.

DIALLO, K., MARCHAND, B., WEI, X., CELLAI, L., GOTTE, M. & WAINBERG, M. A. 2003. Diminished RNA primer usage associated with the L74V and M184V mutations in the reverse transcriptase of human immunodeficiency virus type 1 provides a possible mechanism for diminished viral replication capacity. *J Virol,* 77**,** 8621-32.

DOH. 2004. Department of Health. The South African National Antiretroviral Treatment Guidelines 2004. Available: http://southafrica.usembassy.gov/media/2004-doh-art-guidelines.pdf [Accessed 18 August 2012].

DOH. 2010. Department of Health. The South African Antiretroviral Treatment Guidelines 2010. Available: http://www.uj.ac.za/EN/CorporateServices/ioha/Documentation/Documents/ART%20Guideline.pdf [Accessed 18 August 2012].

FANALES-BELASIO, E., RAIMONDO, M., SULIGOI, B. & BUTTO, S. 2010. HIV virology and pathogenetic mechanisms of infection: a brief overview. *Ann Ist Super Sanita,* 46**,** 5-14.

FRANKEL, F. A., MARCHAND, B., TURNER, D., GOTTE, M. & WAINBERG, M. A. 2005. Impaired rescue of chain-terminated DNA synthesis associated with the L74V mutation in human immunodeficiency virus type 1 reverse transcriptase. *Antimicrob Agents Chemother,* 49**,** 2657-64.

GALLANT, J. E. & DERESINSKI, S. 2003. Tenofovir disoproxil fumarate. *Clin Infect Dis,* 37**,** 944-50.

GALLO, R. C., SARIN, P. S., GELMANN, E. P., ROBERT-GUROFF, M., RICHARDSON, E., KALYANARAMAN, V. S., MANN, D., SIDHU, G. D., STAHL, R. E., ZOLLA-PAZNER, S., LEIBOWITCH, J. & POPOVIC, M. 1983. Isolation of human T-cell leukemia virus in acquired immune deficiency syndrome (AIDS). *Science,* 220**,** 865-7.

GAO, F., VIDAL, N., LI, Y., TRASK, S. A., CHEN, Y., KOSTRIKIS, L. G., HO, D. D., KIM, J., OH, M. D., CHOE, K., SALMINEN, M., ROBERTSON, D. L., SHAW, G. M., HAHN, B. H. & PEETERS, M. 2001. Evidence of two distinct subsubtypes within the HIV-1 subtype A radiation. *AIDS Res Hum Retroviruses,* 17**,** 675-88.

GIANELLA, S. & RICHMAN, D. D. 2010. Minority variants of drug-resistant HIV. *J Infect Dis,* 202**,** 657-66.

HALVAS, E. K., ALDROVANDI, G. M., BALFE, P., BECK, I. A., BOLTZ, V. F., COFFIN, J. M., FRENKEL, L. M., HAZELWOOD, J. D., JOHNSON, V. A., KEARNEY, M., KOVACS, A., KURITZKES, D. R., METZNER, K. J., NISSLEY, D. V., NOWICKI, M., PALMER, S., ZIERMANN, R., ZHAO, R. Y., JENNINGS, C. L., BREMER, J., BRAMBILLA, D. & MELLORS, J. W. 2006. Blinded, multicenter comparison of methods to detect a drug-resistant mutant of human immunodeficiency virus type 1 at low frequency. *J Clin Microbiol,* 44**,** 2612-4.

HAMERS, R. L., SIGALOFF, K. C., WENSING, A. M., WALLIS, C. L., KITYO, C., SIWALE, M., MANDALIYA, K., IVE, P., BOTES, M. E., WELLINGTON, M., OSIBOGUN, A., STEVENS, W. S., RINKE DE WIT, T. F. & SCHUURMAN, R. 2012. Patterns of HIV-1 drug resistance after first-line antiretroviral therapy (ART) failure in 6 sub-Saharan African countries: implications for second-line ART strategies. *Clin Infect Dis,* 54**,** 1660-9.

HARRIGAN, P. R. & COTE, H. C. 2000. Clinical utility of testing human immunodeficiency virus for drug resistance. *Clin Infect Dis,* 30 Suppl 2**,** S117-22.

HARTMAN, T. L. & BUCKHEIT, R. W., JR. 2012. The Continuing Evolution of HIV-1 Therapy: Identification and Development of Novel Antiretroviral Agents Targeting Viral and Cellular Targets. *Mol Biol Int,* 2012**,** 401965.

HAUSER, A., MUGENYI, K., KABASINGUZI, R., BLUETHGEN, K., KUECHERER, C., HARMS, G. & KUNZ, A. 2009. Detection and quantification of minor human immunodeficiency virus type 1 variants harboring K103N and Y181C resistance mutations in subtype A and D isolates by allele-specific real-time PCR. *Antimicrob Agents Chemother,* 53**,** 2965-73.

HENRY, M., TOURRES, C., COLSON, P., RAVAUX, I., POIZOT-MARTIN, I. & TAMALET, C. 2006. Coexistence of the K65R/L74V and/or K65R/T215Y mutations on the same HIV-1 genome. *J Clin Virol,* 37**,** 227-30.

HICKS, C. & GULICK, R. M. 2009. Raltegravir: the first HIV type 1 integrase inhibitor. *Clin Infect Dis,* 48**,** 931-9.

HOFFMANN-LA_ROCHE. LightCycler® Real-Time PCR Systems - Application Manual Version 1. Available: http://www.roche-diagnostics.ch/content/dam/corporate/roche-dia_ch/documents/broschueren/applied_science/qPCR-NAP/LightCycler/05444217001_EN_EA_LightCycler-480-Real-Time-PCR-Systems-Application-Manual.pdf.

HOFFMANN, C. J., LEDWABA, J., LI, J. F., JOHNSTON, V., HUNT, G., FIELDING, K. L., CHAISSON, R. E., CHURCHYARD, G. J., GRANT, A. D., JOHNSON, J. A.,

CHARALAMBOUS, S. & MORRIS, L. 2013. Resistance to tenofovir-based regimens during treatment failure of subtype C HIV-1 in South Africa. *Antivir Ther*.

JACOBS, G. B., WILKINSON, E., ISAACS, S., SPIES, G., DE OLIVEIRA, T., SEEDAT, S. & ENGELBRECHT, S. 2014. HIV-1 subtypes B and C unique recombinant forms (URFs) and transmitted drug resistance identified in the Western Cape Province, South Africa. *PLoS One,* 9**,** e90845.

JOHNSON, J. A., LI, J. F., WEI, X., LIPSCOMB, J., IRLBECK, D., CRAIG, C., SMITH, A., BENNETT, D. E., MONSOUR, M., SANDSTROM, P., LANIER, E. R. & HENEINE, W. 2008. Minority HIV-1 drug resistance mutations are present in antiretroviral treatment-naive populations and associate with reduced treatment efficacy. *PLoS Med,* 5**,** e158.

KLIMAS, N., KONERU, A. O. & FLETCHER, M. A. 2008. Overview of HIV. *Psychosom Med,* 70**,** 523-30.

LARDER, B. A., DARBY, G. & RICHMAN, D. D. 1989. HIV with reduced sensitivity to zidovudine (AZT) isolated during prolonged therapy. *Science,* 243**,** 1731-4.

LEITNER, T., HALAPI, E., SCARLATTI, G., ROSSI, P., ALBERT, J., FENYO, E. M. & UHLEN, M. 1993. Analysis of heterogeneous viral populations by direct DNA sequencing. *Biotechniques,* 15**,** 120-7.

LI, J. Z. & KURITZKES, D. R. 2013. Clinical implications of HIV-1 minority variants. *Clin Infect Dis,* 56**,** 1667-74.

LITTLE, S. J., HOLTE, S., ROUTY, J. P., DAAR, E. S., MARKOWITZ, M., COLLIER, A. C., KOUP, R. A., MELLORS, J. W., CONNICK, E., CONWAY, B., KILBY, M., WANG, L., WHITCOMB, J. M., HELLMANN, N. S. & RICHMAN, D. D. 2002. Antiretroviral-drug resistance among patients recently infected with HIV. *N Engl J Med,* 347**,** 385-94.

MASQUELIER, B., TAMALET, C., MONTES, B., DESCAMPS, D., PEYTAVIN, G., BOCKET, L., WIRDEN, M., IZOPET, J., SCHNEIDER, V., FERRE, V., RUFFAULT, A., PALMER, P., TRYLESINSKI, A., MILLER, M., BRUN-VEZINET, F. & COSTAGLIOLA, D. 2004. Genotypic determinants of the virological response to tenofovir disoproxil fumarate in nucleoside reverse transcriptase inhibitor-experienced patients. *Antivir Ther,* 9**,** 315-23.

MELONI, S. T., KIM, B., SANKALE, J. L., HAMEL, D. J., TOVANABUTRA, S., MBOUP, S., MCCUTCHAN, F. E. & KANKI, P. J. 2004. Distinct human immunodeficiency virus type 1 subtype A virus circulating in West Africa: sub-subtype A3. *J Virol,* 78**,** 12438-45.

METZNER, K. J., RAUCH, P., WALTER, H., BOESECKE, C., ZOLLNER, B., JESSEN, H., SCHEWE, K., FENSKE, S., GELLERMANN, H. & STELLBRINK, H. J. 2005. Detection of minor populations of drug-resistant HIV-1 in acute seroconverters. *AIDS,* 19**,** 1819-25.

MURPHY, R. A., SUNPATH, H., KURITZKES, D. R., VENTER, F. & GANDHI, R. T. 2007. Antiretroviral therapy-associated toxicities in the resource-poor world: the challenge of a limited formulary. *J Infect Dis,* 196 Suppl 3**,** S449-56.

NDUNG'U, T. & WEISS, R. A. 2012. On HIV diversity. *AIDS,* 26**,** 1255-60.

NISSLEY, D. V., HALVAS, E. K., HOPPMAN, N. L., GARFINKEL, D. J., MELLORS, J. W. & STRATHERN, J. N. 2005. Sensitive phenotypic detection of minor drug-resistant human immunodeficiency virus type 1 reverse transcriptase variants. *J Clin Microbiol,* 43**,** 5696-704.

ORRELL, C., WALENSKY, R. P., LOSINA, E., PITT, J., FREEDBERG, K. A. & WOOD, R. 2009. HIV-1 clade C resistance genotypes in naïve patients and after first virological failure in a large community ART programme. *Antivir Ther,* 14**,** 523-531.

PAREDES, R., MARCONI, V. C., CAMPBELL, T. B. & KURITZKES, D. R. 2007. Systematic evaluation of allele-specific real-time PCR for the detection of minor HIV-1 variants with pol and env resistance mutations. *J Virol Methods,* 146**,** 136-46.

PARIKH, U. M., BACHELER, L., KOONTZ, D. & MELLORS, J. W. 2006. The K65R mutation in human immunodeficiency virus type 1 reverse transcriptase exhibits bidirectional phenotypic antagonism with thymidine analog mutations. *J Virol,* 80**,** 4971-7.

PILLAY, S., BLAND, R. M., LESSELLS, R. J., MANASA, J., DE OLIVEIRA, T. & DANAVIAH, S. 2014. Drug resistance in children at virological failure in a rural KwaZulu-Natal, South Africa, cohort. *AIDS Research and Therapy,* 11.

POMERANTZ, R. J. & HORN, D. L. 2003. Twenty years of therapy for HIV-1 infection. *Nat Med,* 9**,** 867-73.

REITER, M. & PFAFFL, M. W. 2011. RT-PCR Optimization Strategies. *In:* KENNEDY, S. & OSWALD, N. (eds.) *PCR Troubleshooting and Optimization - The Essential Guide*. U.K: Caister Academic Press.

ROWLEY, C. F., BOUTWELL, C. L., LOCKMAN, S. & ESSEX, M. 2008. Improvement in allele-specific PCR assay with the use of polymorphism-specific primers for the analysis of minor variant drug resistance in HIV-1 subtype C. *J Virol Methods,* 149**,** 69-75.

SANTORO, M. M. & PERNO, C. F. 2013. HIV-1 Genetic Variability and Clinical Implications. *ISRN Microbiol,* 2013**,** 481314.

SANTOS, A. F. & SOARES, M. A. 2010. HIV Genetic Diversity and Drug Resistance. *Viruses,* 2**,** 503-31.

SCHUURMAN, R., BRAMBILLA, D., DE GROOT, T., HUANG, D., LAND, S., BREMER, J., BENDERS, I. & BOUCHER, C. A. 2002. Underestimation of HIV type 1 drug resistance mutations: results from the ENVA-2 genotyping proficiency program. *AIDS Res Hum Retroviruses,* 18**,** 243-8.

SEN, S., TRIPATHY, S. P. & PARANJAPE, R. S. 2006. Antiretroviral drug resistance testing. *J Postgrad Med,* 52**,** 187-93.

SHAH, F. S., CURR, K. A., HAMBURGH, M. E., PARNIAK, M., MITSUYA, H., ARNEZ, J. G. & PRASAD, V. R. 2000. Differential influence of nucleoside analog-resistance

mutations K65R and L74V on the overall mutation rate and error specificity of human immunodeficiency virus type 1 reverse transcriptase. *J Biol Chem,* 275**,** 27037-44.

SHARMA, P. L. & CRUMPACKER, C. S. 1999. Decreased processivity of human immunodeficiency virus type 1 reverse transcriptase (RT) containing didanosine-selected mutation Leu74Val: a comparative analysis of RT variants Leu74Val and lamivudine-selected Met184Val. *J Virol,* 73**,** 8448-56.

SHARP, P. M., SHAW, G. M. & HAHN, B. H. 2005. Simian Immunodeficiency Virus Infection of Chimpanzees. *J Virol* 79**,** 3891-3902.

SIERRA, S., KUPFER, B. & KAISER, R. 2005. Basics of the virology of HIV-1 and its replication. *J Clin Virol,* 34**,** 233-44.

SLUIS-CREMER, N., SHEEN, C. W., ZELINA, S., TORRES, P. S., PARIKH, U. M. & MELLORS, J. W. 2007. Molecular mechanism by which the K70E mutation in human immunodeficiency virus type 1 reverse transcriptase confers resistance to nucleoside reverse transcriptase inhibitors. *Antimicrob Agents Chemother,* 51**,** 48-53.

SUNPATH, H., WU, B., GORDON, M., HAMPTON, J., JOHNSON, B., MOOSA, M. Y., ORDONEZ, C., KURITZKES, D. R. & MARCONI, V. C. 2012. High rate of K65R for antiretroviral therapy-naive patients with subtype C HIV infection failing a tenofovir-containing first-line regimen. *AIDS,* 26**,** 1679-84.

SVAROVSKAIA, E. S., MARGOT, N. A., BAE, A. S., WATERS, J. M., GOODMAN, D., ZHONG, L., BORROTO-ESODA, K. & MILLER, M. D. 2007. Low-level K65R

mutation in HIV-1 reverse transcriptase of treatment-experienced patients exposed to abacavir or didanosine. *J Acquir Immune Defic Syndr,* 46**,** 174-80.

TANG, M. W. & SHAFER, R. W. 2012. HIV-1 antiretroviral resistance: scientific principles and clinical applications. *Drugs,* 72**,** e1-25.

TAYLOR, B. S. & HAMMER, S. M. 2008. The challenge of HIV-1 subtype diversity. *N Engl J Med,* 359**,** 1965-6.

TRIQUES, K., BOURGEOIS, A., SARAGOSTI, S., VIDAL, N., MPOUDI-NGOLE, E., NZILAMBI, N., APETREI, C., EKWALANGA, M., DELAPORTE, E. & PEETERS, M. 1999. High diversity of HIV-1 subtype F strains in Central Africa. *Virology,* 259**,** 99-109.

TRIQUES, K., BOURGEOIS, A., VIDAL, N., MPOUDI-NGOLE, E., MULANGA-KABEYA, C., NZILAMBI, N., TORIMIRO, N., SAMAN, E., DELAPORTE, E. &PEETERS, M. 2000. Near-full-length genome sequencing of divergent African HIV type 1 subtype F viruses leads to the identification of a new HIV type 1 subtype designated K. *AIDS Res Hum Retroviruses,* 16**,** 139-51.

TRIVEDI, V., VON LINDERN, J., MONTES-WALTERS, M., ROJO, D. R., SHELL, E. J., PARKIN, N., O'BRIEN, W. A. & FERGUSON, M. R. 2008. Impact of human immunodeficiency virus type 1 reverse transcriptase inhibitor drug resistance mutation interactions on phenotypic susceptibility. *AIDS Res Hum Retroviruses,* 24**,** 1291-300.

TURNER, D., BRENNER, B. & WAINBERG, M. A. 2004. Relationships among various nucleoside resistance-conferring mutations in the reverse transcriptase of HIV-1. *J Antimicrob Chemother,* 53**,** 53-7.

UNAIDS 2011. UNAIDS World Aids Day Report 2011.

UNAIDS 2013. Report on the Global HIV/AIDS epidemic.

VAN ZYL, G. U., LIU, T. F., CLAASSEN, M., ENGELBRECHT, S., DE OLIVEIRA, T., PREISER, W., WOOD, N. T., TRAVERS, S. & SHAFER, R. W. 2013. Trends in Genotypic HIV-1 Antiretroviral Resistance between 2006 and 2012 in South African Patients Receiving First- and Second-Line Antiretroviral Treatment Regimens. *PLoS One,* 8**,** e67188.

VIDAL, N., BAZEPEO, S. E., MULANGA, C., DELAPORTE, E. & PEETERS, M. 2009. Genetic characterization of eight full-length HIV type 1 genomes from the Democratic Republic of Congo (DRC) reveal a new subsubtype, A5, in the A radiation that predominates in the recombinant structure of CRF26_A5U. *AIDS Res Hum Retroviruses,* 25**,** 823-32.

VIDAL, N., MULANGA, C., BAZEPEO, S. E., LEPIRA, F., DELAPORTE, E. & PEETERS, M. 2006. Identification and molecular characterization of subsubtype A4 in central Africa. *AIDS Res Hum Retroviruses,* 22**,** 182-7.

VON WYL, V., YERLY, S., BONI, J., BURGISSER, P., KLIMKAIT, T., BATTEGAY, M., BERNASCONI, E., CAVASSINI, M., FURRER, H., HIRSCHEL, B., VERNAZZA,

P. L., RICKENBACH, M., LEDERGERBER, B. & GUNTHARD, H. F. 2008. Factors associated with the emergence of K65R in patients with HIV-1 infection treated with combination antiretroviral therapy containing tenofovir. *Clin Infect Dis,* 46**,** 1299-309.

WAINBERG, M. A., BRENNER, B. G. & TURNER, D. 2005. Changing patterns in the selection of viral mutations among patients receiving nucleoside and nucleotide drug combinations directed against human immunodeficiency virus type 1 reverse transcriptase. *Antimicrob Agents Chemother,* 49**,** 1671-8.

WALLIS, C. L., MELLOR, S. L., VENTER, F., SANNE, I. & STEVENS, W. 2010. Varied Patterns of HIV-1 Drug Resistance on Failing First-Line Antiretroviral Therapy in South Africa. *J Acquir Immune Defic Syndr,* 53**,** 480-484.

WATERS, L., NELSON, M., MANDALIA, S., BOWER, M., POWLES, T., GAZZARD, B. & STEBBING, J. 2008. The risks and incidence of K65R and L74V mutations and subsequent virologic responses. *Clin Infect Dis,* 46**,** 96-100.

WEBER, J., CHAKRABORTY, B., WEBEROVA, J., MILLER, M. D. & QUINONES-MATEU, M. E. 2005. Diminished replicative fitness of primary human immunodeficiency virus type 1 isolates harboring the K65R mutation. *J Clin Microbiol,* 43**,** 1395-400.

WENSING, A. M. & BOUCHER, C. A. 2003. Worldwide transmission of drug-resistant HIV. *AIDS Rev,* 5**,** 140-55.

WIRDEN, M., LAMBERT-NICLOT, S., MARCELIN, A. G., SCHNEIDER, L., AIT-MOHAND, H., BRUNET, C., ANGLERAUD, F., AMARD, S., KATLAMA, C. & CALVEZ, V. 2009. Antiretroviral combinations implicated in emergence of the L74I and L74V resistance mutations in HIV-1-infected patients. *AIDS,* 23**,** 95-9.

WONG, M. L. & MEDRANO, J. F. 2005. Real-time PCR for mRNA quantitation. *Biotechniques,* 39**,** 75-85.

YERLY, S., VORA, S., RIZZARDI, P., CHAVE, J. P., VERNAZZA, P. L., FLEPP, M., TELENTI, A., BATTEGAY, M., VEUTHEY, A. L., BRU, J. P., RICKENBACH, M., HIRSCHEL, B. & PERRIN, L. 2001. Acute HIV infection: impact on the spread of HIV and transmission of drug resistance. *AIDS,* 15**,** 2287-92.